MODELS AND SOLUTION APPROACHES FOR EMERGENCY RESPONSE NETWORK DESIGN INTEGRATING SUPPLY AND DEMAND SIDES

A Dissertation

by

JYOTIRMOY DALAL

Submitted to the Office of Graduate and Professional Studies of
Texas A&M University
in partial fulfillment of the requirements for the degree of

DOCTOR OF PHILOSOPHY

Chair of Committee,	Halit Üster
Co-chair of Committee,	Guy L. Curry
Committee Members,	Sila Çetinkaya
	Neil Geismar
Head of Department,	César O. Malavé

December 2014

Major Subject: Industrial Engineering

ABSTRACT

We present three models for emergency response network design. First, in a deterministic setting, we focus on two critical aspects of emergency logistics: evacuation and relief distribution. We consider a three-tier system comprising evacuation sources, shelters, and distribution centers (DC). Applying a multi-objective mixed integer programming model, we minimize the evacuees' maximum travel distance and total system cost. To solve large scale instances, we implement Benders Decomposition (BD) with callback feature, solving the master problem only once, thereby, saving significant solution time. We also find that tuning of master tree search parameters along with strengthening of the Benders cuts, impact convergence significantly. Next, our model is applied to a GIS-based case study on coastal Texas. We find the effects of changing problem parameters and explain the cost vs. critical distance trade-offs. We conclude that our proposed system works better than the system in practice by comparing them and by providing interesting managerial insights on location decision.

In the second study, for a more detailed network comprising five tiers and multiple modes of transport, we determine the centralized supply locations that serve the region under consideration under any disaster event. Using scenario and interval based representations together, we address uncertainties (1) in disaster location, intensity, and duration, and (2) in demand due to varied compliance rate of the population to the authority's orders. We efficiently solve the large scale instances using a decomposition-based approach. The model is applied to a case study on the Gulf coast of the USA. We find the effects of population density and disaster intensity on location-allocation decisions. Our model captures the trade-offs between

system cost and critical time to start relief distribution, and can aid an emergency manager in strategic decision making under various uncertainties.

Our third study combines the stochastic and robust optimization concepts. Disaster intensity and location related uncertainties are represented by a discrete scenario set. In a problem setting similar to our first study, the DC and shelter opening costs, and the weighted sum of the worst case (robust optimization) and expected (stochastic optimization) flow costs are minimized over all scenarios. We present Benders Decomposition based solution approaches to solve the model with different relative weight vectors. We conduct a case study on coastal Texas and observe the effects of changing certain problem parameters. We find that the underlying demand pattern dictates whether placing the relative emphasis on worst and average cases would alter the location decisions. Our model allows the decision maker to explore several alternatives by changing the emphasis on worst vs. average case cost minimization.

DEDICATION

To *my parents, wife and little son Jishnu*

ACKNOWLEDGMENTS

I would like to thank Dr. Halit Üster for being my advisor through the development of this dissertation under his supervision. I would also like to thank Dr. Guy L. Curry, Dr. Sila Çetinkaya and Dr.Neil Geismar for serving as members of my advising committee and providing valuable suggestions and comments. I am thankful to my friends and officemates: Abhilasha Katariya, Chitra Balasubramaniam, Arupa Mohapatra, Gokhan Memisoglu, Sung Ook Huang, Nannan Chen, and Su Zhao for their valuable suggestions at times.

I thank Texas A&M University for providing me an exciting and unique learning experience. I also thank the department of Industrial and Systems Engineering for providing excellent research facilities. I want to take this opportunity to thank all the staff in the department who helped me over the past years: Judy Meeks, Erin D. Roady, Michele Bork, and Cheryl S. Kocman for administrative help, Mark Henry, Mark Hopcus, and Dennis Allen for their prompt help in technical matters.

I wish to thank my parents without whose blessings and inspirations I could not have arrived at this juncture of my life. I am equally thankful to my parents-in-law for continuous encouragement to keep me focused on my goal. I can not thank my wife, Roopsi, enough for supporting me in my decision of pursuing Ph.D. although it meant a lot of sacrifice, hardship and patience on her part. She has always been the source of my strength, courage and inspiration in the most difficult times.

Finally, I must mention our little powerhouse Jishnu, a boundless flow of energy, for filling our lives with his heart-warming smile and never-ending mischiefs, the ultimate source of inspiration to us to overcome any hurdle in our journey ahead.

NOMENCLATURE

B&C	Branch and Cut
BD	Benders Decomposition
CD	Critical Distance
CSL	Centralized Supply Location
DC	Distribution Center
DSP	Dual Sub Problem
GIS	Geographic Information System
MILP	Mixed Integer Linear Programming
MoT	Mode of Transport
MP	Master Problem
NEEDS	Network for Emergency Evacuation and Distribution of Supplies
PSP	Primal Sub Problem
RO	Robust Optimization
ROC	Robust Optimization Counterpart
SO	Stochastic Optimization
SP	Sub Problem
UDC	Urban Distribution Center
ZCTA	Zip Code Tabulation Area

TABLE OF CONTENTS

Page

LIST OF FIGURES

FIGURE Page

LIST OF TABLES

TABLE Page

1. INTRODUCTION

Disaster is defined as the "situation or event, which overwhelms local capacity, necessitating a request to national or international level for external assistance" (EM-DAT). Even excluding the man-made disasters, the statistics of frequency and damage by the natural disasters are staggering. We present in the Table 1.1 the global natural disaster data over the past decade extracted from EM-DAT, and some further query to the database reveals that the disasters in the hydrological (flood) and meteorological (storm, cyclone, hurricane) categories are the predominant disasters, affecting thousands of human lives every year.

Table 1.1: Natural Disaster Data, 2004-2014 (Source: EM-DAT)

Year	Number of occurrence	Deaths	Affected Population	Damage ($, thousands)
2004	403	244,880	157,420,447	136,340,178
2005	487	93,076	154,250,709	214,202,351
2006	462	29,893	119,931,185	34,104,949
2007	450	22,424	210,535,301	74,420,257
2008	394	242,191	218,359,005	190,548,247
2009	387	16,012	201,254,562	46,801,923
2010	435	308,599	254,804,109	131,082,668
2011	360	34,139	210,716,639	363,989,168
2012	372	11,548	106,638,038	156,480,867
2013	352	22,794	96,080,898	117,838,189
2014	81	1,740	4,234,425	15,723,591

While natural disasters cannot be prevented, efforts should be made to reduce losses and alleviate the suffering of the survivors. Rapid transfer of the injured people, distributing reliefs among the victims are critical post-disaster operations. Bitter

experiences from past mega-disasters such as hurricanes Katrina (2005), Rita (2005), Ike (2008) have taught us the importance of effective pre-disaster preparedness to ensure efficient post-disaster response. While advanced planning is not feasible for earthquake-type disasters, it is definitely an option for the hurricane-type disasters that are predicted fairly in advance. In this dissertation, we only consider these weather-related disasters, and study the strategic response network design problem under different settings.

1.1 Scope of this Dissertation

Emergency management primarily addresses the post-disaster response operations involving two types of flows: relief flow to victims, and flow of injured people to medical centers. However, success of post-disaster efforts largely depends on pre-disaster planning, also involving flows of people and relief resources. Many deaths in natural disasters are avoidable by fast and timely evacuation of the vulnerable population. An equally important issue is distributing relief to these evacuees. For this, pre-positioning of essential relief supplies (e.g., food, medicine, water, personal hygiene products) at strategic locations is critical. In practice, evacuation management efforts are limited to issuing mandatory evacuation order and providing a list of available shelters in the neighborhood areas. Instead of merely instructing the people to self-evacuate, a more comprehensive arrangement can be made by opening shelters at safe locations and informing the people in advance where to go. In this dissertation, we present three related problems where the supply and demand sides of the response network are integrated at strategic level to ensure fast evacuation and cost-effective distribution. We now briefly discuss these three problems, along with our research contribution in these works.

In our first work, presented in Section 2, we introduce the Network for Emergency

Evacuation and Distribution of Supplies (NEEDS) model, where we consider a three tier system comprising evacuation source, shelter and DC. In a deterministic problem setting, we find the optimal shelter and DC locations and capacities, source-to-shelter and DC-to-shelter allocations and flow quantities, while minimizing (1) the maximum travel distance of any evacuee to ensure fast evacuation, and (2) overall logistics cost, comprising the shelter and DC opening, variable, and flow related costs. We model the problem as a multi-objective mixed integer linear programming problem (MILP) and apply Benders Decomposition (BD) based approach to solve the realistic large scale instances. The contributions of this work are as follows:

- Observing that the decisions involved in the pre-disaster stage span the relief and the evacuation sides of the emergency planning activities, a new multi-objective relief network design problem is introduced.
- A piecewise linear cost structure is considered for the shelters, to represent the economy of scale in both the fixed and variable cost components.
- We devise a BD-based efficient solution approach.
- We apply the NEEDS model to solve a realistic problem with available GIS-based data and study the effects of fixed cost, evacuation area, and critical distance on location decisions. We compare our solution with the existing evacuation and sheltering system in practice, and gain interesting insights.

For our second work presented in Section 3, the network solution obtained by solving the NEEDS model becomes part of the input to the network. Similar to our first work, we consider integration of supply and demand sides in strategic network designing. Here, we consider a more detailed, five tier system comprising very large central supply location (CSL), DC, small urban DC (UDC), shelter, and source. Instead of

solving the deterministic problem, we consider various sources of data-uncertainties. We use scenario-based representation for disaster location and intensity uncertainties. Further, the demands at sources are modeled using the box uncertainty representation due to (1) inaccurate estimate of disaster duration,(2) non-compliance of the affected people to the suggested action plan. In this work, our planning region is of much larger scale, a vast expanse of the coastline, e.g., entire Gulf coast. We assume that by applying the Network for Emergency Evacuation and Distribution of Supplies model locally to several smaller regions along the entire coast, the DC and shelters, that are suitable for disaster management at that level, are already built. Moreover, several smaller candidate UDCs are pre-selected in the vicinity of the source nodes. However, which ones of these DC, shelter, or UDC locations will be operative for the realization of a particular disaster scenario, is unknown. Geographically the source, UDC, shelter, DC, and CSL are located from the disaster-prone coastline in an increasing order of distance. On demand side, during a disaster, part of the population of a source leave for shelters and a fraction of the stay-back population go to UDCs to collect reliefs. On the supply side, the CSLs send reliefs to the DC and UDC locations, which finally get distributed among evacuees at shelters and the stay-back population, respectively. With a number of scenarios representing disasters at different intensities and landfall locations, to try to minimize the sum of the CSL opening cost and the worst case scenario flow cost. These opened CSLs are responsible to supply to the entire study region for any realization of the disaster event, however, the shelters, DCs, and UDCs can *turn on/off* based on individual scenarios. We capture an interesting inter-relation among (1) the critical time to start distribution, (2) system cost, and (3) demand uncertainty. Emergency managers should ensure the availability of reliefs at the shelters and UDCs by starting the relief movement early to avoid a situation where evacuees and stay-back people reach the shelters

and UDCs, respectively, only to find the supplies are yet to come. For large critical time, distribution begins early, using less expensive ground transport, avoiding late hour hurry and traffic congestion, however, starting distribution too early may prove counterproductive as the storm's direction may change later. On the other hand, waiting too long for more accurate weather prediction decreases the critical time. In that case, we reduce the uncertainty about the storm's intensity and impact area, but at the cost of using very expensive air transport option, thereby, increasing overall cost. Thus, by considering different modes of transport with varied unit costs to distribute reliefs, we capture the trade-off between the critical time to start sending reliefs from CSLs and the overall system cost. The contributions of this work are as follows:

- A robust optimization problem using the scenario/event-based and interval-based uncertainties together is modeled.
- A mixed integer linear programming (MILP) problem with a detailed five-tier system is developed.
- Different modes of transport with varied unit costs are incorporated. This helps to explore the trade-offs between distribution start time and system cost.
- A Benders Decomposition based solution approach that separates the subproblem into scenario-based smaller flow problems, is adopted. This decomposition enables solving large instances efficiently where commercial solver fails.
- Non-compliance to the instructions, a real issue caused by the affected population, is addressed.
- We conduct a case study with GIS data on Gulf coast and explore the trade-offs

between the system cost and time available to distribute reliefs from CSL. The effects of population density and disaster intensity on the solution are observed.

The third work is an attempt to combine the concepts of stochastic and robust optimization when data uncertainty is represented by scenario-indexed vectors of the uncertain model parameters. We revisit the problem setting of NEEDS model: a three-tier emergency response network, consisting of evacuation sources (demand points), shelters, and DCs (supply points). In this work, we consider the uncertainty in location and intensity of a disaster causing fluctuation in the demand induced at sources. Similar to NEEDS, we consider a multi-objective problem with two objectives: (1) fast evacuation, and (2) a variation from the regular cost minimization due to evacuee- and relief-flows. In a two-stage model, we consider minimizing the fixed cost to open DCs and shelters at the first stage. For the second stage, over all scenarios, we consider minimizing a weighted sum of two more flow-related cost components : (1) maximum flow cost (robust optimization), and (2) average flow cost (stochastic optimization). Here, we are interested to understand the change in the prescribed solution while a decision maker specifies his emphasis on either of the two extremes: worst cast or average case, or chooses some intermediate, balanced approach. As the two previous studies, we face difficulty in solving the large scale problem instances by off-the-shelf solver. For that, we develop an efficient decomposition based solution approach with three variations, based on whether we choose minimizing the system cost only for the worst case, average, or the weighted sum of both sides. We present the detailed modeling and solution schemes for these three approaches. The contributions of this work are listed as follows.

- Decision models with data uncertainty are treated by either stochastic or robust optimization approaches, but we combine both, in the form of the objective as

weighted sum of the relevant cost components.

- Decision-maker gets the flexibility to specify his emphasis on worst case or average system cost minimization, or an intermediate of these two.
- We develop a Benders Decomposition based efficient solution approach, with three variations, to solve the model with different weight combinations. State-of-the-art solver fails to solve instances with large number of scenarios.
- A GIS-based case study is conducted and the effects of changing specific model parameters are observed.

1.2 Gaps in the Literature and Our Contributions

Although work addressing the evacuation and distribution problem exists in the humanitarian logistics literature, we have not yet found their strategic integration. Also, the literature apparently does not contain any multi-objective model where the objectives are connected to both evacuation (demand side) and distribution (supply side). Works addressing data uncertainty primarily adopt stochastic optimization, that heavily rely on assumed probability values for each scenario occurrence, to minimize the expected performance measure, generally, the overall system cost. These models mostly consider uncertainties in demand and infrastructural availabilities (due to partial damage of roads, shelters, DCs). The logistics literature contains no realistically detailed model considering *together* the following: (1) three or more tiers, (2) multiple modes of transport, (3) criticality of relief distribution starting time, while explaining the time and system cost interaction. In robust optimization literature, studies exist on two-stage robust network design, but with no applications in humanitarian logistics. There exist a number of emergency related papers in stochastic optimization and some work in robust optimization settings, but no at-

tempt has been made for a comparative study in a common problem context. Also, no work connects the stochastic and robust optimization settings under a single framework, solves realistic problem, and analyzes the outcomes.

Studies in this dissertation contribute to the existing literature in several ways. In the first work, we introduce a multi-objective integrated model to help with a multitude of important decisions for emergency response network design in a strategic pre-disaster setting so as to enable fast evacuation and cost-effective relief distribution. In our second work, we introduce a robust optimization model, that integrates the demand and supply sides in a detailed, five-tier emergency logistics network. This model ensures fast evacuation, on-time and adequate supply to the affected population, irrespective of the disaster location, intensity, and duration. Moreover, we address demand uncertainty caused by human behavior during emergency altering the estimated fraction of source population requiring relief. Our model adopts an absolute robustness criterion to minimize the worst case system cost, and therefore, does not require probability information about the disaster events. In the third work, we combine the stochastic and the robust optimization problem settings by introducing a mixed integer programming model. Considering a large number of emergency scenarios, we attempt to minimize the sum of initial infrastructure building cost, and the weighted sum of the average case (stochastic part) and worst case (robust part) transportation costs due to evacuee- and relief-flows. We provide an emergency manager a flexible tool, where, by changing the weights of the average and worst case parts in the objective function, one can explore the alternative location decisions and system costs.

Our work also contributes to the related literature from methodological perspective. Since realistic problems of this nature are of large scale, in our first work, we develop a decomposition-based approach to efficiently solve large scale

problem instances. We execute detailed computational experiments and conduct GIS-data based case studies with realistic size problems. In our second and third works, we demonstrate efficient modeling approaches that allow application of the decomposition-based techniques and scenario- or event-specific subproblem separation, thereby enabling the solution of large scale problems, that are hard to solve by the commercial solvers.

1.3 Organization of the Dissertation

The dissertation is organized as follows. In Section 2, we consider a multi-objective integrated Network for Emergency Evacuation and Distribution of Supplies (NEEDS) model, to ensure fast evacuation by minimizing the source-to-shelter *critical distance*, and the overall logistics cost in a deterministic setting. In Section 3, we consider various sources of uncertainties, present those using the scenario- and interval-based uncertainty representations together in a robust optimization model. We consider a five-tier system, where optimal location decisions for very large CSLs are made. These CSLs are responsible for relief supply to a very large coastal region, in all disaster scenarios. In Section 4, we consider a simplified version of the problem setting of Section 2 with demand uncertainty, represented by discrete disaster scenarios. We combine the concepts of stochastic and robust optimization, consider the objective function to minimize the weighted sum of worst case and average case system cost over all scenarios. This model enables the decision-maker to explore the trade-offs between the absolute robust and stochastic approaches, or an in-between solution by varying the weights of respective cost terms in the objective function. Finally, in Section 5, we conclude with a brief summary of the research results and a discussion of the potential impact of this dissertation in the future.

2. EMERGENCY RESPONSE NETWORK DESIGN INTEGRATING SUPPLY AND DEMAND SIDES IN A MULTI-OBJECTIVE APPROACH

2.1 Introduction and Motivation

Natural disasters pose a threat to mankind every year in the form of storms, hurricanes, tsunamis, and earthquakes. The result is enormous damage to property, infrastructure and, above all, the loss of human lives. The Indian Ocean tsunami in 2004 caused more than 250,000 deaths. The southern coast of the United States (U.S.) was hit by Hurricane Katrina the next year, causing about 1,800 deaths and a staggering loss of 108 billion U.S. dollars, making it the costliest disaster in U.S. history. Within the U.S., the hurricanes Rita (2005), Ike (2008), Irene (2011), Sandy (2012), internationally the earthquakes in China (2008), Haiti (2010) and the earthquake-turned-tsunami-turned-nuclear disaster in Japan (2011) remind us of the vulnerability of mankind to mega-disasters.

Past experience has taught us an important lesson: effective preparedness leads to efficient response. Planning in advance to open emergency shelters and arranging for the logistics to provide those shelters with essential supplies in a timely manner are crucial for the survival of the affected population. At the same time, one cannot emphasize enough the importance of saving the population near the impact area by conducting fast evacuation.

In Figure 2.1, we illustrate these two critical components, *relief* and *evacuation*, along with the important strategic decisions involved during the *pre- and post-disaster* situations. In practice, evacuation management is primarily concerned with timing the mandatory evacuation order and providing a list of potential locations (e.g., neighborhood towns) for evacuees to choose as shelters for themselves. It can

be argued that, at the strategic level, a good choice of shelters as well as the assignment of evacuees to these shelters are important for a less chaotic evacuation event. Thus, on the evacuation side, we consider two primary decisions that involve the determination of *shelter locations* and the *assignment of evacuees* to these shelters. On the relief side, we need to strategically locate enough supplies for evacuees at predetermined center locations so that their efficient distribution to shelters is facilitated at the post-disaster stage. Thus, as shown on the left-side of Figure 2.1, we are primarily concerned with the (supply) pre-positioning and distribution problems pertaining the decisions in the pre- and post-disaster stages, respectively. Since it is possible that shelter assignment and usage may continue in post-disaster, we also include shelter assignment in this stage in a pseudo manner (dashed lines in Figure 2.1). Observing that the decisions involved in the pre-disaster stage span the relief and the evacuation sides of the emergency planning activities, we are motivated to consider these decisions in an integrated fashion. The interface between these two sides is composed of shelters whose locations and capacities are decisions variables affecting both the supply (relief) and the demand (evacuation) side activities. This is further illustrated in Figure 2.2. Therefore, unlike past studies in humanitarian logistics that focusing either on resource pre-positioning or on evacuation planning mainly in operational level, we introduce a strategic network design problem that integrates pre-disaster decisions pertaining to both supply and demand sides of shelters by taking their specific objectives into account in a multi-objective setting.

For the integrated design, we consider a three-tier system with evacuation zone, potential shelter opening zone and potential distribution center (DC) opening zone. On receiving evacuation instruction, the evacuees move to the shelters and relief is sent there from the DCs. The shelters should be distant enough from the impact area for safety, but must be reasonably close to the evacuation zone to save time

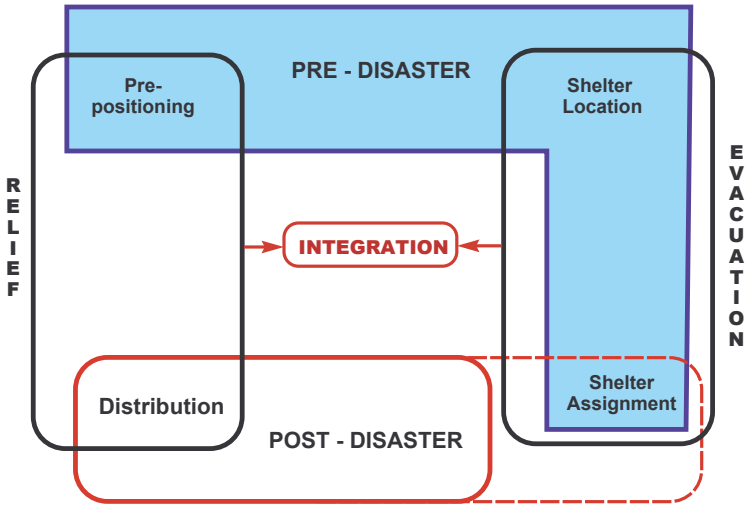

Figure 2.1: Integration of Evacuation and Relief Distribution

and transportation cost. Thus, we define *critical distance* as the maximum distance traveled by some evacuee(s) to reach their designated shelter. Then, in a multi-objective problem setting, our goals are: first, to minimize the critical distance to ensure fast evacuation and second, to minimize the total system cost to ensure cost-effective evacuation and relief distribution. With the decrease of this critical distance that captures the worst case situation, the evacuees' transportation cost to reach the shelters reduces but the relief distribution cost from the DCs to shelters escalates, which may increase the total system cost. This indicates an underlying trade-off between these two objectives, a prevailing fact in multi-objective optimization. It is also interesting to note that the total evacuation side transportation cost can also be perceived as a proxy to the total time spent by the evacuees on the road, which is another common measure of evacuation efficiency. Since our problem has multiple objectives, it has a set of non-dominating Pareto-optimal solutions instead of only one optimal solution. Exploration of the frontier offers the decision-maker the flexibility

to examine multiple solutions and trade-offs in a complex, resource-limited situation.

In this study, first, we develop a regional strategic response network design model. Our model can aid an emergency manager to comprehend the trade-offs between the conflicting objectives. We propose a mixed-integer linear programming model (MILP) for efficient evacuation and cost-effective relief distribution. Second, since a realistic problem of this nature is of large scale, from the methodological perspective, we develop a Benders Decomposition-based solution approach and present a detailed computational study. Finally, we demonstrate the usefulness of the proposed model by conducting a case study with realistic data (based on GIS) on coastal Texas region which is vulnerable to hurricanes. We discuss the effects of (1) increasing the demand for shelters by gradually expanding the evacuation area from coast to inland, (2) increasing an evacuee's maximum allowable travel distance, and (3) fixed costs of shelter locations. We also compare the existing State Evacuation and Sheltering Plan (Texas) with limited number of shelter hubs, to an alternative scheme with more distributed potential shelter locations. We present insights on better strategic planning by comparing these two systems on total cost, evacuees' maximum travel distance, and underlying trade-offs between cost and the maximum travel distance.

The remainder of this study is organized as follows. Section 2.2 provides a review of the related literature. We formally introduce the problem with notation and mathematical formulation in section 2.3. In section 2.4, we discuss a general solution approach for our multi-objective model, followed by Benders Decomposition (BD) framework with performance enhancements to solve large scale problems efficiently. We report the computational results and comparisons of the solution methodologies in section 2.5. In section 2.6, we present a GIS-based case study with numerical analysis, highlighting important managerial insights. Finally, we summarize our conclusions in section 2.7.

2.2 Related Literature

Comprehensive reviews of the works on humanitarian logistics problems are found in the literature (e.g., Altay and Green III, 2006; Apte, 2009; Çelik et al., 2012). Brachman and Church (2009) provide a literature review from the transportation analysis and planning perspective. Since our work focuses on integrating relief distribution and evacuation at the strategic level, studies on strategic pre-positioning of resources and strategic pre-disaster evacuation planing, as well as the integration of the two are relevant to us.

We first discuss the deterministic models on supply pre-positioning. Several studies in this category ignore the issue of data uncertainty, an inherent characteristic of any emergency-related model. We first mention some of these deterministic models followed by those addressing uncertainty issues. Jia et al. (2007) introduce a medical facility location problem for large-scale emergencies with specific coverage-quantity and coverage-quality, to serve each demand point by multiple facilities, located at varied distances.

Horner and Downs (2010) present a system consisting of: (1) pre-existing logistical staging areas (LSA), (2) two types of distribution facilities namely, point of distribution (POD) and break of bulk points (BOB) with different capacity levels, and (3) demand points. With the distribution cost minimization objective, they determine the optimal locations and capacities of the PODs and BOBs to fulfill each demand point's requirement.

Duran et al. (2011) present a two-tier system with DC and demand points where the number of new DCs is fixed. They determine the DC locations with single capacity level, flows of multiple relief items, and the inventory to stockpile while minimizing the post-disaster average response time. Though cost minimization is not

their objective, specifying the maximum allowable new facilities and the maximum inventory holding, indicate the implicit budgetary restriction.

We next discuss the pre-positioning models addressing uncertainty. Balçik and Beamon (2008) consider a two-tier, multiple relief item distribution system comprising DCs with single capacity level and the demand points. They address demand uncertainty by constructing scenarios from historical disaster data. Although the number of new DCs is not fixed, the pre- and post-disaster budget constraints implicitly address the limitation on that number. The model, while maximizing the total expected demand fulfillment, determines the optimal DC locations, the amount of supplies to stockpile at each DC, and the relief flows. The model is tested on a network comprising of 167 demand points and 45 potential DCs with 286 scenarios. Rawls and Turnquist (2010) integrate location, inventory management, and distribution problems in a two-stage stochastic programming model with the objective to minimize the total expected cost, which is the sum of new DC opening cost, transportation cost, inventory procurement, and holding or shortage costs. Given the demand points, the model determines the optimal locations and capacities (multiple levels) of the DCs, stocking quantities of multiple relief supplies, and the DC to demand point relief flows. Their case study considers 51 scenarios on a network with 30 nodes and 58 links. An extension to this model with additional constraints for service quality and average distance limit is found in Rawls and Turnquist (2011) in which a network with 30 nodes and 56 links is considered for study under 51 scenarios. In Rawls and Turnquist (2012), the authors also include a response phase to their model in terms of time periods. Their case study instance considers 33 scenarios with 4 time periods, 16 counties as potential DCs, and 19 demand points. Doyen et al. (2012) present their multiple relief item distribution model with regional relief center (RRC), local relief center (LRC) and the demand points. Their model

determines the location of both the RRC and the LRC (at single capacity level), but in two successive stages, while minimizing the total cost under demand and transportation cost uncertainty. The model allows for supply shortage at a center subject to heavy penalty cost. For computational study, they consider two scenario-types (based on probability values), and 4 distinct scenarios within each type (based on disaster intensity values). They generate random test instances of 15 classes having up to 10 potential RRC sites, up to 40 potential LRC sites, and up to 800 demand points. Lastly, Bozorgi-Amiri et al. (2013) present a three-tier model with supplier, regional distribution center (RDC), and affected areas (AA). They consider multiple capacity levels at the RDCs and multiple relief items. Their multi-objective, robust, stochastic optimization model address uncertainty in terms of scenarios where supply, demand, unit transportation cost, procurement cost, and the road network availability vary. With two objectives to minimize (1) the total expected cost and cost-variability, and (2) sum of maximum shortage at affected demand points, the model determines the optimum number, location, and capacities of the RDCs. Thus, the decisions include only the RDC locations and flows. A case study based on a region of Iran including 5 suppliers, 15 demand points, and 4 scenarios is presented. All the above pre-positioning related works primarily focus on cost-effective relief distribution to known demand points and ensure full or maximum possible demand coverage of the population. These do not emphasize on strategic evacuation and/or shelter location decisions.

We now discuss the works focusing on the evacuation side. Sherali et al. (1991) present a network flow model where the sets of potential shelters and evacuees are specified. With the objective to minimize total evacuation time for all evacuees, the model determines the evacuee-flow to each shelter and thereby decides which ones to open. Maximum number of shelters are fixed similar to the p-median facilities

location problem (Daskin (1995)). The authors conduct the computational study on a realistic network instance, based on the Princess Anne District in Virginia Beach consisting of 74 nodes, also including 9 origin nodes and up to 15 shelter nodes, and 118 arcs. Given the origin and destination (shelter) locations, Lu and George (2005) consider an evacuation route generation problem on a static network with arc and node capacities. With the overall objective of minimizing total evacuation time, they develop a heuristic based on iterative flow augmentation along shortest paths (using Dijkstra's algorithm). They conduct numerical tests on random large networks with up to 5000 nodes (up to 4000 source node; number of destination nodes is not specified) and the arcs being three times the number of nodes. In the Dynamic Traffic Assignment (DTA) literature, focusing on analysis of urban traffic networks (given origin-destination pair and the underlying network), we identify some recent works related to evacuation. Based on simulation approach and driver route choice data, the DTA models focus on real-time traffic management. Noh et al. (2009) present a DTA model for short-notice evacuation where an estimation process is used to feed a dynamic simulation model. Such short-notice models can be very useful for evacuation under extreme events with little to no warning.

In the above-mentioned evacuation-related works, the emphasis is on determining evacuation route while optimizing some time-based objective function (e.g., minimize total evacuation time). In the context of emergency management, only fast evacuation of the affected population is not enough. To ensure their survival in the hostile situation, pre-disaster planning to move them to safe shelters and provide essential reliefs is equally critical. This integration of evacuation and relief at strategic level is not yet addressed in literature.

We have so far come across only one paper that consider both evacuee- and relief-flows, however, in a different problem setting. Specifically, Li et al. (2011) present

a three-tier model with specified sets of evacuees' origins and DCs, and pre-existing temporary or permanent shelter with known capacity levels. The model considers decisions on addition of shelters with fixed capacity levels, DC-to-shelter relief flows and origin-to-shelter evacuees flows under uncertainty in demand, unit transportation cost, and unit operating cost which is captured via a set of scenarios. Demand satisfaction is not guaranteed but penalty cost is applied for any supply shortage at the shelters. The model is constructed as a two-stage stochastic model and solved by L-shaped method to determine the new shelter locations while minimizing the total expected system cost. The approach is then tested on an instance with 45 scenarios in a setting of 31 temporary and 57 permanent existing shelters, 26 potential new shelters, 7 DCs, and 19 evacuation origins.

In summary, although a past work addressing the evacuation and distribution problem exist in the humanitarian logistics literature, we did not find their strategic integration in any three-tier system where location decisions for the DCs and shelters, and evacuee- and relief-flows are taken simultaneously. Also, we have not come across any multi-objective model where the objectives are connected to both evacuation (demand side) and distribution (supply side). With these observations, we introduce a multi-objective integrated model to help with a multitude of important decisions for emergency response network design in a strategic pre-disaster setting so as to enable fast evacuation and cost-effective relief distribution. Our work also contributes to the related literature from methodological perspective. Since realistic problems of this nature are of large scale, we develop a decomposition-based approach to efficiently solve instances considerably larger than those mentioned in this section. We present an extensive computational study with instances up to 3510 nodes (up to 3200 origins, 250 shelters, and 60 DCs, respectively) and also conduct a case study comprising up to 1085 origins, 56 potential shelters, and 48 potential DC locations.

2.3 Problem Definition and Formulation

We consider a three-tier system as depicted in Figure 2.2 to establish an integrated emergency response network, consisting of evacuation sources, shelters, and DCs. The rightmost tier is the evacuation zone, which consists of the habitats of people close to coastline. We refer to the habitats as origins or evacuation sources interchangeably. The middle tier consists of the candidate shelter locations that are geographically farther away from the evacuation zone. The third (leftmost) tier consists of the potential DC locations. On receiving an evacuation order from the authorities, the residents of the impact area should evacuate to the shelters that are assigned to them beforehand. Relief supplies in previously estimated quantities should be distributed from the DCs to those shelters. The shelters should be distant enough from the evacuation sources to remain safe during a disaster, but must be located judiciously to ensure fast evacuation and reduce the transportation cost for the evacuees. We have several reasons to separate DC zone from the shelter zone. Large centralized DCs can have appropriate storage and material handling equipment. Pre-positioning the relief items at every shelter is cost prohibitive (Brachman and Church, 2009). Therefore, instead of holding inventory at each shelter in a decentralized fashion, stockpiling those in the DCs and serving the shelters on need basis can reduce overhead cost. Also, from the administrative point of view, it is preferable to keep the large stock of supplies away from the inbound evacuees to avoid any hostile situation. Keeping the DCs farther away from the evacuation zone can also help with fast relief distribution to the shelters while avoiding the possible traffic congestion between the sources and the shelters.

We design a response network for a study region with two objectives: (1) fast evacuation and (2) cost-effective relief distribution. To ensure fast evacuation, we

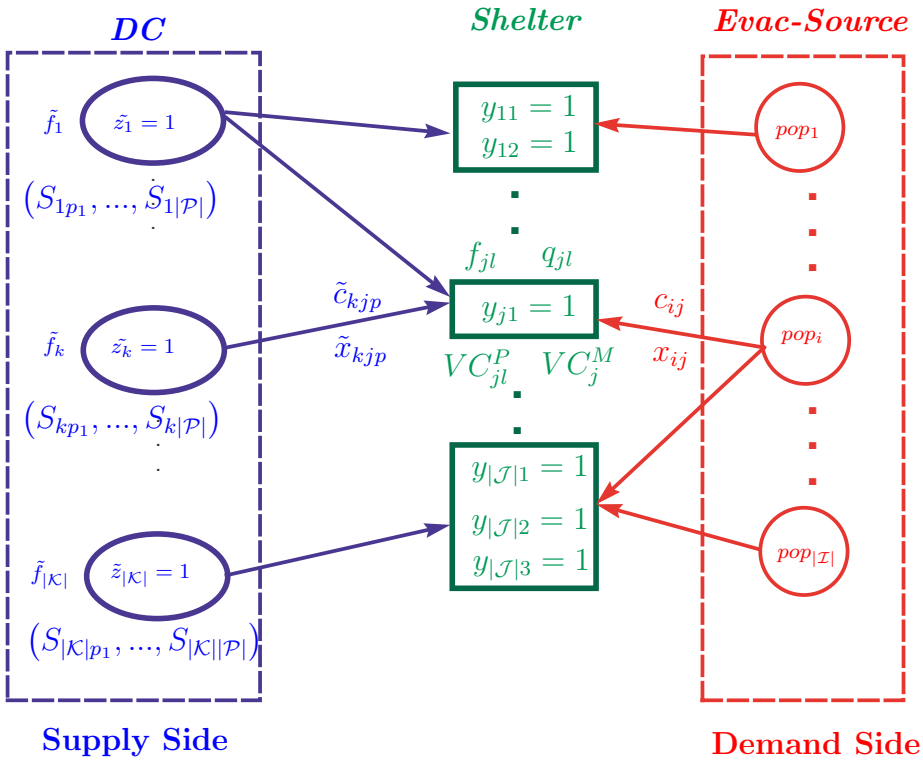

Figure 2.2: Underlying Network Structure and Notation

minimize the maximum distance that any evacuee travels to reach his/her designated shelter. We define this distance as the *critical distance* in this study. Next, for objective (2), we minimize total system cost that comprises the fixed costs to open DCs and shelters, the variable costs to manage the inbound evacuees and relief supplies at the shelters, and the transportation costs for the evacuee- and relief-flows. Opening shelters at reasonably safe places close to the evacuation sources can reduce both the critical distance and the evacuees' transportation cost, but, the DC-to-shelter distribution cost escalates, most likely increasing the total system cost. To capture this trade-off, we introduce a multi-objective optimization model with these

objectives to design a strategic network. Before presenting our integrated Network for Emergency Evacuation and Distribution of Supplies (NEEDS) model, we first summarize the **important design characteristics and assumptions**.

- Our system is multi-sourcing. Evacuees from an origin can go to multiple shelters and a shelter can receive evacuees from multiple origins. Similarly, a shelter can receive supplies from multiple DCs, and a DC can serve multiple shelters. Both the DCs and shelters are capacitated.

- Unlike studies in humanitarian logistics that introduce the notion of service level to represent the proportion of coverage provided to the population (Rawls and Turnquist, 2011), we assume total coverage for the population in the impact area. Several studies on evacuees' response during past disasters reveal that many citizens self-evacuate to their relatives' places or commercial establishments (Wu et al., 2012). Also, the trend of the shelter-going people largely depends on their age, gender, and socio-economic background (Huang et al., 2012). But, in the presence of accessible demographic and economic data, emergency managers can make estimates of the demand for shelters in a region and use these as input to the model.

- Several relief items, e.g., medicine, drinking water, and food packets are sent from the DCs to the shelters. We assume that an estimate of the per-head-demand for each item is known. We consider different unit transportation costs for the evacuees and for the relief items, which is a reasonable assumption since temperature-sensitive items such as frozen foods, medicines, and vaccines have special handling requirements, affecting their unit transportation costs.

- To open a DC, we consider a fixed cost, accounting for an aggregated estimate of

the annualized rental and insurance of the infrastructure, utilities, maintenance, equipment and manpower for storage and handling of the relief items. We consider that installation of refrigeration units or other temperature-controlling equipment at a DC can increase its fixed cost.

- Finally, we discuss the cost components associated with opening shelters. Since establishing and maintaining dedicated shelters for disaster mitigation is not economically viable, in practice public buildings and infrastructures (e.g., schools, churches, auditoriums, stadiums) are converted to makeshift shelters, incurring separate fixed opening and variable operating costs. A shelter can have multiple capacity levels, but the fixed cost for construction need not be proportional to the capacity. In real life, remodeling or expanding an existing infrastructure is generally less expensive than building one from scratch. The variable operating cost is incurred due to deployment of trained professionals and volunteers in the shelters to attend inbound evacuees, distribute reliefs, and provide medical care to the elderly and sick people. We assume this variable cost as proportional to the number of inbound evacuees. However, with the expansion of a shelter capacity resulting in more evacuee-inflow, one can expect a drop in the variable operating cost per person. Thus, for the shelters, to represent the economy of scale in both the fixed and variable cost components, we use a piecewise linear cost structure following the incremental model of Croxton et al. (2003) to make our model more realistic. For shelters, we consider another variable cost component, proportional to the inbound volume of the relief items, due to receiving, record keeping, unpacking, and distributing those supplies.

For an integrated relief network with these assumptions and design characteristics, we determine (1) optimal locations to open the shelters and DCs, (2) shelter

capacities, (3) source-to-shelter and DC-to-shelter assignments and corresponding flows, and (4) the critical travel distance for an evacuee to reach a shelter, so as to minimize total cost on both the supply and demand sides and maximum travel distance for evacuees. We next present our integrated multi-objective Network for Emergency Evacuation and Distribution of Supplies (NEEDS) model.

2.3.1 Model Formulation

We first introduce the notation.

Sets and Indices

$\mathcal{I}$	Set of sources of evacuation, $i \in \mathcal{I}$
$\mathcal{J}$	Set of potential shelter locations, $j \in \mathcal{J}$
$\mathcal{K}$	Set of potential DC locations, $k \in \mathcal{K}$
$\mathcal{L}$	Set of different capacity levels of the potential shelters, $l \in \mathcal{L}$
$\mathcal{P}$	Set of relief supplies for the evacuees, $p \in \mathcal{P}$

Model Parameters

pop_i	Population at origin $i \in \mathcal{I}$
w_p	Demand of product $p \in \mathcal{P}$ for each person
q_{jl}	Capacity of the shelter at location $j \in \mathcal{J}$ with level $l \in \mathcal{L}$
Δq_{jl}	$:= q_{jl} - q_{jl-1}$, where $q_{j0} := 0 \qquad \forall j, l$
	Shelter Capacity increment if opened at $j \in \mathcal{J}$ with level $l \in \mathcal{L}$
VC_j^M	Variable cost for relief flow at location $j \in \mathcal{J}$ (\$ / unit)
VC_{jl}^P	Variable cost for evacuee in shelter $j \in \mathcal{J}$ of level $l \in \mathcal{L}$ (\$/person)
f_{jl}	Fixed cost for opening a shelter at location j with level $l \in \mathcal{L}$
Δf_{jl}	$:= f_{jl} - f_{jl-1} + (VC_{jl}^P - VC_{jl-1}^P)q_{jl-1}$, where $f_{j0} := 0 \qquad \forall j, l$
	Fixed cost increment for opening a shelter at $j \in \mathcal{J}$ with level $l \in \mathcal{L}$
$\tilde{f}_k$	Fixed cost of opening a DC at location $k \in \mathcal{K}$
d_{ij}	Distance between origin $i \in \mathcal{I}$ and shelter location $j \in \mathcal{J}$

α Unit transportation cost for a person (\$/person-mile)

c_{ij} ($:= \alpha\ d_{ij}$) Transportation cost to move one person from i to j

β_p Unit transportation cost for item $p \in \mathcal{P}$ (\$/unit-mile)

$\tilde{c}_{kjp}$ ($:= \beta_p\ d_{kj}$) Transportation cost to move one unit of $p \in \mathcal{P}$ from DC $k \in \mathcal{K}$ to shelter $j \in \mathcal{J}$

S_{kp} Capacity of DC at $k \in \mathcal{K}$ for storing relief $p \in \mathcal{P}$

Decision Variables

x_{ij} Number of people evacuating from origin $i \in \mathcal{I}$ going to shelter $j \in \mathcal{J}$

$\tilde{x}_{kjp}$ Units of relief $p \in \mathcal{P}$ shipped from DC $k \in \mathcal{K}$ to shelter $j \in \mathcal{J}$

t_{jl} Number of evacuees staying in level $l \in \mathcal{L}$ of shelter at $j \in \mathcal{J}$

$\tilde{z}_k$ 1, if a DC opens at $k \in \mathcal{K}, 0$ otherwise

y_{jl} 1, if a shelter of level $l \in \mathcal{L}$ opens at $j \in \mathcal{J}, 0$ otherwise

u_{ij} 1, if origin $i \in \mathcal{I}$ is allocated to shelter $j \in \mathcal{J}, 0$ otherwise

Then, we formulate the NEEDS model as follows:

$$\text{Min} \qquad Z_1 = \{\max_{i\in\mathcal{I}, j\in\mathcal{J}} u_{ij} d_{ij}\} \tag{2.1}$$

$$\begin{aligned}\text{Min} \qquad Z_2 = &\sum_{i\in\mathcal{I}}\sum_{j\in\mathcal{J}} c_{ij}\, x_{ij} + \sum_{k\in\mathcal{K}}\sum_{j\in\mathcal{J}}\sum_{p\in\mathcal{P}} \tilde{c}_{kjp}\, \tilde{x}_{kjp} + \sum_{k\in\mathcal{K}} \tilde{f}_k\, \tilde{z}_k \\ &+ \sum_{j\in\mathcal{J}}\sum_{l\in\mathcal{L}} \Delta f_{jl}\, y_{jl} + \sum_{j\in\mathcal{J}}\sum_{l\in\mathcal{L}} VC^P_{jl}\, t_{jl} + \sum_{j\in\mathcal{J}}\sum_{l\in\mathcal{L}}\sum_{p\in\mathcal{P}} VC^M_j\, w_p\, t_{jl}\end{aligned} \tag{2.2}$$

subject to

$$\sum_{j\in\mathcal{J}} \tilde{x}_{kjp} \le S_{kp}\tilde{z}_k \qquad \forall k \in \mathcal{K},\, \forall p \in \mathcal{P} \qquad (2.3)$$

$$\sum_{k\in\mathcal{K}} \tilde{x}_{kjp} \ge w_p \sum_{i\in\mathcal{I}} x_{ij} \qquad \forall j \in \mathcal{J},\, \forall p \in \mathcal{P} \qquad (2.4)$$

$$\sum_{j\in\mathcal{J}} x_{ij} = pop_i \qquad \forall i \in \mathcal{I} \qquad (2.5)$$

$$\sum_{i\in\mathcal{I}} x_{ij} = \sum_{l\in\mathcal{L}} t_{jl} \qquad \forall j \in \mathcal{J} \qquad (2.6)$$

$$t_{jl} \le \Delta q_{jl} y_{jl} \qquad \forall j \in \mathcal{J},\, \forall l \in \mathcal{L} \qquad (2.7)$$

$$t_{jl-1} \ge \Delta q_{jl-1} y_{jl} \qquad \forall j \in \mathcal{J},\, \forall l \in \mathcal{L} \setminus \{1\} \qquad (2.8)$$

$$\sum_{k\in\mathcal{K}} S_{kp}\tilde{z}_k \ge w_p \sum_{i\in\mathcal{I}} pop_i \qquad \forall p \in \mathcal{P} \qquad (2.9)$$

$$\sum_{j\in\mathcal{J}}\sum_{l\in\mathcal{L}} \Delta q_{jl} y_{jl} \ge \sum_{i\in\mathcal{I}} pop_i \qquad (2.10)$$

$$x_{ij} \le M\, u_{ij}, \;\; u_{ij} \le \sum_{l\in\mathcal{L}} y_{jl} \qquad \forall i \in \mathcal{I},\, \forall j \in \mathcal{J} \qquad (2.11)$$

$$x_{ij}, \tilde{x}_{kjp}, t_{jl} \ge 0 \qquad \forall i \in \mathcal{I}, \forall j \in \mathcal{J}, \forall k \in \mathcal{K}, \forall l \in \mathcal{L}, \forall p \in \mathcal{P} \qquad (2.12)$$

$$u_{ij}, y_{jl}, \tilde{z}_k \in \{0,1\} \qquad \forall i \in \mathcal{I}, \forall j \in \mathcal{J}, \forall k \in \mathcal{K}, \forall l \in \mathcal{L}. \qquad (2.13)$$

The model consists of two objective functions. The objective (2.1) minimizes the maximum distance between any origin and shelter. The objective (2.2) minimizes the total cost incurred by the system. The first and second terms of (2.2) are the transportation costs for flows of evacuees and relief supplies respectively. The third and fourth terms are the fixed costs associated with the DCs and the shelters. The last two terms of (2.2) represent the variable costs at the shelters due to the inbound people and the relief items. Among the constraints, (2.3) represents the capacity constraint for each DC for each relief item and constraint (2.4) ensures that the

demand for each item at each shelter is satisfied by the relief coming from the DCs. Constraint (2.5) is the demand constraint of each origin, ensuring full coverage for all the people. Constraint (2.6) ensures that for each shelter, all the inbound evacuees are accommodated within some of its open capacity level. For each shelter, constraint (2.7) and (2.8) together ensure that the number of evacuees occupying a certain capacity level, actually corresponds to the correct level of the piecewise linear cost function. We note that by combining appropriate terms from constraints (2.7) and (2.8), we obtain $y_{jl+1} \leq y_{jl}, \forall j, l \in \mathcal{L} \setminus \{|\mathcal{L}|\}$ which is a constraint to enforce that if the incremental capacity of a higher level is added, then the incremental capacity of the smaller levels must be added, too. Also, we observe that (2.6) and (2.7) together imply capacity constraint of each shelter. Constraints (2.9) and (2.10) are the surrogate constraints, to ensure that the total capacities of the DCs and shelters are enough to handle their respective total demands. Although not essential, addition of these surrogate constraints considerably helps to solve our model by commercial MIP solver. Constraints (2.11) ensure that shelters and origin-to-shelter links are created properly based on flow. In the first part of (2.11), M stands for a very large value (big-M), to ensure appropriate upper bound of x_{ij} variables, based on the u_{ij} values. Finally, constraints (2.12) and (2.13) state variable range requirements.

In the NEEDS model, we observe that the minimax-type objective (2.1) can be simplified to minimization-type (2.14) by introducing an auxiliary non-negative variable CD (2.16) for the critical distance. After adding its corresponding new constraint (2.15) we obtain the following:

$$\text{Min} \qquad Z_1 = CD \tag{2.14}$$

$$\text{Min} \qquad Z_2$$

subject to

$$CD \geq u_{ij} d_{ij} \qquad \forall i \in \mathcal{I}, \forall j \in \mathcal{J} \tag{2.15}$$

$$CD \geq 0 \tag{2.16}$$

(2.3) to (2.13).

2.4 Solution Approaches

Since multi-objective models cannot have a single optimal solution, by solving the NEEDS model, we should obtain a Pareto-optimal Front (PF) of non-dominated solutions. This gives a decision-maker the flexibility to accept a Pareto-optimal solution that suits his/her notion of the relative priorities of the objectives under consideration (Deb, 2001). To convert our model from multi- to single-objective, we first observe that the distance between any $[i, j]$ pair, d_{ij}, is known a-priori, because we know each source i and candidate shelter j location. Thus, we can pre-process to populate a set $\mathcal{D} := \{d_{ij} | i \in \mathcal{I}, j \in \mathcal{J}\}$. Clearly, an optimum value for our decision variable CD must be in the set $\mathcal{D}$. However, when $|\mathcal{I}|$ and $|\mathcal{J}|$ are large, the set $\mathcal{D}$ is too large to consider its entries individually. Therefore, we populate the set $\mathcal{D}$ with a finite number of gradually increasing integers, with meaningful differences between each element. For each given $\widehat{CD} \in \mathcal{D}$, we solve the NEEDS model to minimize the total cost. But, in order to avoid any source-to-shelter assignment where $d_{ij} > \widehat{CD}$, we first construct a binary accessibility matrix as follows:

$$a_{ij} = \begin{cases} 1, & \text{if } d_{ij} \leq \widehat{CD} \qquad \forall i \in \mathcal{I},\ j \in \mathcal{J} \\ 0, & \text{otherwise,} \end{cases} \tag{2.17}$$

and, with big-M, we redefine the unit transportation cost of the evacuees using

$[a_{ij}]$ matrix:

$$\widehat{c}_{ij} := \alpha \times d_{ij} + M\,(1 - a_{ij}) \qquad \forall i \in \mathcal{I}, \forall j \in \mathcal{J}. \tag{2.18}$$

Therefore, the model is discouraged from assigning a source i to shelter j if $d_{ij} > \widehat{CD}$.

We note at this point that our approach is similar to the ϵ-constraint method in the multi-objective optimization literature. In this method, out of a number of objectives, only one is retained and the remaining ones are converted to constraints, bounded by some specified $\boldsymbol{\epsilon}$ vector. However, we do not face the usual issues regarding the judicious choice of $\boldsymbol{\epsilon}$ that strongly influences the success of the ϵ-constraint method because we know in advance the potential optimal values of the CD variable. Thus, for a given $\widehat{CD}$, we convert our model to a single-objective model, NEEDS($\widehat{CD}$) as follows:

$$\begin{aligned} \text{Min} \qquad Z_2 \;=\; & \sum_{i\in\mathcal{I}}\sum_{j\in\mathcal{J}} \widehat{c}_{ij}\, x_{ij} + \sum_{k\in\mathcal{K}}\sum_{j\in\mathcal{J}}\sum_{p\in\mathcal{P}} \tilde{c}_{kjp}\, \tilde{x}_{kjp} + \sum_{k\in\mathcal{K}} \tilde{f}_k\, \tilde{z}_k + \sum_{j\in\mathcal{J}}\sum_{l\in\mathcal{L}} \Delta f_{jl}\, y_{jl} \\ & + \sum_{j\in\mathcal{J}}\sum_{l\in\mathcal{L}} VC^P_{jl}\, t_{jl} + \sum_{j\in\mathcal{J}}\sum_{l\in\mathcal{L}}\sum_{p\in\mathcal{P}} VC^M_j\, w_p\, t_{jl} \end{aligned} \tag{2.19}$$

$$\text{subject to} \qquad (2.3) \text{ to } (2.10), \quad \text{and} \quad (2.12) \text{ to } (2.13).$$

Observe that constraint (2.11) involving the binary assignment variable u_{ij} is no longer required as we remove the objective (2.1). Solving NEEDS($\widehat{CD}$) model repetitively with different values of $\widehat{CD} \in \mathcal{D}$ yields a collection of multi-objective solutions. By applying Kung et al.'s method (Deb, 2001), we discard the dominated solutions from this collection and obtain the non-dominated or Pareto-optimal solutions for our multi-objective model.

2.4.1 Benders Decomposition-based Framework

Solving large instances of the mixed integer programming (MIP) model NEEDS($\widehat{CD}$) can be computationally challenging. We observe that, if the binary variables y_{jl} and $\tilde{z}_k$ are fixed in NEEDS($\widehat{CD}$), the remaining problem is a linear program (LP) with only the continuous variables x_{ij}, t_{jl}, and $\tilde{x}_{kjp}$. Therefore, large instances of NEEDS($\widehat{CD}$) can be efficiently solved by Benders Decomposition (BD). In BD, the overall formulation is decomposed into a master problem (**MP**) and a sub-problem (**SP**), and solved by transferring one-another's solution within an iterative framework (Benders, 1962). The **MP** mainly contains integer variables and only one continuous auxiliary variable that connects **MP** to **SP**, which is a linear program. Our specific decomposition-based implementation method for improved efficiency is described in detail in §3.5.2.

2.4.1.1 Benders Subproblem and its Dual

For the given binary vectors $\widehat{\mathbf{y}}$ and $\widehat{\mathbf{z}}$, representing the opened shelters and DCs, respectively, we obtain the primal subproblem PSP($\mathbf{x}, \tilde{\mathbf{x}}, \mathbf{t}|\widehat{\mathbf{y}}, \widehat{\tilde{\mathbf{z}}}$) which is a linear program. The binary vectors are supplied by the **MP**, described in §2.4.1.2. The primal subproblem **PSP**(.) is as follows:

$$\text{Min} \qquad Z_{\text{PSP}} = \sum_{i\in\mathcal{I}}\sum_{j\in\mathcal{J}} \widehat{c}_{ij}\, x_{ij} + \sum_{k\in\mathcal{K}}\sum_{j\in\mathcal{J}}\sum_{p\in\mathcal{P}} \tilde{c}_{kjp}\, \tilde{x}_{kjp} + \sum_{j\in\mathcal{J}}\sum_{l\in\mathcal{L}} VC^P_{jl}\, t_{jl} + \sum_{j\in\mathcal{J}}\sum_{l\in\mathcal{L}}\sum_{p\in\mathcal{P}} VC^M_{j}\, w_p\, t_{jl} \quad (2.20)$$

subject to

$$\sum_{j\in\mathcal{J}} \tilde{x}_{kjp} \leq S_{kp}\widehat{\tilde{z}}_k \qquad \forall k \in \mathcal{K},\, \forall p \in \mathcal{P} \qquad (2.21)$$

$$\sum_{k\in\mathcal{K}} \tilde{x}_{kjp} \geq w_p \sum_{i\in\mathcal{I}} x_{ij} \qquad \forall j \in \mathcal{J},\, \forall p \in \mathcal{P} \qquad (2.22)$$

$$\sum_{j\in\mathcal{J}} x_{ij} = pop_i \qquad \forall i \in \mathcal{I} \qquad (2.23)$$

$$\sum_{i\in\mathcal{I}} x_{ij} = \sum_{l\in\mathcal{L}} t_{jl} \qquad \forall j \in \mathcal{J} \qquad (2.24)$$

$$t_{jl} \leq \Delta q_{jl}\widehat{y}_{jl} \qquad \forall j \in \mathcal{J},\, \forall l \in \mathcal{L} \qquad (2.25)$$

$$t_{jl-1} \geq \Delta q_{jl-1}\widehat{y}_{jl} \qquad \forall j \in \mathcal{J},\, \forall l \in \mathcal{L} \setminus \{1\} \qquad (2.26)$$

$$x_{ij},\ \tilde{x}_{kjp},\ t_{jl} \geq 0 \qquad \forall i \in \mathcal{I}, \forall j \in \mathcal{J}, \forall k \in \mathcal{K}, \forall l \in \mathcal{L}, \forall p \in \mathcal{P}. \qquad (2.27)$$

By defining α_{kp}, β_{jp}, γ_i, π_j, μ_{jl} and ν_{jl} as the dual variables associated with constraints (2.21) - (2.26) respectively, the dual subproblem $\mathbf{DSP}(\boldsymbol{\alpha}, \boldsymbol{\beta}, \boldsymbol{\gamma}, \boldsymbol{\pi}, \boldsymbol{\mu}, \boldsymbol{\nu} | \widehat{\mathbf{y}}, \widehat{\tilde{\mathbf{z}}})$ is obtained as follows:

$$\text{Max } Z_{\text{DSP}} = -\sum_{k\in\mathcal{K}}\sum_{p\in\mathcal{P}} S_{kp}\,\widehat{\tilde{z}}_k\,\alpha_{kp} + \sum_{i\in\mathcal{I}} pop_i\gamma_i - \sum_{j\in\mathcal{J}}\sum_{l\in\mathcal{L}} \Delta q_{jl}\,\widehat{y}_{jl}\mu_{jl} + \sum_{j\in\mathcal{J}}\sum_{l\in\mathcal{L}\setminus\{1\}} \Delta q_{jl-1}\,\widehat{y}_{jl}\nu_{jl} \qquad (2.28)$$

subject to

$$-\alpha_{kp} + \beta_{jp} \leq \tilde{c}_{kjp} \qquad \forall k \in \mathcal{K},\, \forall j \in \mathcal{J},\, \forall p \in \mathcal{P} \qquad (2.29)$$

$$\gamma_i - \pi_j - \sum_{p\in\mathcal{P}} w_p\beta_{jp} \leq c_{ij} \qquad \forall i \in \mathcal{I},\, \forall j \in \mathcal{J} \qquad (2.30)$$

$$\pi_j - \mu_{jl} + \nu_{jl+1} \leq VC^P_{jl} + VC^M_j \sum_{p\in\mathcal{P}} w_p \qquad \forall j \in \mathcal{J},\, \forall l \in \mathcal{L} \setminus \{|\mathcal{L}|\} \qquad (2.31)$$

$$\pi_j - \mu_{jl} \leq VC^P_{jl} + VC^M_j \sum_{p\in\mathcal{P}} w_p \qquad \forall j \in \mathcal{J},\, l = |\mathcal{L}| \qquad (2.32)$$

$$\alpha_{kp},\ \beta_{jp},\ \mu_{jl},\ \nu_{jl} \geq 0 \qquad \forall k \in \mathcal{K},\, \forall p \in \mathcal{P},\, \forall j \in \mathcal{J},\, \forall l \in \mathcal{L} \qquad (2.33)$$

$$\gamma_i,\ \pi_j \qquad \text{unrestricted} \qquad \forall i \in \mathcal{I},\, \forall j \in \mathcal{J}. \qquad (2.34)$$

Let Θ denote the set of all extreme points of the **DSP** polyhedron specified by (2.29) - (2.34). For each extreme point $\theta \in \Theta$, we denote the associated variables $\alpha^\theta_{kp}, \beta^\theta_{jp}, \gamma^\theta_i, \pi^\theta_j, \mu^\theta_{jl}, \nu^\theta_{jl}$ and the objective function D^θ. If the optimal objective value is D^*, then $D^* \geq D^\theta, \forall\theta \in \Theta$. We can restate **DSP** as $\min_{D\geq 0}\{D : D \geq D^\theta, \forall\theta \in \Theta\}$ where

$$D^\theta = -\sum_{k\in\mathcal{K}}\sum_{p\in\mathcal{P}} S_{kp}\,\widehat{\tilde{z}}_k\,\alpha^\theta_{kp} + \sum_{i\in\mathcal{I}} pop_i\gamma^\theta_i - \sum_{j\in\mathcal{J}}\sum_{l\in\mathcal{L}} \Delta q_{jl}\,\widehat{y}_{jl}\mu^\theta_{jl} + \sum_{j\in\mathcal{J}}\sum_{l\in\mathcal{L}\setminus\{1\}} \Delta q_{jl-1}\,\widehat{y}_{jl}\nu^\theta_{jl}$$

$$\forall\theta \in \Theta.$$

2.4.1.2 Benders Master Problem

With the above representation of **DSP** by using the extreme points of its polyhedron, we reformulate the overall problem as:

$$\text{Min} \qquad Z_{\text{MP}} = \sum_{k\in\mathcal{K}} \tilde{f}_k\,\tilde{z}_k + \sum_{j\in\mathcal{J}}\sum_{l\in\mathcal{L}} \Delta f_{jl}\,y_{jl} + D \qquad (2.35)$$

subject to

$$\sum_{k\in\mathcal{K}} S_{kp}\tilde{z}_k \geq w_p \sum_{i\in\mathcal{I}} pop_i \qquad \forall p \in \mathcal{P} \qquad (2.36)$$

$$\sum_{j\in\mathcal{J}}\sum_{l\in\mathcal{L}} \Delta q_{jl}y_{jl} \geq \sum_{i\in\mathcal{I}} pop_i \qquad (2.37)$$

$$\sum_{j\in\mathcal{J}}\sum_{l\in\mathcal{L}\setminus\{1\}} \Delta q_{jl-1}y_{jl} \leq \sum_{i\in\mathcal{I}} pop_i \qquad (2.38)$$

$$y_{jl+1} \leq y_{jl} \qquad \forall j \in \mathcal{J},\, \forall l \in \mathcal{L} \setminus \{|\mathcal{L}|\} \tag{2.39}$$

$$D \geq -\sum_{k\in\mathcal{K}}\sum_{p\in\mathcal{P}} S_{kp}\,\tilde{z}_k\,\widehat{\alpha}^{\theta}_{kp} + \sum_{i\in\mathcal{I}} pop_i\widehat{\gamma}^{\theta}_i - \sum_{j\in\mathcal{J}}\sum_{l\in\mathcal{L}} \Delta q_{jl}\,y_{jl}\widehat{\mu}^{\theta}_{jl} + \sum_{j\in\mathcal{J}}\sum_{l\in\mathcal{L}\setminus\{1\}} \Delta q_{jl-1}\,y_{jl}\widehat{\nu}^{\theta}_{jl} \quad \forall\,\theta \in \Theta \tag{2.40}$$

$$D \geq 0 \tag{2.41}$$

$$y_{jl},\ \tilde{z}_k \in \{0,1\} \qquad \forall k \in \mathcal{K},\, \forall j \in \mathcal{J},\, \forall l \in \mathcal{L}. \tag{2.42}$$

This model is difficult to solve due to a huge number of type (2.40) constraints, however, not all of those are binding. Therefore, in Benders Decomposition, we start by solving a relaxed model, called the master problem (**MP**), by considering only a subset of (2.40). The **MP** is a relaxation of the original model since it does not contain all (2.40) type constraints in the overall problem's reformulation, hence, its optimal solution provides a valid lower bound of our overall problem. At an iteration θ, we solve the $\mathbf{DSP}(\boldsymbol{\alpha}, \boldsymbol{\beta}, \boldsymbol{\gamma}, \boldsymbol{\pi}, \boldsymbol{\mu}, \boldsymbol{\nu} | \widehat{\mathbf{y}}, \widehat{\tilde{\mathbf{z}}})$, and using the obtained dual solution $(\widehat{\boldsymbol{\alpha}}^{\theta}, \widehat{\boldsymbol{\beta}}^{\theta}, \widehat{\boldsymbol{\gamma}}^{\theta}, \widehat{\boldsymbol{\pi}}^{\theta}, \widehat{\boldsymbol{\mu}}^{\theta}, \widehat{\boldsymbol{\nu}}^{\theta})$ we generate a cut (2.40) corresponding to the θ-th extreme point of the **DSP** polyhedron, and add it to the **MP**.

We note that even if the distance d_{ij} between an evacuation source i and a shelter j is larger than given $\widehat{CD}$, we assume link (i, j) as connected, however, usage of such link incurs a huge penalty cost. Therefore, the **PSP** is always feasible with respect to any $(\mathbf{y}, \tilde{\mathbf{z}})$ pair and the corresponding **DSP** is always bounded. This way, the **DSP** solution always provides Benders optimality cuts rather than feasibility cuts, based on the extreme rays of the **DSP**, that hampers the convergence rate of the approach. To this end, we also utilize surrogate constraints to ensure that the network provided

by the **MP** solution, based on the values of $\mathbf{y}$ and $\tilde{\mathbf{z}}$, does not lead to subproblem infeasibility. Specifically, constraint (2.36) ensures aggregate demand satisfaction for each relief item by the open DCs and constraint (2.37) ensures all evacuees' accommodation by opening enough shelters. Constraint (2.38) prevents opening shelters in excess amount. Notice that constraints (2.5), (2.6), and (2.8), when considered together, imply (2.38). Since this information is lost after decomposition as (2.6) and (2.8) are in the subproblem, we add (2.38) as a surrogate constraint. Finally, (2.39) establishes that opening a higher capacity level at a shelter location implies that the lower capacity levels are already available.

2.4.2 Approaches to Accelerate Benders Decomposition

A traditional Benders Decomposition (BD) implementation to solve a large MIP problem, which relies on solving **MP** and **SP** successively, often does not perform satisfactorily. Therefore, over time, researchers prescribe several algorithmic improvements to accelerate BD. Some of these techniques include employing ϵ-optimal approach to obtain a first feasible solution of **MP** to save considerable solution time (Geoffrion and Graves, 1974), solving LP relaxation of the **MP** in a number of initial iterations (McDaniel and Devine, 1977), and early-stopping of **MP** in some initial iterations (Üster et al., 2007). For the network optimization problems with inherent degeneracy, resulting in alternate optima, strengthening of Benders cut(s) also proves to be helpful. In our study, we first attempted traditional BD implementation with some of these acceleration mechanisms. We started the first BD iteration with a bunch of heuristically generated initial cuts added to the **MP**. Although it significantly improved the initial optimality gap compared to the original BD algorithm, total solution time did not improve in any significant way. We also attempted the improvement approach of Saharidis et al. (2010) where instead of a single Benders

cut, a covering cut bundle is generated and added to the **MP** at each iteration. Additionally, we examined the maximum density cut suggested by Azad et al. (2013). However, the primary drawback in each of these approaches is the waste of considerable time for repeated solving of the **MP** at every iteration. Therefore, to avoid this repetition and make a significant performance improvement, we explore three avenues to accelerate our BD framework: (1) use of callback feature of CPLEX to solve the Benders master problem, (2) CPLEX parameter tuning, and (3) strengthening of Benders cuts.

2.4.2.1 Callback and CPLEX Parameter Tuning

We use lazy constraint callback of CPLEX (version 12.4 or later) in our BD implementation (Rubin, 2011). This is one type of control callbacks that CPLEX offers its users to intervene the branch-and-cut tree search process. Unlike the traditional BD framework, where the **MP** is solved repeatedly in each iteration with one or more additional cuts, the callback implementation solves the **MP** only once. During the branch-and-cut execution, whenever an incumbent is found, a new cut is added to the **MP** and the tree search proceeds till the stopping criteria are met or the optimal solution is obtained. This saves significant computation time. However, it is important to note that the use of callback turns off dynamic search and deterministic parallelism of the solver (CPLEX, 2009).

In this framework, clearly how the branch-and-cut tree is explored has an expected impact on the strength and the timing of the bounds obtained in solving the **MP**. Thus, we examine tuning of certain tree search parameters to increase efficiency of our implementation. For tree search, conventional search needs to be utilized instead of dynamic search (these are specified through the parameter *MIPSearch*) which does not allow the use of callbacks. Specifically, we tune two CPLEX parameters. First,

for *MIPEmphasis*, we try balancing between optimality and feasibility, and emphasizing optimality over feasibility. After some initial trials, we choose emphasizing optimality, because for our problem it is important to add good quality cuts at the early stage of BD execution. Although it may take longer than a feasibility-emphasized run to obtain a solution, our choice ultimately helps in terms of lesser but deeper cuts to **MP** leading to faster convergence. Second, we tune variable selection strategy for branching at an incumbent node (*Varsel*). This parameter influences which variable should be chosen for branching in the search tree after a node is selected. We tried default, pseudo, pseudo reduced, and strong branching alternatives, and after initial trial runs, we decided only to use strong branching for our computational study.

We now explain our BD implementation with callback and performance tuning in Figure 2.3. We set several CPLEX parameters at the beginning, to specify the stopping criteria (tolerance and runtime), and others as described above. Initially there are no Benders cuts in **MP** and the branch-and-cut (B&C) tree is explored until an integer-feasible solution is found. Once one is found, we check whether any stopping criterion is met. If not, the lazy constraint callback is invoked to solve the **SP**, using the **MP** solution vector as input. Next, an optimality cut is constructed from the **SP** solution and added to the **MP** before resuming the B&C tree search. This process continues until either of the stopping criteria is met. Finally, we solve the **SP** corresponding to the final **MP** solution and report the complete solution.

2.4.2.2 Cut Strengthening

As the $\mathbf{PSP}(\mathbf{x}, \tilde{\mathbf{x}}, \mathbf{t}|\widehat{\mathbf{y}}, \widehat{\tilde{\mathbf{z}}})$ is a network flow problem usually containing degeneracy, the $\mathbf{DSP}(\boldsymbol{\alpha}, \boldsymbol{\beta}, \boldsymbol{\gamma}, \boldsymbol{\pi}, \boldsymbol{\mu}, \boldsymbol{\nu}|\widehat{\mathbf{y}}, \widehat{\tilde{\mathbf{z}}})$ can have alternate optima, each able to define a different Benders cut. We attempt to get a strengthened Benders cut, whose in-

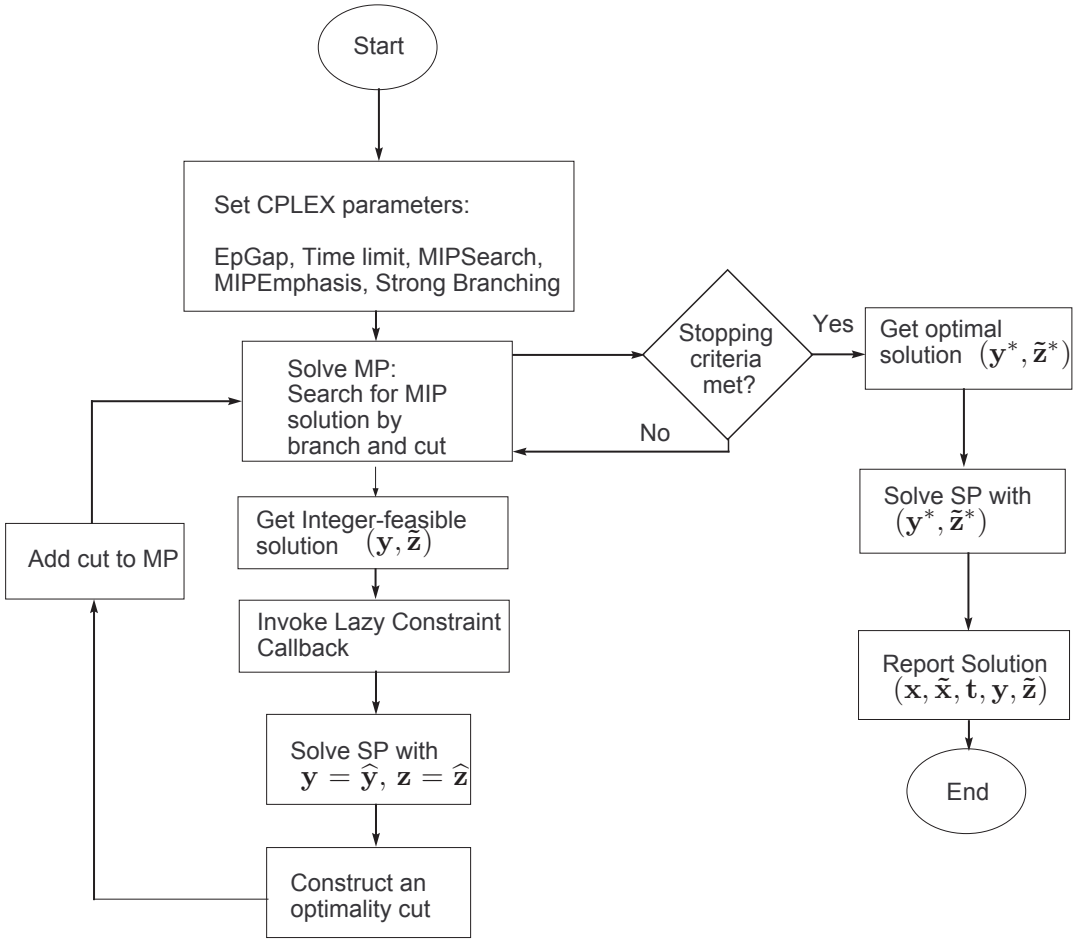

Figure 2.3: Benders Decomposition with Callback and CPLEX Parameter Tuning

clusion to **MP**, instead of the regular cut helps faster convergence. Strength of a cut for an optimization problem $\text{Min}_{y\in Y, z\in\mathbb{R}}\{z : z \geq f(w) + yg(w), \forall w \in W\}$ is defined by Magnanti and Wong (1981) as follows: A cut $z \geq f(v) + yg(v)$ is stronger than another cut $z \geq f(w) + yg(w)$ if $f(v) + yg(v) \geq f(w) + yg(w)$, $\forall y \in Y$ and for at least one $y \in Y$ we have $f(v) + yg(v) > f(w) + yg(w)$. Based on this result, we implement a two-phase method to strengthen a Benders cut before adding it to the **MP** (e.g., Van Roy, 1986; Üster and Agrahari, 2011; Üster

and Kewcharoenwong, 2011). In Phase-I, we solve the $\mathbf{DSP}(\boldsymbol{\alpha}, \boldsymbol{\beta}, \boldsymbol{\gamma}, \boldsymbol{\pi}, \boldsymbol{\mu}, \boldsymbol{\nu} | \widehat{\mathbf{y}}, \widehat{\widetilde{\mathbf{z}}})$ and obtain the dual variable vectors $\boldsymbol{\alpha}^{(1)}, \boldsymbol{\beta}^{(1)}, \boldsymbol{\gamma}^{(1)}, \boldsymbol{\pi}^{(1)}, \boldsymbol{\mu}^{(1)}$, and $\boldsymbol{\nu}^{(1)}$. We compute the upper bound of our problem using the Phase-I solution in the usual manner. Then, we fix the dual variables corresponding to the terms appearing in (2.28) with nonzero coefficients (i.e., nonzero binary solution values from the **MP** solution) and, consider the remaining ones as the decision variables in a Phase-II problem $\mathbf{DSP_{II}}(\boldsymbol{\alpha}, \boldsymbol{\beta}, \boldsymbol{\gamma}, \boldsymbol{\pi}, \boldsymbol{\mu}, \boldsymbol{\nu} | \boldsymbol{\alpha}^{(1)}, \boldsymbol{\beta}^{(1)}, \boldsymbol{\gamma}^{(1)}, \boldsymbol{\pi}^{(1)}, \boldsymbol{\mu}^{(1)}, \boldsymbol{\nu}^{(1)}, \widehat{\mathbf{y}}, \widehat{\widetilde{\mathbf{z}}})$ given as

$$\text{Max } Z_{\text{DSP}_{\text{II}}} = -\sum_{k \in \mathcal{K}} \sum_{p \in \mathcal{P}} S_{kp}\, \alpha_{kp} - \sum_{j \in \mathcal{J}} \sum_{l \in \mathcal{L}} \Delta q_{jl} \mu_{jl} + \sum_{j \in \mathcal{J}} \sum_{l \in \mathcal{L} \setminus \{1\}} \Delta q_{jl-1} \nu_{jl} \qquad (2.43)$$

$$\text{subject to (2.29) to (2.34).}$$

Essentially, the dual variables associated with zero coefficients based on **MP** solution can assume any value without changing the optimum objective value as long as they are feasible. Thus, the Phase-II problem determines their values in such a way that the Benders cut generated is stronger in the sense of strongness defined by Magnanti and Wong (1981). Observe that the second term of (2.28) containing γ_i variables is no longer included in the Phase-II objective (2.43). Since each γ_i has a nonzero coefficient pop_i, we fix all the $\gamma_i = \widehat{\gamma}_i$, obtained from Phase-I and the corresponding term of the objective function becomes a constant.

2.5 Computational Study

To examine the performance of our solution methodology in a series of computational studies, we randomly generate eight test problem classes with varying number of nodes in all three tiers of our network as outlined in Table 2.1. Every class contains five network instances, each having two randomly generated parameter sets, making

10 instances per class and 80 instances in total. To generate the efficient frontier, we solve all 80 instances with eight fixed critical distance values ($\widehat{CD}$).

Table 2.1: Problem Classes for Computational Study

Class	$\|\mathcal{I}\|$	$\|\mathcal{J}\|$	$\|\mathcal{K}\|$	Total ($\mathcal{N}$)	Class	$\|\mathcal{I}\|$	$\|\mathcal{J}\|$	$\|\mathcal{K}\|$	Total ($\mathcal{N}$)
C1	2500	200	50	2750	C5	3200	200	50	3450
C2	2500	200	60	2760	C6	3200	200	60	3460
C3	2500	250	50	2800	C7	3200	250	50	3500
C4	2500	250	60	2810	C8	3200	250	60	3510

2.5.1 Computational Experiments

At the first analysis phase, we attempt to solve all 80 instances with two early-stopping criteria: 2% optimality gap between the incumbent and the best lower bound, and 3600 sec. time limit, whichever is reached first. Our computational experiments are summarized as follows:

- We apply traditional branch-and-cut (B&C) with CPLEX default settings for cut generation, preprocessing, and upper bound heuristics to solve our test instances. We use this B&C result to benchmark the performance of our proposed BD-approaches.

- We implement BD in which we use default settings to solve the **MP** as described in § 2.4.2.1. Our aim is to observe any possible performance improvement over B&C in terms of solution time and optimality gap. We hereafter call this experiment BD-I.

- We conduct tuning of the parameters as given in §2.4.2.1 to further improve the BD-I results, and we call this experiment BD-II.

- Finally, we extend tuned BD-II by adding Benders cut strengthening feature (as explained in §2.4.2.2), and call this experiment BD-III.

At this point, we note that our preliminary trials using cut-strengthened BD without parameter tuning does not improve runtime in general. This is attributed to the computational overhead of repeatedly solving the DSP model in two phases. Therefore, we do not consider using only cut-strengthened BD in our computational study. Moreover, since we improve BD-I by parameter tuning, we explore tuning possibilities in B&C (CPLEX) as well for a fair comparison. For this, we first check whether parameter tuning improves B&C's performance for our test instances. To find that, we design an experiment with our B&C implementation using the same two parameters (*MIPEmphasis, and Varsel*) used in BD-II. We choose three levels of MIPEmphasis ("balanced", "feasibility", and "optimality"), and two levels Varsel ("default" and "strong branching"). Conducting ANOVA tests for all six combinations on runtimes of our selected samples (10% of the test bed), we do not observe any significant main or interaction effect of changing the parameters at 95% confidence level, therefore, decide to keep the default settings for B&C.

Analyzing the results of first round from the above four computational experiments, we identify the difficult instances and re-solve those with a 2% gap as the only early-stopping criterion. In §2.5.3, we present the results of each experiment and make important remarks.

We implement both B&C and BD using Concert Technology (CPLEX 12.4 with Java API). In BD implementations, we employ CPLEX to solve the (**MP**) as well as the dual subproblems (both $\mathbf{DSP}_{\mathrm{I}}$ and $\mathbf{DSP}_{\mathrm{II}}$ in cut strengthening). We take all

runs on desktop computers with Intel Core 2 Duo processor and 8 GB RAM.

2.5.2 Random Test Instance Generation

For the computational study, we generate random test instances, geographically close to the real problem for coastal Texas in terms of scale and spatial distribution of the nodes. We also randomly generate several model parameters whose values are close to the real data available at online GIS databases. We represent the study region by a 440×350 rectangle, divided into: evacuation, potential shelter opening, and potential DC opening zones, from right to left, as shown in Figure 2.4.

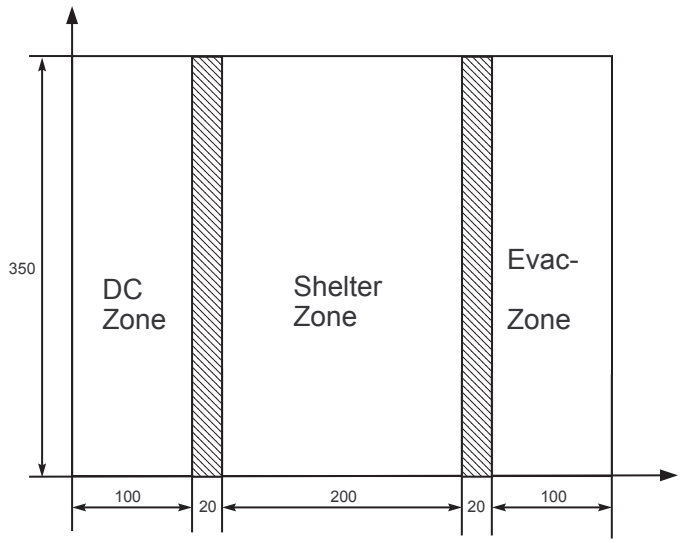

Figure 2.4: Setting for Test Instance Generation

To avoid opening shelters very close to the evacuation zone, we consider a 20 unit wide strip separating the evacuation and shelter zones. Similarly, another 20 unit wide strip ensures a safe distance between the DC and shelter zones. Using the uniform distribution, we randomly generate $|\mathcal{I}|$, $|\mathcal{J}|$ and $|\mathcal{K}|$ point coordinates

within these three rectangles, representing the three zones as per the combinations listed in Table 2.1. The distributions used for the model parameter generation are presented in Table 2.2.

Table 2.2: Distribution of Model Parameters

Parameter	Distribution	Parameter	Distribution
pop_i	Uniform [250; 2500]	$\bar{Q}_j$	$pop_j\times$ Uniform [0.8; 1.2]
pop_j	Uniform [1; 2] $\times\frac{\sum_{i\in\mathcal{I}} pop_i}{\lvert\mathcal{J}\rvert}$		$l=1$: Uniform [0.3; 0.5] $\times\bar{Q}_j$
α	Uniform [0.12; 0.15]	q_{jl}	$l=2$: Uniform [0.5; 0.7] $\times\bar{Q}_j$
	$p=1$: Uniform [0.001; 0.005]		$l=3$: Uniform [0.8; 1.1] $\times\bar{Q}_j$
β_p	$p=2$: Uniform [0.02; 0.05]		$l=1$: Uniform [100; 200] $\times q_{jl}$
	$p=3$: Uniform [0.01; 0.03]	f_{jl}	$l=2$: Uniform [1.1 ; 1.5] $\times f_{j1}$
VC_j^M	Uniform [1; 3]		$l=3$: Uniform [2.5 ; 4.0] $\times f_{j1}$
	$l=1$: Uniform [4; 6]	S_{kp}	Uniform [0.9; 1.1]* $\bar{Q}_p$
VC_{jl}^P	$l=2$: Uniform [2; 3]	$\tilde{f}_k$	$\sum_p \theta_p S_{kp}$,
	$l=3$: Uniform [1; 2]		where $\sum_p \theta_p = 1, \theta_p \in [0,1]$

We use uniform distributions to generate population parameters at the sources of evacuation (pop_i) and at the potential shelter locations (pop_j). We assume a candidate shelter's capacity as proportional to its population. If pop_j is large, generally there should be existing infrastructure and public buildings to accommodate a large flow of inbound evacuees. We generate pop_j as shown in Table 2.2 to avoid infeasibility of any instance due to inadequate shelter capacity. We further generate $\bar{Q}_j$, the base capacity of a shelter at j using uniform distribution, but as a function of pop_j. We consider three capacity levels namely small, medium, and large for a shelter j that are, in turn, functions of $\bar{Q}_j$. Other parameters include unit transportation cost for the evacuees (α), unit distribution cost for each relief item p (β_p), variable cost to manage inbound relief items at a shelter j (VC_j^M), and variable cost to serve an

evacuee at the shelter j in capacity level l (VC_{jl}^{P}). As mentioned, the capacity of a shelter (q_{jl}) depends on $\bar{Q}_j$, and the fixed cost f_{jl} to open a shelter is a function of it. Considering ϕ as the percentage of total potential DCs expected to open, we randomly generate DC capacity S_{kp} for each relief item p, where $\bar{Q}_p$ is calculated as $\frac{\sum_i pop_i * w_p}{\phi * |\mathcal{K}|}$. The fixed cost to open a DC depends on the equipment installation cost for different relief items. For example, medical supplies require a temperature controlled storage environment, which is costlier to build. Since we assume that each DC can store various relief items, we define $\tilde{f}_k$, the fixed cost for DC as the weighted sum of the storage capacities S_{kp} for each item p, with weight θ_p.

2.5.3 Computational Results

We now summarize the results of our four computational experiments. We solve our NEED($\widehat{CD}$) model with a list of eight $\widehat{CD}$ values starting from 170 increasing with a step size of 20 up to 310. In our preliminary trial runs on the C1 to C8 classes, we observe that tail-off effect makes the B&C computationally expensive for reaching optimality. Therefore, at first round, setting two early-stopping criteria as 2% gap and 3600 sec. time limit for all experiments, we identify the difficult instances and the promising solution approach(es) in Table 2.3. In each of the classes C1 to C8, we solve 10 instances, each with eight $\widehat{CD}$ values. The sequence of eight digits in each row represents the number of NEEDS($\widehat{CD}$) instances that are not solved for the corresponding $\widehat{CD}$ values within an hour. If all 10 instances of a class are solved within one hour for one value of $\widehat{CD}$, we put a "-" in the corresponding position. For example, in Table 2.3, the B&C sequence for C3, "1 3 2 3 2 2 - 2", means that by applying B&C on 10 instances of C3, we get one, three, two, three, two, two, none, and two difficult instances with $\widehat{CD}$ values of 170, 190, 210, 230, 250, 270, 290, and 310, respectively.

Table 2.3: Snapshot of Difficult Instances (with $\epsilon = 2\%$, after 3600 sec.)

Class	B&C	Total	BD-I	Total	BD-II	Total	BD-III	Total
C1	- - - - - - - -	0	- - - - - - - -	0	- - - - - - - -	0	- - - - - - - -	0
C2	- - 2 - - - 1 -	3	- - - - - - - -	0	- - - - - - - -	0	- - - - - - - -	0
C3	1 3 2 3 2 2 - 2	15	- 1 2 - - - - -	3	- - - - - - - -	0	- - - - - - - -	0
C4	1 3 2 2 1 2 2 1	14	- - 1 - - - - -	1	- - - - - - - -	0	- - - - - - - -	0
C5	- 4 - 1 4 1 2 1	13	- - - - - - - -	0	- - - - - - - -	0	- - - - - - - -	0
C6	- 2 2 1 1 1 -	7	- - 1 - - - -	1	- - - - - - - -	0	- - - - - - - -	0
C7	1 1 1 3 1 1 1 1	10	- 4 2 - - - - -	6	- - - - - - - -	0	- - - - - - - -	0
C8	2 2 4 2 3 1 3 2	19	2 1 3 - - - - -	6	- - - - - - - -	0	- - - - - - - -	0
		81		17		0		0

It is observed in Table 2.3 that the solution approaches from left to right are generally more efficient since more instances are solved within the one hour time limit. Furthermore, since BD-I cannot solve 17 instances to 2% optimality in one hour while BD-II and BD-III can solve all, we do not consider BD-I in the next phase of computational study.

In the second phase, we again apply B&C to solve the instances in Table 2.3 under B&C column without time limit but only under a 2% optimality gap stopping rule. This gives us a common ground to compare different solution approaches with respect to runtime. Table 2.4 presents a comparison of the average and maximum solution times for B&C, BD-II, and BD-III to solve instances of C1 to C8 with $\epsilon = 2\%$. Row minimums are highlighted in bold. We now summarize our key observations on performance comparison of three approaches.

- The average runtimes show that BD-III performs better than other approaches in general. Across all the classes and all $\widehat{CD}$ values, either BD-II or BD-III is the fastest. For B&C, the average runtime increases with the instance class size in general.

- In our hardware setting, under the default parallel mode of CPLEX, B&C uses eight threads. On the other hand, in all callback-based BD implementations, CPLEX turns off this parallel mode and uses single thread; but still BD outperforms B&C.

- Maximum runtime for B&C is always higher than BD. Moreover, the maximum runtime is primarily lowest in BD-III, followed by BD-II. Therefore, from the worst case perspective, the combination of tuning and cut strengthening is the most efficient approach for our test instances. For several row entries where the maximum runtime for BD-II is lower than BD-III's, the difference is very small. This happens for a few instances due to BD-III's computational overhead for cut strengthening.

- We also observe that the increase of $\widehat{CD}$ has no apparent effect on the runtime of B&C. But in BD, there is noticeable drop in runtime after $\widehat{CD} = 210$, in all eight classes. Our modeling approach for BD can explain this difference. In BD, to avoid adding feasibility cut corresponding to any infeasible solution from **MP**, we accept any source-to-shelter allocation even if it exceeds $\widehat{CD}$, but impose a large penalty in transportation cost. At the initial stage of BD, the **MP** locates shelters and DCs only to minimize total fixed opening cost. Since **MP** has no information of the cost structure of the underlying network, it may end up opening shelters at places that force the evacuees to travel more than given $\widehat{CD}$. Consequently, the upper bound of the overall problem gets very large, and this initial huge optimality gap takes a long time to converge. For smaller $\widehat{CD}$s, more source-to-shelter links are associated with this penalty cost, causing large optimality gap at the beginning. As the $\widehat{CD}$ increases, the problem becomes less restricted, and, thus, less solution time is required.

Table 2.4: Average and Maximum Runtimes (secs.) for 8 Classes ($\epsilon = 2\%$)

	Average runtimes (sec.)						Maximum runtimes (sec.)					
$\widehat{CD}$	B&C	BD-II	BD-III	B&C	BD-II	BD-III	B&C	BD-II	BD-III	B&C	BD-II	BD-III
	Class c1			Class c2			Class c1			Class c2		
170	862	265	**231**	1236	323	**286**	3310	**367**	411	3663	679	**443**
190	885	478	**372**	1130	544	**310**	1424	923	**507**	3247	1845	**446**
210	757	470	**302**	1571	**356**	362	2571	835	**516**	7140	622	**613**
230	1026	283	**155**	628	179	**145**	3530	437	**321**	3200	269	**213**
250	645	266	**127**	909	204	**163**	1706	726	**258**	3432	325	**265**
270	703	278	**121**	604	257	**164**	2758	647	**196**	2320	508	**442**
290	574	214	**130**	1148	230	**151**	1286	321	**216**	4801	697	**292**
310	786	245	**131**	512	215	**130**	3660	429	**234**	1618	447	**189**
	Class c3			Class c4			Class c3			Class c4		
170	1449	**509**	543	4177	**884**	919	6832	**723**	911	34334	3600	**3600**
190	4825	561	**560**	6899	1104	**752**	16277	**838**	917	47845	3600	**2477**
210	1530	710	**573**	4948	**748**	755	4499	1366	**1226**	36785	3600	**3600**
230	2497	401	**292**	2982	342	**278**	9765	732	**719**	17611	762	**762**
250	2206	411	**309**	1567	286	**175**	6838	855	**853**	10370	579	**230**
270	1520	333	**290**	3324	376	**252**	4705	642	**640**	21168	737	**736**
290	918	410	**317**	2726	428	**243**	2127	1031	**1001**	19204	1555	**495**
310	1552	449	**300**	2780	320	**233**	5746	1591	**841**	18906	492	**488**
	Class c5			Class c6			Class c5			Class c6		
170	815	581	**478**	709	478	**416**	1948	1061	**631**	2525	650	**648**
190	3241	**701**	731	3146	**633**	642	7592	**1692**	1695	16168	**1732**	1733
210	1692	959	**625**	1661	**444**	466	3561	3600	**1147**	9077	819	**818**
230	1552	311	**285**	1205	369	**295**	5233	**434**	437	8261	946	**643**
250	2555	340	**312**	1469	308	**252**	6541	**717**	725	12691	695	**475**
270	1637	**305**	313	356	450	**305**	7772	**609**	613	824	1295	**648**
290	2000	309	**291**	866	277	**268**	6845	768	**765**	4966	463	**461**
310	2020	310	**305**	785	328	**300**	12637	**617**	624	4445	**612**	615
	Class c7			Class c8			Class c7			Class c8		
170	2028	1271	**840**	2976	920	**873**	8573	3600	**1371**	10873	**1408**	1427
190	2392	**890**	905	3673	914	**793**	9501	**1519**	1599	12409	1369	**1196**
210	2434	994	**955**	4108	1051	**1016**	12437	**1814**	1943	11727	3685	**3600**
230	2735	**487**	514	3044	620	**411**	7083	**1089**	1155	12489	1518	**1145**
250	2015	510	**485**	2636	643	**457**	8381	**877**	933	9631	1347	**1253**
270	2185	630	**578**	2105	741	**379**	8280	**996**	1054	7439	2478	**1034**
290	2129	571	**568**	2816	624	**505**	10042	**1131**	1207	8808	1824	**1480**
310	2325	459	**447**	3158	587	**489**	9358	**903**	955	15547	2144	**2046**

Thus, our results show that the BD with callback implementation improves the computational efficiency as opposed to the traditional Benders decomposition implementation. Moreover, CPLEX parameter tuning for solving the Benders **MP** in this specific implementation can improve the efficiency significantly. Strengthening of Benders cuts, in spite of having computational overhead, can further accelerate BD. Therefore, an implementation of BD, integrated with these performance improvement features, is a viable solution procedure for large-scale problem instances.

2.6 Case Study

We demonstrate the application of the integrated NEEDS model by conducting a case study with realistic GIS data in the coastal Texas region. For this purpose, we first present our data collection approach and then an experimental setting to devise a strategic evacuation and distribution plan, followed by important insights based on the results.

2.6.1 Data Collection and Experiments on Varying Evacuation Zones

We identify the most vulnerable areas to hurricane in five coastal Texas counties: Brazoria, Chambers, Galveston, Harris, and Matagorda from the Texas DPS evacuation planning map (Polonis et al., 2013). Based on the hurricane-intensity, they categorize the 5-digit ZIPcode-based evacuation area as: Coastal, A, B, and C zones. We consider the same sources, however, to represent the evacuee-origins more accurately, we acquire the demographic data at block-group level from census 2010 (source: socialexplorer.com) and integrate those to the census 2010 TIGER/Line shapefiles and construct the evacuation zone as shown in Figure 2.6.1.

The State of Texas has a "State Evacuation and Sheltering Plan" (SESP) (Fort Bend County Office of Emergency Management, 2012) where 16 sheltering hubs are identified to accommodate a large population. All these hubs are around the densely

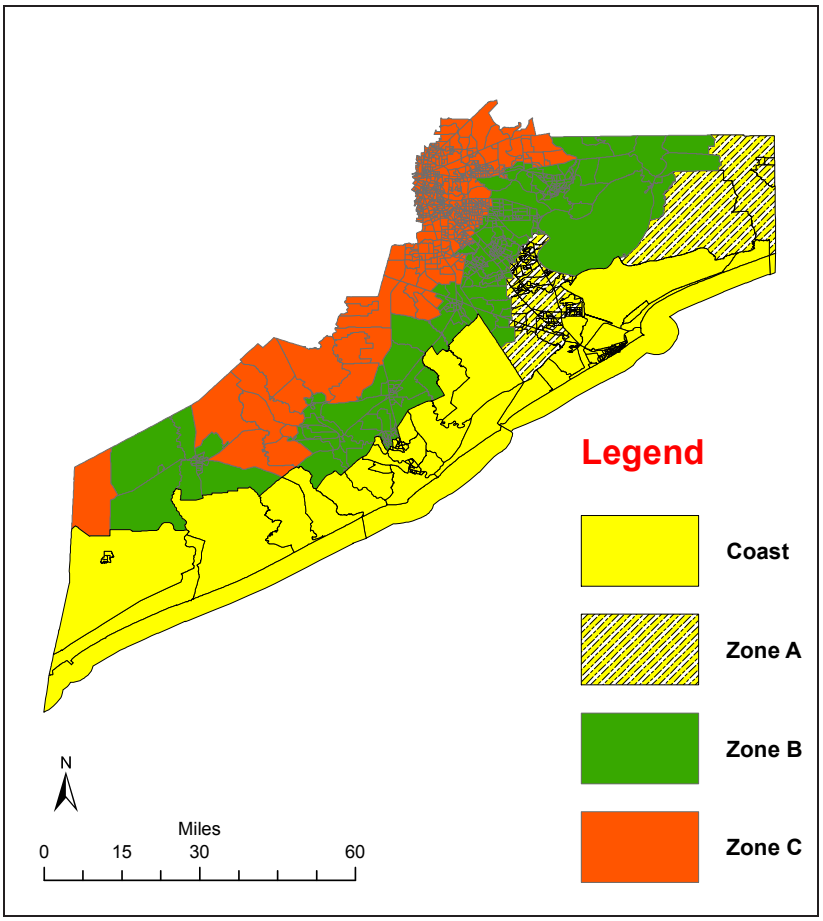

Figure 2.5: Evacuation Zone

populated cities e.g., Dallas, Austin, San Antonio (see Figure 2.7). We consider nine out of those 16 hubs that are close to the coastal Texas and augment the set of potential shelters by 47 more neighboring counties, to form the candidate shelter zone. These 56 counties, spatially spread-out and located far away from the coast, envelop the entire evacuation zone. List of the counties considered to construct these three zones is given in Table 2.5.

Potential DC zone consists of 48 counties that are farther away from the coast and envelops the shelter zone. As a hurricane gradually loses its intensity after making the landfall, we assume that the potential shelter and DC zones are relatively safer

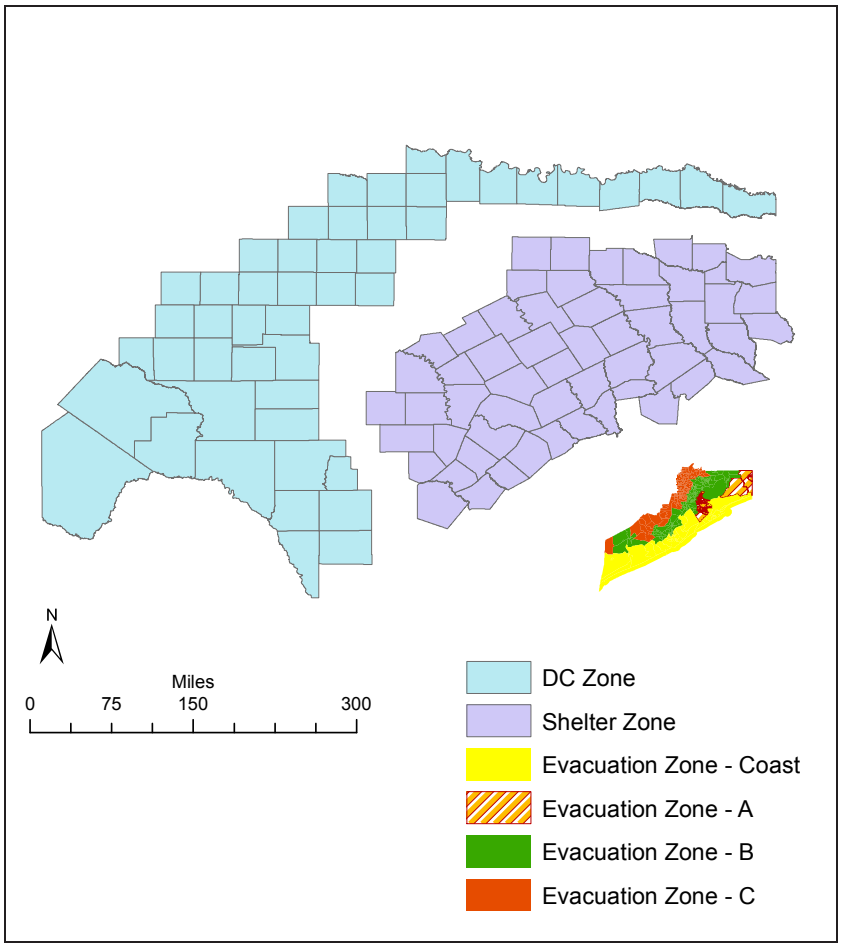

Figure 2.6: Three Zones

than the evacuation zone. Figure 2.6 presents all these three zones considered for our case study.

We use the census 2010 demographic data to estimate the shelter capacities. Since many existing buildings (school, public library, church, and auditorium) are used as emergency shelters, we assume that the shelter capacity in a county is proportional to its existing infrastructure, which, in turn, is proportional to its population. Therefore, we assume the maximum capacity of a potential shelter at j as $U[0.4, 0.6] * pop_j$, i.e., 40-60% of its existing population. We assume that the fixed cost of opening a

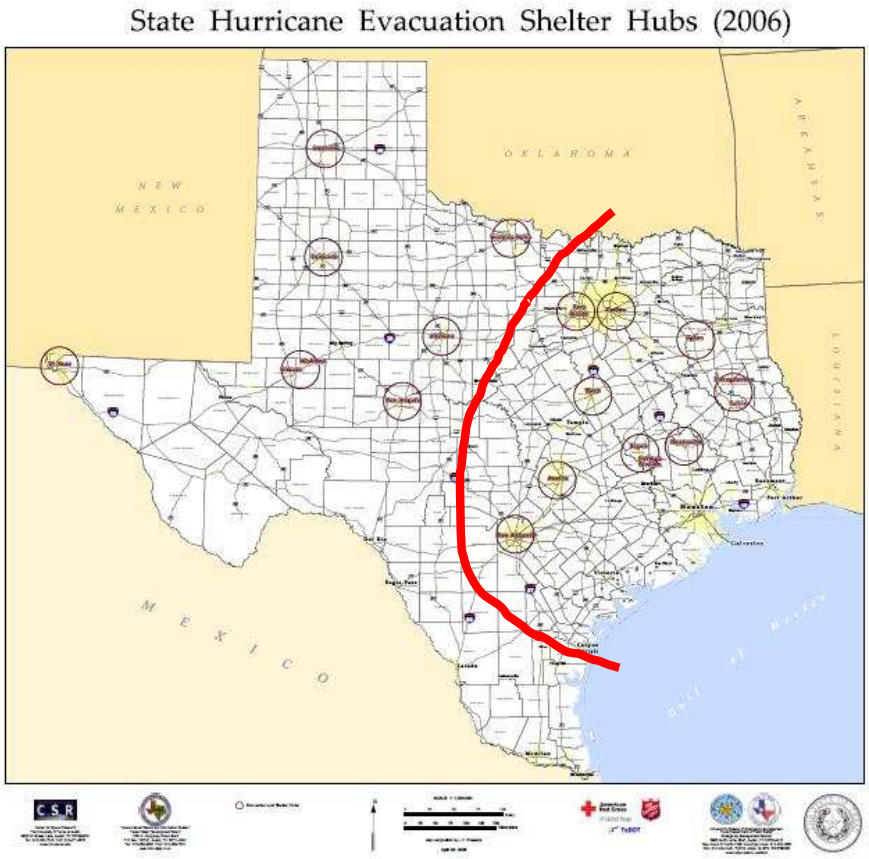

Figure 2.7: Shelter Hubs identified in State Evacuation and Sheltering Plan (Texas, 2006)

shelter is proportional to its capacity. Consequently, a candidate shelter at a densely populated county has large capacity but a high fixed cost. We use uniform distribution for all other model parameters as summarized in Table 2.2.

The objective of this case study is to devise a strategic evacuation and distribution plan for the population in a region under consideration. However, with the intensity of the incoming hurricane, the span of the evacuation zone may change. For instance, a low-intensity emergency needs evacuation of only the coast. In a more intense situation, both the coast and zone A should be evacuated. Similarly, for much

Table 2.5: Counties Considered in Three Zones

Evacuation Zone	Shelter Zone	DC Zone
Selected block groups of the following 5 counties, closely resembling the evacuation map by Texas DPS (Figure 2.6.1): Brazoria, Chambers, Galveston, Harris, Matagorda.	Anderson, Angelina, Bastrop, Bell, Bexar*, Blanco, Bosque, Brazos*, Burleson, Burnet, Caldwell, Cherokee, Comal, Coryell, Dallas*, Ellis, Falls, Freestone, Gillespie, Gregg, Guadalupe, Hamilton, Harrison, Hays, Henderson, Hill, Houston, Johnson, Kaufman, Kendall, Lampasas, Lee, Leon, Limestone, Llano, Madison, Mason, McLennan*, Milam, Mills, Nacogdoches*, Navarro, Panola, Robertson, Rusk, San Saba, Shelby, Smith*, Tarrant*, Travis*, Trinity, Upshur, Vanzandt, Walker*, Williamson, Wood. (56 counties)	Archer, Baylor, Bowie, Brewster, Callahan, Clay, Coke, Cooke, Crane, Crockett, Edwards, Fannin, Fisher, Glasscock, Grayson, Haskell, Howard, Irion, Jones, Kinney, Knox, Lamar, Martin, Maverick, Midland, Mitchell, Montague, Nolan, Pecos, Reagan, Real, Red river, Schleicher, Scurry, Shackelford, Sterling, Stonewall, Sutton, Taylor, Terrell, Throckmorton, Tomgreen, Upton, Uvalde, Val verde, Wichita, Young, Zavala. (48 counties)
Source of evacuation: Centroid of Block Group.	**Candidate Shelter:** Centroid of County.	**Candidate DC:** Centroid of County.

* Counties considered as Shelter Hubs in State Evacuation and Sheltering Plan.

stronger hurricanes, the authorities should evacuate areas such as "coast + zone A + zone B", or "coast + zone A + zone B + zone C" respectively. We summarize the number of sources and evacuees in Table 2.6 for each setting.

We solve the NEEDS models corresponding to each setting with an increasing series of critical distance (CD) values in order to obtain a Pareto-optimal front, where the trade-offs between CD and system cost can possibly provide some managerial insights. We present a representative sample of the results obtained by solving the

Table 2.6: Settings Considered in Case Study

Setting	Evacuation Area	Number of sources	Number of Evacuees
1	Coast	108	98,609
2	Coast + A	222	287,969
3	Coast + A + B	543	827,075
4	Coast + A + B + C	1085	1,813,273

NEEDS model under the four settings in Figures 2.9 - 2.10 for different CDs in 10-mile intervals such as 140, 150, ..., 330. Each row of Figures 2.9 and 2.10 represents an evacuation setting, for example, first row shows setting 1, second row shows setting 2 and so on. We mention the associated CD values in parenthesis in the captions of the individual maps. The first map in each row corresponds to the first feasible CD, i.e., all evacuees are accommodated in some shelters, no evacuee requiring to travel more that the specified CD value. We present the results for two other CDs, where the shelter and DC locations are significantly different, as the second and third maps in each row. We use a gradient color scheme of ArcGIS (ESRI Inc.) symbology, in which the candidate shelter counties with larger population are shown in darker color.

We summarize our observations of the outcomes in the four settings as follows:

1. **Effect of demand change on location decision:** Column-wise comparison of the four maps in Figures 2.9 - 2.10 (combined) indicates the need for more shelters as evacuation zone expands. Moreover, while one DC is sufficient for settings 1 and 2, in settings 3 and 4 we need 3 and 5 DCs, respectively. As a result, the fixed costs for opening the shelters and DCs gradually increase. The variable costs, evacuees' transportation cost, and relief distribution cost also increase with the number of evacuees. Due to the capacity limitation in

the nearby shelters, as the demand grows, more shelters open up at locations that are farther from the evacuation zone, causing a gradual increase of the first feasible CD (see Figures 2.9a, 2.9d, 2.10a, 2.10d) with the evacuation zone expansion. In other words, if the demand for shelters increases and the nearby locations do not have enough capacity to accommodate all evacuees, some of them have to travel farther, thereby increasing the critical distance and affecting the evacuation completion time.

2. **Effect of changing CD within each setting:** An increase of CD implies that the evacuees are allowed to travel longer to reach a shelter. Then, we solve a more relaxed version of the problem, which gives an opportunity to locate the DCs and shelters close to each other, reduce the distribution cost and possibly decrease the system cost. Therefore, we observe a general pattern of shifting the shelters more towards the candidate DC zone for larger CDs. If there is adequate evacuation time, emergency managers may direct the evacuees to travel to distant shelters, which, in turn, may reduce the DC to shelter relief distribution cost.

3. **Effect of fixed cost on shelter choice:** We note that a number of shelters open up in the low-population counties, instead of fewer large shelters in the highly populated locations. Dependence of the fixed cost for opening shelters on the population is its underlying reason. Therefore, even if a densely populated county is within the specified CD, it is generally not chosen to avoid a substantial fixed cost. As CD increases, with new possibilities of DC-shelter proximity, we sometimes observe a *consolidation*, i.e., instead of a bunch of small or medium size shelters, fewer large shelters open up closer to the DC zone (compare Figures 2.9b and 2.9c).

By studying these different settings, we try to develop a prudent strategy to prepare for the worst situation. In this study, Setting 4 is the worst case where all the four zones are evacuated, gets the maximum number of evacuees, and needs a large number of shelters. We focus on the first feasible solution under Setting 4 (see Figure 2.10d), where all the shelters are close to the evacuation zone.

A comparison of this set of open shelters to those under Setting 1 - Setting 3 with different CDs reveals that a large percentage of the shelters in the latter solutions is included in the former set. We note that this similarity is at least 60% and at most 100%. Therefore, the first feasible solution under Setting 4, although the costliest one in its associated frontier, is worth considering.The choice of this particular solution can be considered as a trade-off between the system cost and system adaptability. It gives some insight to a policy maker to strategically locate the shelters and DCs to handle an emergency response at various intensity levels.

2.6.2 Experiments on the Candidate Shelter Set

As fore mentioned, the State Evacuation and Sheltering Plan (SESP) currently considers nine shelter hubs in our study region. We compare two systems: one having nine large and densely populated candidate shelters (mentioned as *SH-9*), and the other having 56 widely spread shelters enveloping the evacuation zone (mentioned as *SH-56*). We wish to answer the following questions:

1. Which system provides a lower CD value with a feasible solution?
2. Which system is more sensitive to CD change, providing more CD-vs.-cost trade-off?
3. Which system is less expensive, and which cost component is most dominant?
4. What is the effect of increasing CD on the number and location of shelters and DCs?

We re-solve the NEEDS model with a candidate shelter set containing only the nine large and densely populated hubs considered in the SESP. We plot the total costs of the two systems (i.e., *SH-56* and *SH-9*) for common CDs in Figure 2.8 for all the four experiment settings mentioned in §3.7.3. The cost percentage differences, presented in the plot, are calculated as: 100*[(*SH-9* system cost) - (*SH-56* system cost)]/(*SH-9* system cost).

In response to our above questions, we summarize our key observations as follows:

1. In all four experiments, *SH-56* gives lower first feasible CD, suggesting that some evacuees have to travel longer in *SH-9*. Figures 2.9a, 2.9d, 2.10a, 2.10d (four settings in *SH-56*) show the first feasible CDs as 140, 150, 160, and 170 miles, respectively. In *SH-9* system (see Figure 2.8), corresponding CD values are 150, 170, 180, and 230 miles. The reason is: in *SH-56* there are more close-by candidate shelters than in *SH-9*. Therefore, *SH-56* is the better option since evacuees have to travel less to reach shelters.

2. In *SH-9*, the Pareto-optimal Front (PF) contains fewer non-dominated solutions, indicating that the system cost is now less sensitive to CD. As we have fewer and sparsely distributed candidate shelters, the problem remains unaltered for small CD increase. However, *SH-56* provides richer PF with more trade-off opportunities (see Figure 2.8).

3. Comparing the system cost between *SH-9* and *SH-56* for the common CDs in the two PFs, we find that *SH-9* is always costlier. Further analysis of the cost components at the *SH-9*'s PF points reveals that the fixed cost for a shelter is the dominant component (about 50% of total cost), because all the nine candidate shelters have very large capacity and thereby, high fixed cost. Therefore, if shelter opening cost is proportional to its capacity, which

is a realistic assumption, fewer large shelters may be a costlier option than widespread, smaller, but less expensive shelters.

4. As CD increases, we observe more *consolidation* in *SH-9*. A few huge shelters in *SH-9* are sufficient to accommodate all evacuees. Particularly, for some large CDs, only one or two shelters open at the most populated counties. But, implementation of such optimal solution, by convincing all to evacuate only to one or two counties is unrealistic. Moreover, sudden high volume of evacuee-inflow can jeopardize the traffic system of the large city during emergency, raising several administrative issues. However, the *SH-56*'s solution suggests opening more shelters in lower capacities at less crowded counties. Instead of huge evacuee-inflow to few large cities, dispersion to multiple spatially distributed shelters can help smoother evacuation.

2.7 Concluding Remarks

In this work, we introduce a multi-objective emergency relief network design problem. We integrate two crucial actions of emergency management, evacuation and relief distribution, to obtain a holistic strategic decision. We develop a new mixed integer linear model (NEEDS) with two objectives, first, to minimize the maximum travel distance for an evacuee, and second, to minimize the overall system cost. By exploring the problem structure, we convert the model from multi- to a series of single-objective problems, and devise a method to construct the Pareto-optimal front. We observe that a state-of-the-art branch-and-cut approach is computationally expensive for large test instances. Thus, we devise a BD-based solution approach and conduct a detailed computational study on the efficiency of its three different implementations incorporating algorithmic enhancements. We first implement BD using lazy constraint callback function during the master problem (**MP**) solution

whose search tree is maintained throughout the solution procedure (rather than repeatedly solving the **MP** after each Benders cut addition) and observe significant improvement in solution time. Then, we conduct performance tuning of tree search parameters to solve the **MP** faster and further enhance the BD performance. Our attempt to strengthen the Benders cuts in addition to parameter tuning is very effective to further reduce solution time for most of the instances in our testbed while maintaining acceptable solution quality. In summary, we observe a gradual improvement in average solution time in three BD implementations, each of which outperforms B&C as implemented in CPLEX.

We apply our model to solve a realistic problem with available GIS-based data and study the effects of fixed cost, evacuation area, and critical distance on location decision. We compare the existing evacuation and sheltering system with ours and gain interesting counter-intuitive insights. We observe that the current practice of locating shelters in fewer densely-populated areas due to availability of infrastructure may prove costlier than an alternative of opening more low-capacity shelters in less populated, widely-spread areas. Having more spatially distributed shelters may keep the evacuees' critical distance lower, while accommodating all of them. Moreover, an emergency manager can use our model as a decision-making tool to explore the trade-offs between cost and critical distance before taking strategic decision.

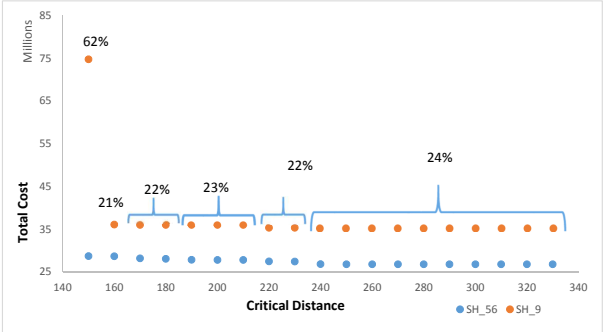

(a) Evacuate Coast Only

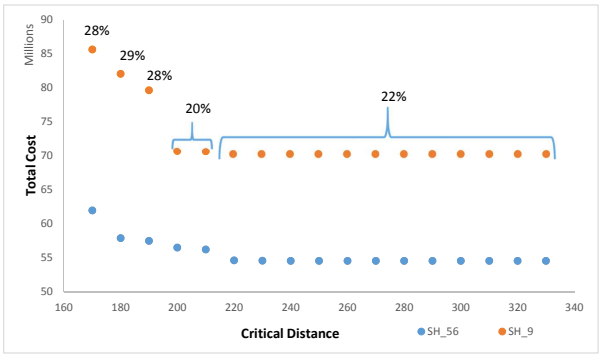

(b) Evacuate Coast and zone A

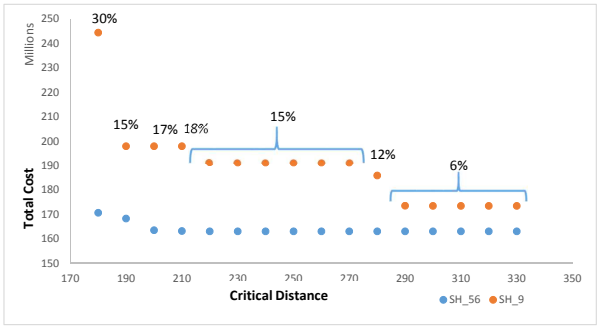

(c) Evacuate Coast, zones A and B

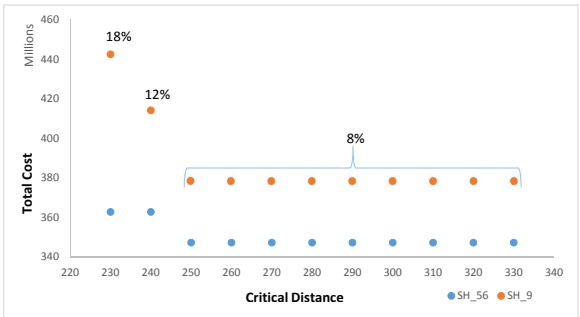

(d) Evacuate Coast, zones A, B and C

Figure 2.8: System Cost Comparison with 56 vs. 9 Candidate Shelters

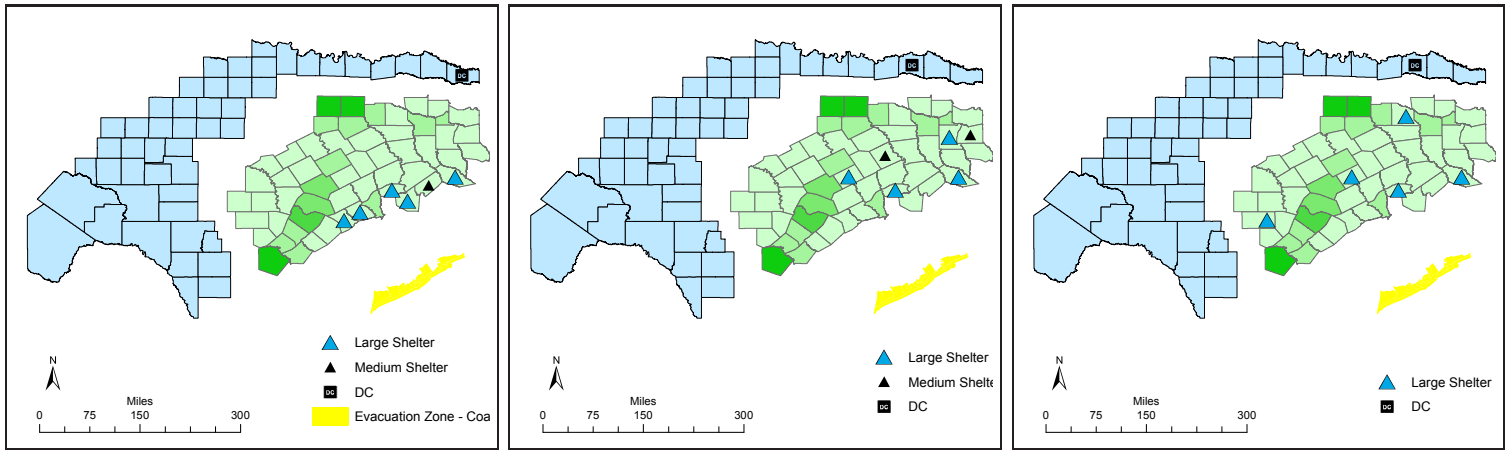

(a) Evacuate: Coast only (140) (b) Evacuate: Coast only (210) (c) Evacuate: Coast only (250)

(d) Evacuate: Coast, A (150) (e) Evacuate: Coast, A (200) (f) Evacuate: Coast, A (240)

Figure 2.9: Change of Location Decision Based on Evacuation Zone and Critical Distance - Part 1

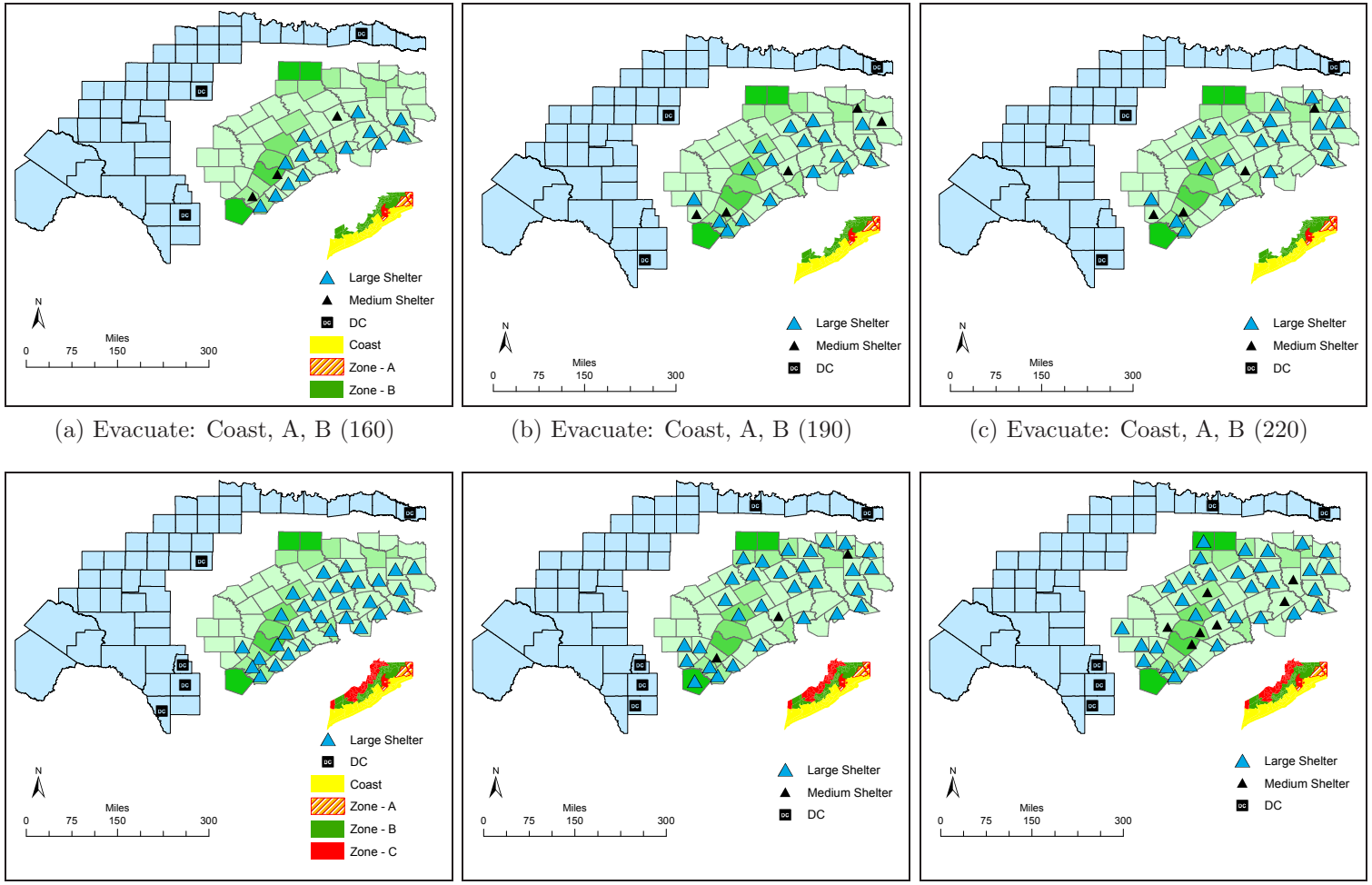

(a) Evacuate: Coast, A, B (160)

(b) Evacuate: Coast, A, B (190)

(c) Evacuate: Coast, A, B (220)

(d) Evacuate: Coast, A, B, C (170)

(e) Evacuate: Coast, A, B, C (220)

(f) Evacuate: Coast, A, B, C (270)

Figure 2.10: Change of Location Decision Based on Evacuation Zone and Critical Distance - Part 2

3. EMERGENCY RESPONSE NETWORK DESIGN INTEGRATING SUPPLY AND DEMAND SIDES UNDER DATA UNCERTAINTY: A ROBUST OPTIMIZATION BASED APPROACH

3.1 Introduction and Motivation

Over time, humanitarian logistics has evolved as an emerging research area to address different facets of emergency management and improve the pre- and post-disaster decision making. Every year, at different parts of the world, increasing loss of lives and properties due to natural disasters such as hurricanes, cyclones, tsunamis demand a holistic approach to alleviate the suffering of mankind. Over the past years, studies have investigated different aspects of emergency management by applying various operations research techniques and optimization models ranging from pre-disaster planning to post-disaster operations. Lessons learned from past experiences strongly emphasize on the need for effective preparedness to achieve efficient disaster response. Establishing strong strategic network for fast evacuation and on-time relief distribution are critical to the success of any emergency management endeavor. However, a primary drawback of the optimization models for decision making in emergency logistics domain is the data uncertainty. Solving deterministic models with some estimated parameter values, followed by post-optimality sensitivity analysis can only suggest the effects of data alteration on the obtained solution in a reactive fashion (Mulvey et al., 1995), but it does not recommend an implementable solution to handle the adverse situation.

Realizing the need for integrating data uncertainty in the model itself, many researchers resort to stochastic optimization (SO). Adopting a scenario-based approach, they consider scenario-indexed vectors for the uncertain parameters and

assume probabilities of each scenario occurrence. With such setting, the SO-based models attempt to minimize the expected value of some goodness measure of the solution, primarily, the expected system cost. However, in emergency logistics context, assigning probabilities a-priori to a set of anticipated, highly unpredictable future disaster scenarios resembles an attempt to assign probability to "unknowledge" (Kouvelis and Yu, 1997).

In this paper, we consider a strategic emergency response network design problem to ensure adequate relief supply to the population impacted by a hurricane-type disaster, striking any part of a long coastal region. We divide the problem into evacuation side and relief distribution side. On the evacuation side, in the wake of a hurricane, based on its predicted landfall location and category, the impact area is partially or fully evacuated. The evacuees move to the shelters and out of the remaining population staying back at the sources (if any), a certain fraction go to collect relief items from the urban distribution centers (UDC) that operates on a temporary basis. On the supply side, large central supply locations (CSL) send reliefs to the UDCs and to shelters via distribution centers (DC) well before the evacuation begins, to ensure relief availability at those locations on arrival of the people. We seek a solution that ensures fast evacuation and on time relief supply. Uncertainty in disaster location and/or intensity, incomplete knowledge of the actual number of people adhering to the original evacuation plan, affect the actual demand estimate. In spite of that, we attempt to obtain a solution that proves to be robust to such data uncertainties. Consideration of scenario and interval based uncertainty representations together is an interesting feature of our model formulation. We consider the scenarios for the occurrence of various disaster events, and interval based box uncertainties for the other data uncertainty representation. We model a two-stage problem that minimizes the sum of the cost components for the strategic and the worst case

operational decisions. The first stage decision involves locating the CSLs, while in the second stage, based on realization of one of the disaster events, our model decides which DC, shelter and UDC nodes become operative, and determines the relief- and people-flows. Observing that the location decision involved in the first stage spans relief distribution and evacuation sides, we are motivated to consider these decisions in an integrated fashion. Unlike existing humanitarian logistics literature focusing on either pre-disaster resource pre-positioning (strategic) or post-disaster evacuation or casualty transportation (operational), our work integrates both in a robust optimization setting, giving protection against various data uncertainties.

Our study contributes to the existing literature in several ways. First, in our knowledge, this is the first attempt to model a robust optimization problem using the scenario or event-based and interval-based (box) uncertainties together. Second, we develop a mixed integer linear programming (MILP) problem with a five-tier system, introduce different modes of transport with varied unit costs. The model aids an emergency manager to explore the trade-offs between relief distribution start time and the overall system cost. Third, due to modeling the robust counterpart as a two-stage problem with the objective to minimize the sum of fixed cost and the worst case scenario cost, we can apply Benders Decomposition technique and can further separate the subproblem into scenario-based individual flow problems. This decomposition enables us to solve large instances efficiently where commercial solver fails. Fourth, considering data uncertainty about the actual evacuee-fraction and stay-back population fraction going to shelter and UDC, we address the human behavior during emergency that shows deviation from the original plan. Fifth, we address another concern in emergency logistics about the timely delivery of critical relief items by including different modes of transport in our model that eventually encourages an emergency manager to start distribution early. We also address the

issue of resource stock-out by opening adequate centralized supply locations that fulfill aggregate demand under all disaster events under consideration. Finally, we demonstrate the usefulness of our proposed model by conducting a GIS based case study on Gulf coastal region, vulnerable to hurricanes. We discuss (1) the trade-offs between the system cost and time available to distribute reliefs from CSL, (2) effects of population density and disaster intensity on the solution, and (3) advantages of using robust optimization approach, based on the insights gained.

The remainder of this work is organized as follows. Section 3.2 provides a review of the related literature. We provide an overview of our problem setting, discuss different sources of data uncertainties, and justification for incorporating some problem characteristics in Section 3.3. We formally introduce the problem with notation and mathematical formulation in section 3.4. In section 3.5, we discuss our solution approach using Benders Decomposition (BD) framework, discuss acceleration approaches to solve large scale problems efficiently. We report the computational results and comparisons of the solution methodologies in section 3.6. In section 3.7, we present a GIS-based case study with numerical analysis, highlighting important managerial insights. Finally, we summarize our conclusions in section 3.8.

3.2 Related Literature

Detailed reviews of applications of optimization models on different humanitarian logistics aspects are found in the literature (e.g., Altay and Green III, 2006; Apte, 2009; Çelik et al., 2012; Caunhye et al., 2012). In this work, we focus on integrating the relief distribution side and evacuation side of emergency logistics by strategically establishing central supply locations (CSL) that are robust to uncertainties in disaster location, intensity, and demand. We categorize the related studies into three parts: (1) humanitarian logistics, (2) robust optimization, (3) robust optimization applied

to humanitarian logistics. Literature belonging to the first category are already discussed in Section 2. Therefore, we discuss here the relevant works for the categories (2) and (3).

Next, we briefly review the robust optimization (RO) literature in different logistics problem context. Gabrel et al. (2014) present a detailed review of the widely varied treatment of robustness and highlight the recent developments. For a comprehensive coverage of the RO theory and practice, we refer the reader to Kouvelis and Yu (1997), Ben-Tal et al. (2009), and Bertsimas et al. (2011). Soyster (1973) pioneers the RO concept by not relying on scenario-based uncertainty representation, thus relieving the modeler from estimating probabilities for all scenarios. His approach produces a robust solution, feasible for all data in a convex set, however, the solution is very conservative compared to the nominal (deterministic) problem. For updates on later theoretical advancements in RO that address this excessive conservatism, we refer to Ben-Tal and Nemirovski (2008); Bertsimas and Sim (2003, 2004). Bertsimas and Sim (2004) introduce polyhedral uncertainty set that allows the decision maker to fix Γ, the maximum number of coefficients in each constraint that can deviate from nominal values, and thereby, control the *price of robustness*. By altering Γ, one can exploit the trade-off between uncertainty that the model can handle, and the cost incurred due to this added capability. In Bertsimas and Sim (2003), the authors discuss the application of their proposed framework in various discrete optimization and network flow problems. In literature, data uncertainty representation can be broadly categorized into: (1) uncertainty set-based (e.g., box, ellipsoidal, polyhedral), and (2) scenario-based. In an early RO application, Gutiérrez et al. (1996) consider an uncapacitated network design problem under cost uncertainty. The authors use scenario-based uncertainty to design a robust network for any realizable scenario such that the robust solution lies within a user-specified percentage

from the true optimal solution of each scenario. They devise a multi-master Benders Decomposition (BD) algorithm, computationally superior to a brute-force approach of solving the model for each scenario by traditional BD.

Using absolute robustness criterion (Kouvelis and Yu, 1997) for worst case optimization, Atamtürk and Zhang (2007) present a two-stage robust network design and flow problem under fluctuating demand. They consider applying two types of interval based uncertainties, namely, cardinality restricted uncertainty of Bertsimas and Sim (2003) and budget uncertainty. Baron et al. (2011) consider a multi-period fixed charge network location problem to determine facility location and capacity to satisfy uncertain demand at every period while maximizing profit. The authors use both box and ellipsoidal models to represent the demand uncertainty and explain how this choice affects the outcome. Alem and Morabito (2012) apply robust optimization on a combined lot sizing and cutting stock problem following the approach of Bertsimas and Sim (2004). By developing three models, they study the effects of data uncertainties in demand, cost and both, and highlight their observations. Cacchiani et al. (2012) use a scenario-based uncertainty representation in a robust treatment of large disruptions in passenger trains. They develop a two-stage MIP model to minimize the sum of maximum deviations over all disruption scenarios and the first stage cost. Considering traffic uncertainty, Koster et al. (2013) solve a multi-commodity capacitated network problem.

Finally, we mention the research in strategic pre-disaster planning that use robust optimization to address data uncertainty. We have so far come across only two works in this category. Bozorgi-Amiri et al. (2013) present a multi-objective, robust, stochastic optimization model for location and capacity decisions of regional distribution centers (RDC) in a three-tier system of supplier, RDC, and affected area. Data uncertainties are associated with supply, demand, road network availability,

unit transportation and procurement cost. Using a scenario based approach (with known probability of each scenario) the authors model a bi-objective problem to minimize (1) total expected cost and cost-variability, and (2) sum of maximum shortage at affected demand points. Therefore, although stated as *robust*, this work applies stochastic optimization techniques. Rezaei-Malek and Tavakkoli-Moghaddam (2014) present a model with two objectives to minimize (1) average response time and (2) the sum of fixed cost, holding cost of unused supplies, and penalty cost for unsatisfied demand. This work, too, does not follow more recent robustness concepts that eliminates scenario probabilities.

In summary, we find existing works in humanitarian logistics focusing on evacuation and distribution problems, but not in an integrated fashion. Works addressing data uncertainty primarily adopt stochastic optimization, heavily relying on assumed probability valued for scenario occurrence, to minimize the expected performance measure, generally, the system cost. These models mostly consider uncertainties in demand and infrastructural availabilities (due to partial damage of road, shelter, DC). We have not yet come across any realistically detailed logistical model that consider together more than three tiers, multiple modes of transport, criticality of relief distribution start time, and explain the time and system cost interaction. In RO literature, studies exist on two-stage robust network design, but we do not yet find its application in humanitarian logistics. With these observations, we introduce a robust optimization model integrating demand and supply sides in a detailed, five-tier emergency logistics network, and ensures fast evacuation, on-time and adequate supply to the affected population, irrespective of the disaster location, intensity, and duration. Moreover, we address demand uncertainty caused by human behavior during emergency altering the estimated fraction of source population requiring reliefs. Our model adopts absolute robustness criteria to minimize the worst case system

cost, therefore, does not require probability information about the disaster events. From modeling and methodological perspectives, we contribute to the literature by demonstrating a modeling approach that allows application of decomposition-based technique and event-specific subproblem separation, thereby enabling us to solve large scale problems that are hard to solve directly by the off-the-shelf solvers. Finally, we illustrate our proposed model's practical applicability through a GIS-based case study eliciting interesting managerial insights.

3.3 Problem Setting

3.3.1 Overview

We consider a network with five entities as shown in Figure 3.1: evacuation-source, urban distribution center (UDC), shelter, distribution center (DC), and centralized storage location (CSL). We consider a large belt along a coastal region that is subject to frequent tropical storms and hurricanes. On receiving an evacuation order, all or part of the population from the impact area's sources move to the shelters. Those who stay back, may need to collect reliefs from the UDCs. CSLs supply these relief items in bulk quantities to the DCs and UDCs, which, in turn, arrive at the shelters and sources in smaller quantities. We now elaborate each entity of this network.

Source represents the habitats close to the coastal area that are highly vulnerable to catastrophic storms. Based on a threatening disaster's intensity and predicted landfall location with respect to a source, the authorities issue different levels of evacuation orders (e.g., partial/full, voluntary/mandatory). In response, a part of the population leaves that source for designated shelters, while the remaining population stays back. Except for mandatory evacuation in the wake of devastating storms, generally 100% evacuation does not take place.

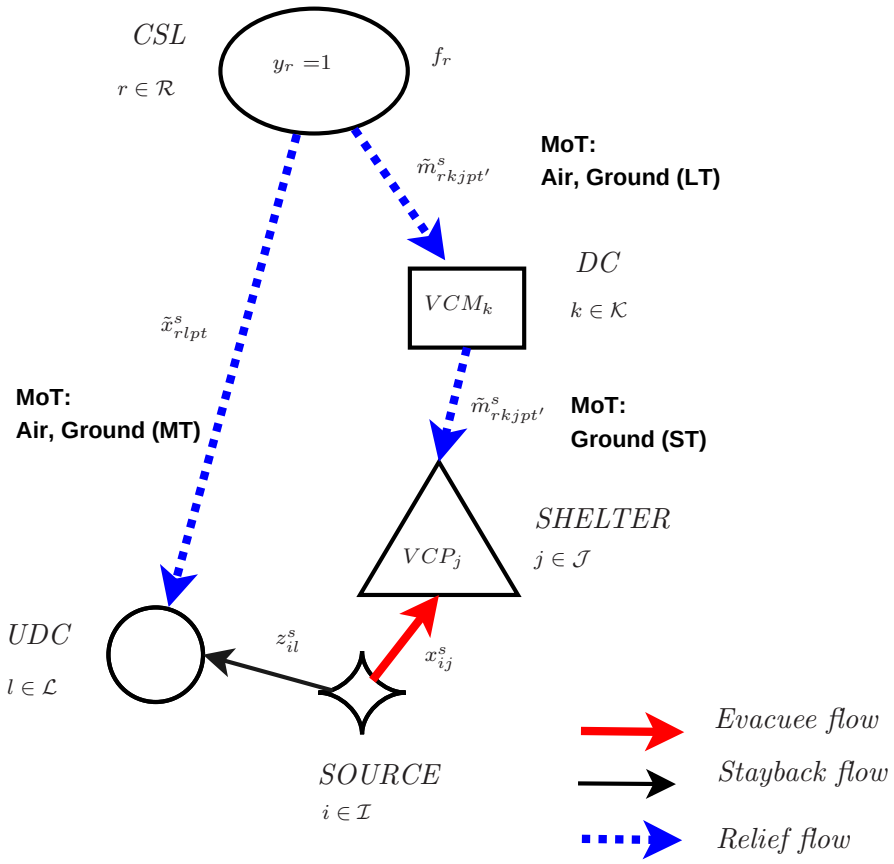

Figure 3.1: Problem Setting with Model Parameters

Part of the stay-back population can self-sufficiently survive during emergency, however, for the others, urban distribution centers (UDC) are opened at large and safe pre-existing establishments near the affected localities to distribute reliefs. These UDCs directly receive reliefs from the CSLs and have necessary manpower, space and equipment to unload and distribute the inbound air-lifted or truck-loaded bulk reliefs to the stay-back population. Since the stay-back population is responsible for going to the UDCs, those are opened reasonably close to the sources where partial/voluntary evacuation is ordered. We do not consider any UDC located close to the coastal area, because in the wake of a high intensity disaster, total evacuation

is enforced there. UDCs cater to the stay-back population because sending reliefs directly to them requires significant amount of scarce resources such as manpower and vehicles, making it logistically cost-prohibitive and inefficient choice for an emergency manager. Moreover, spacious UDCs can receive air-lifted or truck-loaded bulk supplies from CSLs, thus achieve economy of scale in inbound transportation cost. In our problem, we consider existing UDC locations and identify which ones will be operative during a disaster event, using the associated in- and out-flow quantities for a UDC node.

In the previous section, we propose an integrated Network for Emergency Evacuation and Distribution of Supplies (NEEDS) model to determine optimal locations and capacities of DCs and shelters, facilitating fast evacuation and cost-effective relief distribution. Building on this work, we assume that NEEDS model is already applied to determine the shelter and DC locations. Now, we determine which of these shelters and DCs become *operational*, and where the CSLs should be located to enable efficient response to possible disaster events with varied intensity, hitting any location along the coast. The shelters, while safely away from the coast, are located within a specified *critical distance*, the maximum allowed travel distance for any evacuee. Since construction and maintenance of dedicated shelters is not economically viable, public buildings with large accommodation capacities, such as schools, auditoriums, and stadiums are generally used as shelters during emergencies.

The DCs, with necessary manpower, storage and handling equipment to unload supplies, operate as *cross-docks* or *break-of-bulk* points between CSLs and shelters. Therefore, although geographically close to the shelters, we consider DCs as separate entities. In contrast, shelters are neither spacious nor equipped with bulk material handling capability. Similar to shelters, DCs are located at safe distances from the impacted sources.

Lastly, CSLs, large centralized warehousing facilities, stockpile relief items for the entire region under consideration. CSLs are responsible for timely supplying to any affected area along the entire coastal region. A CSL, serving the DCs and UDCs, has access to ground and air transport facilities, the latter for expedited delivery.

These five network entities are geographically located in the order of their critical role in emergency management. First, the sources of evacuation - impacted by tropical storms and hurricanes - represent the habitats located close to the coastline. Second, the UDCs are close to the affected sources, however, they function only as distribution nodes for the stay-back people during medium-to-low intensity disasters. Next, shelters are far from the impact area, and DCs, responsible to supply the shelters are farther away for safety. Finally, the CSLs, holding all the relief inventory in a centralized fashion, are located farthest from the coastal area, for their most critical role in this system.

With this underlying structure, we consider a new strategic network design problem integrating demand (evacuation) and supply (relief distribution) sides, while addressing various uncertainties associated with emergency logistics. We next discuss these various sources of uncertainty.

3.3.2 Sources of Uncertainty

We consider the following sources of uncertainties in this study.

- **Demand location :** Location and intensity of a disaster are uncertain, dictating which source nodes need evacuation and to what degree, i.e., full or partial. Based on the population density in the affected area, the number of evacuees and stay-back population can widely vary.

- **Demand at shelter :** It is difficult to accurately estimate the exact number of evacuees leaving a source for the assigned shelters.

- **Demand at UDC :** As the number of evacuees from a source is uncertain, so is the number of people who stay back at a source. Moreover, entire stay-back population do not go to UDCs to collect reliefs. The exact fraction of them who would ultimately contribute to the UDC's demand, is difficult to precisely quantify.

- **Disaster duration :** The nature of a storm cannot be predicted with 100% accuracy, leading to uncertain estimation of the number of days the evacuees need to stay at the shelters and UDCs have to distribute reliefs. For a medium or low tropical storm, a couple of days' supplies would be sufficient, but to prepare for a high category hurricane, emergency managers should consider adding larger safety stock. Thus, disaster duration uncertainty leads to demand uncertainty.

3.3.3 Importance of Centralized Storage

We consider the relief supplies pre-positioned only at the CSLs. One may argue that stockpiling at the UDCs and shelters would give the affected people faster access to the essential supplies. We now explain the reasons to consider centralized storage.

- CSL reduces wasteful, cost-prohibitive emergency management. Depending on the location and intensity of a disaster, demands are induced at the shelters and UDCs. If CSLs are not used, due to uncertainty in demand quantity and location, to ensure sufficient supply in the wake of any disaster event, all existing UDCs and shelters need stockpiling, although just a fraction of these will be operative. Moreover, from administrative perspective, keeping bulk supplies far from the impact area is preferable to avoid any hostile situation.

- CSL provides inventory aggregation benefit under demand uncertainty by serv-

ing a vast area. UDCs, shelters, and DCs are geographically tied to small regions along the coastline. Those cannot efficiently serve the evacuees outside their region because both the evacuation time and distribution cost escalate. However, the CSLs can cover multiple affected areas along the coast.

- Operating cost to aggregate relief inventory at fewer CSLs is lower than stockpiling at every UDC or shelter, although the latter ensures less expensive, faster distribution. However, in humanitarian logistics context, ignoring this operating-vs.-transportation cost trade-off, one can prioritize fast distribution over any monetary savings, and pre-position the reliefs locally. But, this decision puts the relief items, positioned close to the disaster-prone zone, under the risk of damage, causing stock-out where it is needed most. In this situation, bringing relief from other distant facilities causes delay and transportation cost increase.

- From the operational perspective, dedicated CSLs are best suited for storing bulk quantities of relief supplies as these facilities have infrastructure for storage, trained manpower for loading-unloading operations, and material handling equipments. However, UDCs and shelters are makeshift arrangements, used only during emergencies.

3.3.4 Critical Time and Modes of Transport

In our proposed model, we capture the interaction between the available time to prepare for a disaster and the choice for appropriate mode of transport, influencing the total system cost. For hurricane-like disasters that form over water and gradually move inland, the authorities get prediction about their landfall locations and intensities several days in advance. We assume that all evacuees get sufficient

time of 24 hours to prepare, and can reach their assigned shelters, located within at most 12 hour travel distance. Therefore, at the evacuation side, regular ground transportation options are adequate for the evacuees and stay-back population to reach the shelters and UDCs, respectively. However, the same is not always true for supply side.

Emergency managers should ensure the availability of reliefs at the shelters and UDCs by starting the relief movement early to avoid a situation where evacuees and stay-back people reach the shelters and UDCs, respectively, only to find that the supplies are yet to come. Moreover, to avoid a heavy traffic during the late hours due to high evacuee-flow volume, relief distribution should begin well before the evacuation order is issued.

We define *critical time* (CT) as the time in hand for the emergency managers to send reliefs to the shelters via DCs, and to the UDCs. This CT is equal to the time until a disaster strikes, less the time alloted for evacuation (24 hours). For example, if a hurricane is expected to hit a coastal area in 72 hours from now, emergency managers have 48 hours critical time to send reliefs to the shelters and UDCs.

To make the model more realistic, we consider different types of vehicles from operational perspective (see Figure 3.1). From the large CSLs, supplies are either air-lifted or moved in large trucks (LT) to the DCs. DCs have necessary infrastructure to unload these LTs and reload the small trucks (ST) heading towards shelters. We assume that the UDCs are also spacious, but not as equipped as DCs, therefore, can receive supplies air-lifted or delivered by medium size trucks (MT). Unit costs for air-lifting, ST, MT, and LT follow a decreasing order. In addition to actual travel time, the loading, transfer, and unloading jobs at the CSL, DC, and Shelter or UDC nodes take time. For example, to supply relief along $CSL \rightarrow DC \rightarrow Shelter$, total time required is computed as the sum of actual travel times along $CSL \rightarrow DC$ and

$DC \rightarrow Shelter$, and the processing times at CSLs, DCs, and Shelters.

Next, in Figure 3.2, using an influence diagram, we explain the interaction among *critical time* (CT), transportation cost, and demand uncertainty, influencing overall system cost. CT negatively influences the transportation cost. For large CT, distribution begins early, using less expensive ground transport, avoiding late hour hurry and traffic congestion. However, CT positively influences demand uncertainty. With large CT, starting distribution too early may prove counterproductive due to weather-unpredictability. The location and intensity of an impending storm can significantly alter few days before its landfall, thereby increasing the evacuees' demand uncertainty, both in terms of location and volume. In fact, a storm may not make landfall at all, but still incurs a large transportation cost. Whatever situation arises, as a protection against this increased uncertainty, an emergency manager has to deploy additional resources, that increase overall system cost. On the other hand, waiting too long for more accurate weather prediction may reduce the uncertainty about the storm's intensity and impact area, at the cost of using very expensive air transport option, thereby, increasing total system cost.

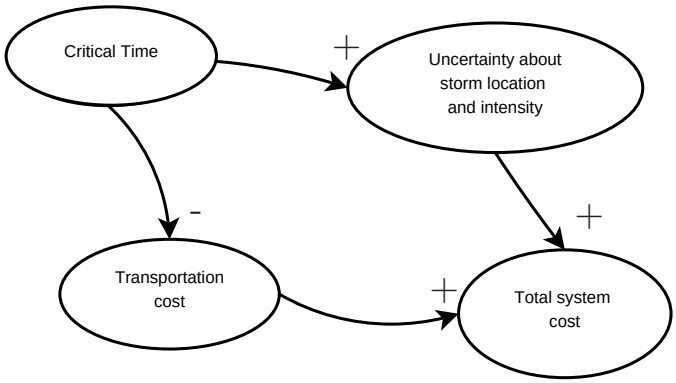

Figure 3.2: Influence Diagram

We introduce an emergency response network design problem that ensures fast evacuation and cost-effective relief supply to the affected population from strategically located centralized storages. To address various sources of uncertainties in the emergency management context (see §3.3.2), we propose a robust optimization based solution approach. We combine both the interval-based and scenario-based uncertainties in the model. Before presenting our model in §3.4, we first summarize the important **design characteristics and assumptions**.

1. Uncertainties about disaster location and intensity are presented using scenarios. Multiple events do not occur simultaneously in our study region. Other uncertain model parameters are represented by box uncertainty.
2. We consider absolute robustness criterion as our performance measure (Kouvelis and Yu, 1997). In a two-stage model, along with minimizing fixed cost of opening the CSLs, we minimize the maximum flow cost across all disaster scenarios.
3. In our multi-sourcing system, people from a source can go to multiple shelters or UDCs, a CSL can supply to multiple DCs and UDCs, and a DC can supply to multiple shelters.
4. Since UDCs operate as temporary relief distribution points, we assume those uncapacitated. An UDC neither stores relief supplies nor provides shelter to inbound people. For the same reason, we do not consider fixed cost for opening an UDC.
5. Shelters have certain accommodation capacity for the evacuees. Similarly, CSL and DC have certain capacity limit for each type of relief item. As the temperature or time sensitive items (e.g., food, vaccine, blood) require specialized storage and handling equipment, we assume a CSL's fixed cost as linear function of its capacity for different relief items.

6. We assume that all DC and shelters are already established. Our model decides which ones among them will be operative in response to different events. Therefore, we do not consider fixed cost to open DC or shelter, however, managing inbound reliefs to DCs and evacuees to shelters need manpower deployment at those facilities, thus, accrue variable costs.
7. We consider two primary modes of transport (MoT): ground and air, between different node pairs (see §3.3.4 for detailed discussion). Unit relief distribution cost varies with item type and MoT. We further assume that the processing time before any relief-carrying fleet movement is higher for air than for ground transportation due to added complexity of the former MoT.
8. Although evacuees get 24 hour time window to act, we assume that the actual source-to-shelter travel time must not exceed 12 hours, to ensure fast evacuation. Similarly, the stay-back people must not travel more than two hours to reach UDCs. Although it seems long, considering post-disaster road damage and adverse conditions, we set this two hour time as an upper limit of the stay-back people's travel time.

With all the above design characteristics and assumptions, we formulate a robust optimization based model to determine: (1) CSL location and capacity that can ensure supply during any disaster event, (2) relief flows, and (3) evacuee and stay-back population flows, for a given value of critical time. Although we do not explicitly determine which DC, shelter and UDC locations will be operative, we implicitly obtain that information from the flow values in the solution. If a DC/shelter/UDC node has no in- or out-flow, it is not operative.

3.4 Model Formulation

We consider a discrete set of disaster events that hit a long coastal region in our study area. Assigning no arbitrary probability value for each of these events as done in stochastic optimization, we attempt to obtain an absolute robust solution, recommending the optimal CSL locations that ensure cost-effective relief distribution even in the worst case in our considered set of disaster events.

3.4.1 Nominal Model

In the robust optimization literature, uncertainty is generally modeled in two ways: (a) scenario-based, with known probability of occurrence of each scenario, (b) uncertainty set based (viz., box, ellipsoidal, polyhedral). Nominal model usually refers to a deterministic model with all known parameters, and its robust counterpart incorporates the corresponding uncertainties as scenarios or augment the feasibility region. However, to include different data uncertainties in our model, we use type (a) to represent varied location and intensity of disaster events, and type (b) to model demand uncertainties in absence of the exact values for disaster duration and the people moving to shelters or UDCs. Since we want a solution that is feasible even under the worst disaster situation, we include the set of discrete events in our nominal model. However, the locations and intensities (expressed in 5-point Saffir-Simpson scale) of the disasters, and the demands induced by those, remain deterministic in the nominal model. We first introduce the notation.

Sets and Indices

$\mathcal{I}$	Set of sources of evacuation, $i \in \mathcal{I}$
$\mathcal{J}$	Set of existing shelter locations, $j \in \mathcal{J}$
$\mathcal{K}$	Set of existing DC locations, $k \in \mathcal{K}$
$\mathcal{L}$	Set of existing urban DC (UDC) locations, $l \in \mathcal{L}$
$\mathcal{R}$	Set of candidate central supply locations (CSL), $r \in \mathcal{R}$
$\mathcal{P}$	Set of relief supplies for the evacuees, $p \in \mathcal{P}$
Θ	Set of MoTs , $t \in \Theta = \{Air, Ground\}$
Θ'	Set of MoTs along the CSL $\rightarrow$ DC $\rightarrow$ shelter paths, $t' \in \Theta' = \{Mixed, Ground\}$
$\mathcal{S}$	Set of disaster events, $s \in \mathcal{S}$

Model Parameters

pop_i	Population at source $i \in \mathcal{I}$
$\bar{\phi}_{is}$	Nominal population fraction of source i evacuating during $s \in \mathcal{S}$
$\bar{\lambda}_{is}$	Nominal stay-back fraction at source $i \in \mathcal{I}$ need relief during $s \in \mathcal{S}$
$\bar{D}_s$	Nominal duration of disaster $s \in \mathcal{S}$ (days)
ω_p	Relief item $p \in \mathcal{P}$ needed for a person, per day (units/person-day)
Q_j^{SH}	Shelter capacity at location $j \in \mathcal{J}$ (persons)
Q_{kp}^{DC}	DC capacity at $k \in \mathcal{K}$ for storing relief $p \in \mathcal{P}$ (units)
Q_{rp}^{CSL}	CSL capacity at $r \in \mathcal{R}$ for storing relief $p \in \mathcal{P}$ (units)
VCM_k	Variable cost to handle relief items at DC $k \in \mathcal{K}$ (\$ / unit)
VCP_j	Variable cost for evacuees in a shelter at $j \in \mathcal{J}$ (\$/person)
f_r	Fixed cost for opening a CSL at location $r \in \mathcal{R}$
d_{ij}	Distance from a node $i \in \mathcal{I} \cup \mathcal{K} \cup \mathcal{R}$ to node $j \in \mathcal{J} \cup \mathcal{K} \cup \mathcal{L}$
α	Transportation cost to move one person by unit distance (\$/person-mile)
c_{ij}	$:= \alpha\ d_{ij}$, Unit transportation cost for people from $i \in \mathcal{I}$ to $j \in \mathcal{J} \cup \mathcal{L}$

β_{pt}	Unit transportation cost for relief $p \in \mathcal{P}$ using MoT $t \in \Theta$ (\$/unit-mile)
$\tilde{c}_{rlpt}$	$:= \beta_{pt}\ d_{rl}$, unit cost to send relief $p \in \mathcal{P}$ from node $r \in \mathcal{R}$ to node $l \in \mathcal{L}$ using MoT $t \in \Theta$
$\tilde{c}_{rkjpt'}$	$:= \beta_{pt'}\ (d_{rk} + d_{kj})$, unit cost for sending relief $p \in \mathcal{P}$ from $r \in \mathcal{R}$ to $l \in \mathcal{L}$ using MoT $t' \in \Theta'$
P^t	fleet preparation time to transport reliefs using MoT $t \in \Theta$
V_t	Average speed of a fleet movement by MoT $t \in \Theta$
Γ	Critical Time.

Based on discrete event set $\mathcal{S}$, we measure the impact of each $s \in \mathcal{S}$ on a source $i \in \mathcal{I}$ in terms of ϕ_{is}, the evacuating fraction of total population at i. For this, we first define a distance factor DF_{is} to capture the impact of event s on source i as follows:

$$DF_{is} = \begin{cases} 1, & d_{is} \leq 20 \text{ units} \\ 0.8, & 20 < d_{is} \leq 40 \text{ units} \\ 0.5, & 40 < d_{is} \leq 50 \text{ units} \\ 0 & d_{is} > 50 \text{ units.} \end{cases}$$

where d_{is} is the distance between source $i \in \mathcal{I}$ and estimated landfall location of $s \in \mathcal{S}$. Now, only for the non-zero values of DF_{is}, using weights W_1 and W_2, we calculate ϕ_{is} as the weighted sum of distance factor and intensity ($Catg_s \in [1, 5]$) as follows:

$$\phi_{is} = W_1\ DF_{is} + W_2 \frac{Catg_s}{5} \mathbb{1}_{(DF_{is}>0)} \qquad \forall i \in \mathcal{I}, \forall s \in \mathcal{S}. \tag{3.1}$$

Next, we construct an indicator matrix $[\tilde{a}_{rkjt'}]$ to identify the directed paths $r \to k \to j$ connecting CSL r to shelter j via DC k, accessible within critical time Γ using

either *Mixed* (Air, Ground) or *Ground* MoT as follows:

$$\tilde{a}_{rkjt'} = \begin{cases} 1, & (P^{Air} + \frac{d_{rk}}{V_{Air}} + P^{Ground} + \frac{d_{kj}}{V_{Ground}}) \leq \Gamma, \text{ when } t' = Mixed \\ 1, & (\frac{(d_{rk}+d_{kj})}{V_{Ground}} + 2P^{Ground}) \leq \Gamma, \text{ when } t' = Ground \\ 0, & otherwise. \end{cases}$$

Similarly, accessible (r, l) links are identified by constructing matrix $[\tilde{b}_{rlt}]$ as follows:

$$\tilde{b}_{rlt} = \begin{cases} 1, & (P^t + \frac{d_{rl}}{V_t}) \leq \Gamma, \qquad t \in \Theta \\ 0, & otherwise. \end{cases}$$

Furthermore, for each source i, we also identify the UDCs l and shelters j within 2-hour and 12-hour travel distances, and construct the respective indicator matrices $[a_{ij}]$ and $[b_{il}]$:

$$a_{ij} = \begin{cases} 1, & \frac{d_{ij}}{V_t} \leq 12 \text{ hour}, t = Ground \\ 0, & otherwise. \end{cases} \qquad b_{il} = \begin{cases} 1, & \frac{d_{il}}{V_t} \leq 2 \text{ hour}, t = Ground \\ 0, & otherwise. \end{cases}$$

Decision Variables

x^s_{ij}	fraction of people from source $i \in \mathcal{I}$ going to shelter $j \in \mathcal{J}$ during $s \in \mathcal{S}$
z^s_{il}	fraction of people stay-back at $i \in \mathcal{I}$, get relief from UDC $l \in \mathcal{L}$ in $s \in \mathcal{S}$
$\tilde{m}^s_{rkjpt'}$	Units of relief $p \in \mathcal{P}$ shipped from CSL $r \in \mathcal{R}$, distributed by DC $k \in \mathcal{K}$, to shelter $j \in \mathcal{J}$ using $t' \in \Theta'$ during $s \in \mathcal{S}$
$\tilde{x}^s_{rlpt}$	Units of relief $p \in \mathcal{P}$ shipped from CSL $r \in \mathcal{R}$ to UDC $l \in \mathcal{L}$ using $t \in \Theta$ during $s \in \mathcal{S}$
y_r	1, if CSL opens at $r \in \mathcal{R}, 0$ otherwise.

We consider a two-stage model to design an emergency response network that ensures adequate relief supply for the affected population under any event realization. With the absolute robustness criteria, we minimize the sum of: (1) fixed cost to open CSLs, and (2) maximum of the flow costs (due to evacuation and relief distribution) across all discrete disaster events $s \in \mathcal{S}$, for available critical time Γ . We present the nominal problem P(Γ) as follows.

$$\begin{aligned}\text{P}(\Gamma)\ \text{Min}\ Z = \sum_{r\in\mathcal{R}} f_r y_r + \max_{s\in\mathcal{S}}\{&\sum_{i\in\mathcal{I}}\sum_{j\in\mathcal{J}} c_{ij} pop_i a_{ij} x^s_{ij} + \sum_{i\in\mathcal{I}}\sum_{l\in\mathcal{L}} c_{il} pop_i b_{il} z^s_{il} \\ &+ \sum_{r\in\mathcal{R}}\sum_{l\in\mathcal{L}}\sum_{p\in\mathcal{P}}\sum_{t\in\Theta} \tilde{c}_{rlpt}\tilde{b}_{rlt}\tilde{x}^s_{rlpt} + \sum_{r\in\mathcal{R}}\sum_{k\in\mathcal{K}}\sum_{j\in\mathcal{J}}\sum_{p\in\mathcal{P}}\sum_{t'\in\Theta'} \tilde{c}_{rkjpt'}\tilde{a}_{rkjt'}\tilde{m}^s_{rkjpt'} \\ &+ \sum_{i\in\mathcal{I}}\sum_{j\in\mathcal{J}} VCP_j pop_i a_{ij} x^s_{ij} + \sum_{r\in\mathcal{R}}\sum_{k\in\mathcal{K}}\sum_{j\in\mathcal{J}}\sum_{p\in\mathcal{P}}\sum_{t'\in\Theta'} VCM_k \tilde{a}_{rkjt'}\tilde{m}^s_{rkjpt'}\} \quad (3.2)\end{aligned}$$

subject to

$$\sum_{j\in\mathcal{J}} a_{ij} x^s_{ij} \geq \bar{\phi}_{is} \qquad \forall i \in \mathcal{I},\ \forall s \in \mathcal{S} \qquad (3.3)$$

$$\sum_{l\in\mathcal{L}} b_{il} z^s_{il} \geq (1-\bar{\phi}_{is})\bar{\lambda}_{is} \qquad \forall i \in \mathcal{I},\ \forall s \in \mathcal{S} \qquad (3.4)$$

$$\sum_{r\in\mathcal{R}}\sum_{k\in\mathcal{K}}\sum_{t'\in\Theta'} \tilde{a}_{rkjt'}\tilde{m}^s_{rkjpt'} \geq \bar{D}^s\omega_p \sum_{i\in\mathcal{I}} pop_i x^s_{ij} \qquad \forall j \in \mathcal{J},\ \forall p \in \mathcal{P},\ \forall s \in \mathcal{S} \qquad (3.5)$$

$$\sum_{r\in\mathcal{R}}\sum_{t\in\Theta} \tilde{b}_{rlt}\tilde{x}^s_{rlpt} \geq \bar{D}^s\omega_p \sum_{i\in\mathcal{I}} pop_i z^s_{il} \qquad \forall l \in \mathcal{L},\ \forall p \in \mathcal{P},\ \forall s \in \mathcal{S} \qquad (3.6)$$

$$\sum_{i\in\mathcal{I}} pop_i a_{ij} x^s_{ij} \leq Q^{SH}_j \qquad \forall j \in \mathcal{J},\ \forall s \in \mathcal{S} \qquad (3.7)$$

$$\sum_{r\in\mathcal{R}}\sum_{j\in\mathcal{J}}\sum_{t'\in\Theta'} \tilde{a}_{rkjt'}\tilde{m}^s_{rkjpt'} \leq Q^{DC}_{kp} \qquad \forall k \in \mathcal{K},\ \forall p \in \mathcal{P},\ \forall s \in \mathcal{S} \qquad (3.8)$$

$$\sum_{k\in\mathcal{K}}\sum_{j\in\mathcal{J}}\sum_{t'\in\Theta'}\tilde{a}_{rkjt'}\tilde{m}^s_{rkjpt'}+\sum_{l\in\mathcal{L}}\sum_{t\in\Theta}\tilde{b}_{rlt}\tilde{x}^s_{rlpt}\le Q^{CSL}_{rp}y_r \quad \forall r\in\mathcal{R},\,\forall p\in\mathcal{P},\,\forall s\in\mathcal{S} \tag{3.9}$$

$$\sum_{r\in\mathcal{R}}Q^{CSL}_{rp}y_r\ge\bar{D}^s\omega_p\sum_{i\in\mathcal{I}}pop_i(\bar{\phi}_{is}+(1-\bar{\phi}_{is})\bar{\lambda}_{is}) \qquad \forall p\in\mathcal{P},\,\forall s\in\mathcal{S} \tag{3.10}$$

$$\sum_{r\in\mathcal{R}}\sum_{t\in\Theta}\tilde{b}_{rlt}y_r\ge 1 \qquad \forall l\in\mathcal{L} \tag{3.11}$$

$$\sum_{r\in\mathcal{R}}\sum_{k\in\mathcal{K}}\sum_{t'\in\Theta'}\tilde{a}_{rkjt'}y_r\ge 1 \qquad \forall j\in\mathcal{J} \tag{3.12}$$

$$0\le x^s_{ij}\le 1,\;\; 0\le z^s_{il}\le 1,\;\; y_r\in\{0,1\} \qquad \forall i\in\mathcal{I},\forall j\in\mathcal{J},\forall l\in\mathcal{L},\forall r\in\mathcal{R},\forall s\in\mathcal{S} \tag{3.13}$$

$$\tilde{x}^s_{rlpt},\tilde{m}^s_{rkjpt'}\ge 0 \qquad \forall r\in\mathcal{R},\forall k\in\mathcal{K},\forall j\in\mathcal{J},\forall l\in\mathcal{L},\forall p\in\mathcal{P},\;\forall t\in\Theta,\forall t'\in\Theta',\forall s\in\mathcal{S}. \tag{3.14}$$

In the objective function (3.2) of problem P(Γ), we minimize sum of: (i) the strategic cost to open the CSLs, and (ii) the maximum of the operational costs, incurred during the disaster events, to distribute supplies from CSLs down to the shelters and UDCs. The first two terms in the minimax part of the objective comprises evacuees' and stay-back population's transportation cost. The third term is the relief distribution cost from CSL to UDC. The fourth term is the relief distribution cost from CSL to shelter via DC. The last two terms express the variable costs incurred at shelters and DCs due to evacuee and supply flows, respectively. The evacuees' demand constraint set (3.3) ensures that for each source i and each event s, the nominal volume of the evacuees must be accommodated at some shelters in set $\mathcal{J}$. Similarly, (3.4) ensures that the population staying back at i who require

relief supply, are allocated to some open UDC in set $\mathcal{L}$. The demand constraint (3.5) ensures that the aggregate relief inflow to a shelter is sufficient to fulfill the aggregate demand of the inbound evacuees. Its left hand side represents the aggregate flow of a relief item p to the shelter j through any feasible path $r \rightarrow k \rightarrow j$ (indicated by binary parameter $\tilde{a}_{rkjt'}$) connecting CSL to shelter via DC, using MoT t' when the disaster event s occurs. The right hand side of (3.5) represents the aggregate demand for relief p at the shelter j due to evacuee-inflow during the event s. Similarly, constraint (3.6) ensures that total supply of item p from CSLs to a UDC l during event s using any MoT t, is sufficient to fulfill the stay-back population's aggregate demand. Constraint sets (3.7), (3.8), and (3.9) represent the shelter, DC, and CSL capacities, respectively. We add surrogate constraint (3.10) to force opening sufficient number of CSLs to satisfy total demand of the evacuees and stay-back population. Next, surrogate constraints (3.11) and (3.12) are added to ensure that for each UDC and each shelter, at least one CSL must open at a location that can send supplies within the critical time Γ. Finally, constraints (3.13) - (3.14) state the variable range requirements.

If all the parameters of problem P(Γ) are known, we solve the nominal model as a deterministic MIP problem to obtain the strategic CSL locations that can send supplies cost-effectively within critical time Γ to any area affected by a disaster event $s \in \mathcal{S}$. However, in presence of data uncertainty, CSL locations obtained from this nominal solution are no longer optimal, even may be infeasible for some disaster event. Therefore, we derive the robust counterpart (ROC) of the problem P(Γ), mentioned hereafter as ROCP(Γ), considering different uncertainty sources (see §3.3.2).

Bertsimas and Sim (2004) suggest removing over-conservatism by balancing robustness and performance by allowing a predetermined number of uncertain coeffi-

cients to deviate from their nominal values. Though it makes sense for many real world problems, where all uncertain parameters do not reach extreme values simultaneously, in the emergency logistics context, it is advisable to be conservative than putting human lives at risk. Therefore, we choose to consider simultaneous attainment of extreme values for all uncertain parameters in ROCP model.

Shelter demand uncertainty: The exact fraction of the evacuees leaving a source i during an event s is an uncertain parameter. To model this uncertainty, we consider the random variable $\tilde{\phi}_{is}$, $i \in \mathcal{I}, s \in \mathcal{S}$, bounded by a symmetric interval around its nominal value $\bar{\phi}_{is}$, i.e., $\tilde{\phi}_{is} \in [\bar{\phi}_{is}(1-\epsilon_1), \bar{\phi}_{is}(1+\epsilon_1)]$, where $\epsilon_1 \in [0,1]$ is the uncertainty measure in the evacuee-fraction estimate. The ROC of (3.3) should ensure that even the maximum of the RHS does not violate the constraint. For this, we substitute the nominal term $\bar{\phi}_{is}$ in RHS by the random variable $\tilde{\phi}_{is}$ which is constrained as $\tilde{\phi}_{is} \in \mathcal{U}_1^{Box} = \bar{\phi}_{is}[1 \pm \epsilon_1]$ and obtain the ROC of (3.3) as follows:

$$\sum_{j \in \mathcal{J}} a_{ij} x_{ij}^s \geq \max_{\tilde{\phi}_{is} \in \mathcal{U}_1^{Box}} \{\tilde{\phi}_{is}\} \qquad \forall i \in \mathcal{I}, \forall s \in \mathcal{S}.$$

Since $\tilde{\phi}_{is} \geq 0$, the optimal solution to the RHS problem is $\tilde{\phi}_{is}^* = \bar{\phi}_{is}(1+\epsilon_1)$. Note, if using equation (3.1) we obtain $\bar{\phi}_{is} = 1$, i.e., source i is 100% evacuated when s occurs, then no uncertainty remains about the number of evacuees from source i, making $\epsilon_1 = 0$. However, to avoid the RHS exceeding 1 as the product of some $\bar{\phi}_{is}$ value close to 1 and a large ϵ_1, final form of constraint (3.3) is as follows:

$$\sum_{j \in \mathcal{J}} a_{ij} x_{ij}^s \geq \min \{1, \bar{\phi}_{is}(1+\epsilon_1)\} \qquad \forall i \in \mathcal{I}, \forall s \in \mathcal{S}. \tag{3.15}$$

UDC demand uncertainty: Among the stay-back population at source i, everyone does not depend on UDC for relief. However, an exact fraction of this

population who depend, is difficult to estimate. With respect to an event $s \in \mathcal{S}$ with low intensity and/or distant landfall location, if ϕ_{is} is calculated as 0 by equation (3.1), then nobody evacuates i, and obviously, no one needs supply from UDC. Therefore, we define the fraction of stay-back population visiting UDC by a random variable $\tilde{\lambda}_{is} \in \bar{\lambda}_{is}[1 \pm \epsilon_2]$ if $\tilde{\phi_{is}} > 0, \forall i \in \mathcal{I}\ \forall s \in \mathcal{S}$, and 0 otherwise. Thus, $\tilde{\lambda}_{is}$ is bounded around its nominal value $\bar{\lambda}_{is}$ by a symmetric uncertainty box $\mathcal{U}_2^{Box} = \bar{\lambda}_{is}[1 \pm \epsilon_2], 0 \leq \epsilon_2 \leq 1$. Now ROC of constraint (3.4) becomes

$$\sum_{l \in \mathcal{L}} b_{il} z_{il}^s \geq \max_{\substack{\tilde{\phi}_{is} \in \mathcal{U}_1^{Box} \\ \tilde{\lambda}_{is} \in \mathcal{U}_2^{Box}}} (1 - \tilde{\phi}_{is})\tilde{\lambda_{is}} \qquad \forall i \in \mathcal{I},\ \forall s \in \mathcal{S}.$$

Since random variables $\tilde{\phi}_{is}$ and $\tilde{\lambda}_{is}$ are independent, we can solve the RHS optimization problem by considering the maximizers of each term in the product as $(1 - \bar{\phi}_{is}(1 - \epsilon_1))$ and $\bar{\lambda}_{is}(1 + \epsilon_2)$, respectively. Again, since the maximum possible value of RHS is 1, the final form of the ROC of constraint (3.4) is as follows:

$$\sum_{l \in \mathcal{L}} b_{il} z_{il}^s \geq \ \min\ \{1, (1 - \bar{\phi}_{is}(1 - \epsilon_1))\bar{\lambda}_{is}(1 + \epsilon_2)\} \qquad \forall i \in \mathcal{I},\ \forall s \in \mathcal{S}. \tag{3.16}$$

Observe, when a source i is fully evacuated, i.e., $\bar{\phi}_{is} = 1$, and ϵ_1 becomes zero, the RHS also reduces to zero.

Disaster duration uncertainty: We assume that the need to stay at the shelters or collect relief supplies from UDCs depends on the disaster's intensity. For simplicity, we assume that for any storm in category 4-5, 2-3, and 1 or below, we keep the provision for four, two, and one days' supply, respectively. However, the model parameter value for disaster duration is a sheer estimate. Therefore, we consider a random variable $\tilde{D}_s \in \mathcal{U}_3^{Box} = \bar{D}_s[1 \pm \epsilon_3], 0 \leq \epsilon_3 \leq 1$, having box uncertainty around its nominal value $\bar{D}_s$. Using the same procedure explained before, we obtain

ROCs of the constraints (3.5) and (3.6) as (3.17) and (3.18), respectively. Note, since the constraints (3.5) and (3.6) have non-negative RHS terms, their maximizers are simply $\tilde{D}^*_s = \bar{D}^s(1+\epsilon_3)$.

$$\sum_{r\in\mathcal{R}}\sum_{k\in\mathcal{K}}\sum_{t'\in\Theta'}\tilde{a}_{rkjt'}\tilde{m}^s_{rkjpt'} \geq \bar{D}^s(1+\epsilon_3)\omega_p\sum_{i\in\mathcal{I}}pop_i a_{ij}x^s_{ij} \qquad \forall j\in\mathcal{J},\ \forall p\in\mathcal{P},\ \forall s\in\mathcal{S}. \tag{3.17}$$

$$\sum_{r\in\mathcal{R}}\sum_{t\in\Theta}\tilde{b}_{rlt}\tilde{x}^s_{rlpt} \geq \bar{D}^s(1+\epsilon_3)\omega_p\sum_{i\in\mathcal{I}}pop_i b_{il}z^s_{il} \qquad \forall l\in\mathcal{L},\ \forall p\in\mathcal{P},\ \forall s\in\mathcal{S}. \tag{3.18}$$

Finally, we observe that the surrogate constraint set (3.10) contains all the above mentioned uncertain parameters in the RHS. With box uncertainties around each random variable associated with these uncertain parameters, we present the ROC of the constraint (3.10) as follows:

$$\sum_{r\in\mathcal{R}}Q^{CSL}_{rp}y_r \geq \max_{\substack{\tilde{\phi}_{is}\in\mathcal{U}_1^{Box}\\ \tilde{\lambda}_{is}\in\mathcal{U}_2^{Box}\\ \tilde{D}_s\in\mathcal{U}_3^{Box}}} \omega_p\tilde{D}^s\sum_{i\in\mathcal{I}}pop_i(\tilde{\phi}_{is}+(1-\tilde{\phi}_{is})\tilde{\lambda}_{is}) \qquad \forall p\in\mathcal{P},\ \forall s\in\mathcal{S}.$$

On solving the optimization problem in the RHS, we obtain the following final form:

$$\sum_{r\in\mathcal{R}}Q^{CSL}_{rp}y_r \geq \omega_p\bar{D}^s(1+\epsilon_3)\sum_{i\in\mathcal{I}}pop_i\{\bar{\phi}_{is}(1+\epsilon_1)+(1-\bar{\phi}_{is}(1-\epsilon_1))\bar{\lambda}_{is}(1+\epsilon_2)\} = \omega_p\Upsilon_s$$
$$\forall p\in\mathcal{P},\ \forall s\in\mathcal{S}. \tag{3.19}$$

Therefore, ROCP(Γ), the robust counterpart of our original problem P(Γ) becomes:

$$\text{ROCP}(\Gamma)\ \text{Min}\ Z$$

$$\text{subject to} \qquad (3.7)\text{ - }(3.9), (3.11)\text{ - }(3.19).$$

We simplify the ROCP(Γ) objective's minimax part by converting it to minimization-type (3.20) by introducing an auxiliary variable $\rho \geq 0$:

$$\text{Min } Z = \sum_{r \in \mathcal{R}} f_r y_r + \rho \tag{3.20}$$

subject to

$$\sum_{i \in \mathcal{I}} \sum_{j \in \mathcal{J}} c_{ij} pop_i a_{ij} x^s_{ij} + \sum_{i \in \mathcal{I}} \sum_{l \in \mathcal{L}} c_{il} pop_i b_{il} z^s_{il} + \sum_{r \in \mathcal{R}} \sum_{l \in \mathcal{L}} \sum_{p \in \mathcal{P}} \sum_{t \in \Theta} \tilde{c}_{rlpt} \tilde{b}_{rlt} \tilde{x}^s_{rlpt}$$
$$+ \sum_{r \in \mathcal{R}} \sum_{k \in \mathcal{K}} \sum_{j \in \mathcal{J}} \sum_{p \in \mathcal{P}} \sum_{t' \in \Theta'} \tilde{c}_{rkjpt'} \tilde{a}_{rkjt'} \tilde{m}^s_{rkjpt'} + \sum_{i \in \mathcal{I}} \sum_{j \in \mathcal{J}} VCP_j pop_i a_{ij} x^s_{ij}$$
$$+ \sum_{r \in \mathcal{R}} \sum_{k \in \mathcal{K}} \sum_{j \in \mathcal{J}} \sum_{p \in \mathcal{P}} \sum_{t' \in \Theta'} VCM_k \tilde{a}_{rkjt'} \tilde{m}^s_{rkjpt'} \leq \rho \qquad \forall s \in \mathcal{S} \tag{3.21}$$

$$(3.7) \text{ - } (3.9), (3.11) \text{ - } (3.19).$$

.

3.5 Solution Approaches

3.5.1 Benders Decomposition Framework

Solving large instances of the mixed integer programming (MIP) model ROCP(Γ) is computationally challenging. Presence of the minimax term in the objective also adds to this difficulty. However, if we consider that the strategic decision has already been taken in terms of the binary variables y_r, then the remaining model becomes an easily solvable LP. Therefore, Benders Decomposition (BD) can be employed to solve the large instances of ROCP(Γ). In BD, we split the overall problem into a master problem (**MP**) and a subproblem (**SP**), and then solve it by transferring one-another's solution within an iterative framework. Moreover, we observe that all constraints are separable over the discrete events $s \in \mathcal{S}$. Exploiting this structural

property of ROCP(Γ), we can further decompose the **SP** into $|\mathcal{S}|$ independent smaller subproblems, one for each $s \in \mathcal{S}$. Note that the number of surrogate constraints in (3.19) can be reduced from $|\mathcal{P}| \times |\mathcal{S}|$ to $|\mathcal{P}|$ by taking the maximum of the RHS over all s, for each p, thereby, reducing the **MP** size.

3.5.1.1 Benders Subproblem and its Dual

For the given binary vector $\widehat{\mathbf{y}}$ representing the open CSLs, we obtain the LP called primal subproblem or $\mathbf{PSP}(\mathbf{x}, \mathbf{z}, \tilde{\mathbf{x}}, \tilde{\mathbf{m}} | \widehat{\mathbf{y}})$. Since **PSP** constraints are completely separable over events $s \in \mathcal{S}$, we can solve a problem $\mathbf{PSP}^s$ for each event separately. The $\widehat{\mathbf{y}}$ vector for each $\mathbf{PSP}^s$ comes by solving the model **MP** as explained in §3.5.1.2. The $\mathbf{PSP}^s$ is as follows:

$$\begin{aligned}\text{Min } \mathbf{Z}_{\text{PSP}^s} = &\sum_{i\in\mathcal{I}}\sum_{j\in\mathcal{J}} c_{ij} pop_i a_{ij} x^s_{ij} + \sum_{i\in\mathcal{I}}\sum_{l\in\mathcal{L}} c_{il} pop_i b_{il} z^s_{il} + \sum_{r\in\mathcal{R}}\sum_{l\in\mathcal{L}}\sum_{p\in\mathcal{P}}\sum_{t\in\Theta} \tilde{c}_{rlpt}\tilde{b}_{rlt}\tilde{x}^s_{rlpt} \\ &+ \sum_{r\in\mathcal{R}}\sum_{k\in\mathcal{K}}\sum_{j\in\mathcal{J}}\sum_{p\in\mathcal{P}}\sum_{t'\in\Theta'} \tilde{c}_{rkjpt'}\tilde{a}_{rkjt'}\tilde{m}^s_{rkjpt'} + \sum_{i\in\mathcal{I}}\sum_{j\in\mathcal{J}} VCP_j pop_i a_{ij} x^s_{ij} \\ &+ \sum_{r\in\mathcal{R}}\sum_{k\in\mathcal{K}}\sum_{j\in\mathcal{J}}\sum_{p\in\mathcal{P}}\sum_{t'\in\Theta'} VCM_k \tilde{a}_{rkjt'}\tilde{m}^s_{rkjpt'} \quad (3.22)\end{aligned}$$

subject to

$$a_{ij} x^s_{ij} \le 1 \qquad \forall i \in \mathcal{I}, \forall j \in \mathcal{J} \quad (3.23)$$

$$b_{il} z^s_{il} \le 1 \qquad \forall i \in \mathcal{I}, \forall l \in \mathcal{L} \quad (3.24)$$

$$\sum_{j\in\mathcal{J}} a_{ij} x^s_{ij} \ge \min\{1, \bar{\phi}_{is}(1+\epsilon_1)\} \qquad \forall i \in \mathcal{I} \quad (3.25)$$

$$\sum_{l\in\mathcal{L}} b_{il} z^s_{il} \ge \min\{1, (1-\bar{\phi}_{is}(1-\epsilon_1))\bar{\lambda}_{is}(1+\epsilon_2)\} \qquad \forall i \in \mathcal{I} \quad (3.26)$$

$$\sum_{r\in\mathcal{R}}\sum_{k\in\mathcal{K}}\sum_{t'\in\Theta'} \tilde{a}_{rkjt'}\tilde{m}^s_{rkjpt'} \ge \bar{D}^s(1+\epsilon_3)\omega_p \sum_{i\in\mathcal{I}} pop_i a_{ij} x^s_{ij} \qquad \forall j \in \mathcal{J}, \forall p \in \mathcal{P} \quad (3.27)$$

$$\sum_{r\in\mathcal{R}}\sum_{t\in\Theta}\tilde{b}_{rlt}\tilde{x}^s_{rlpt} \geq \bar{D}^s(1+\epsilon_3)\omega_p\sum_{i\in\mathcal{I}}pop_i b_{il}z^s_{il} \qquad \forall l\in\mathcal{L},\,\forall p\in\mathcal{P} \qquad (3.28)$$

$$\sum_{i\in\mathcal{I}}pop_i a_{ij}x^s_{ij} \leq Q^{SH}_j \qquad \forall j\in\mathcal{J} \qquad (3.29)$$

$$\sum_{r\in\mathcal{R}}\sum_{j\in\mathcal{J}}\sum_{t'\in\Theta'}\tilde{a}_{rkjt'}\tilde{m}^s_{rkjpt'} \leq Q^{DC}_{kp} \qquad \forall k\in\mathcal{K},\,\forall p\in\mathcal{P} \qquad (3.30)$$

$$\sum_{k\in\mathcal{K}}\sum_{j\in\mathcal{J}}\sum_{t'\in\Theta'}\tilde{a}_{rkjt'}\tilde{m}^s_{rkjpt'} + \sum_{l\in\mathcal{L}}\sum_{t\in\Theta}\tilde{b}_{rlt}\tilde{x}^s_{rlpt} \leq Q^{CSL}_{rp}\widehat{y}_r \qquad \forall r\in\mathcal{R},\,\forall p\in\mathcal{P} \qquad (3.31)$$

$$x^s_{ij}, z^s_{il}, \tilde{x}^s_{rlpt}, \tilde{m}^s_{rkjpt'} \geq 0 \qquad \forall r\in\mathcal{R},\forall k\in\mathcal{K},\forall j\in\mathcal{J},\forall l\in\mathcal{L},\forall p\in\mathcal{P},\forall t\in\Theta,\forall t'\in\Theta'. \qquad (3.32)$$

Defining dual vectors $\boldsymbol{\tau}, \boldsymbol{\psi}, \boldsymbol{\kappa}, \boldsymbol{\eta}, \boldsymbol{\gamma}, \boldsymbol{\delta}, \boldsymbol{\pi}, \boldsymbol{\theta}, \boldsymbol{\mu}$ associated with the constraints (3.23) - (3.31), respectively, we obtain the $\mathbf{DSP}^s(\boldsymbol{\tau}, \boldsymbol{\psi}, \boldsymbol{\kappa}, \boldsymbol{\eta}, \boldsymbol{\gamma}, \boldsymbol{\delta}, \boldsymbol{\pi}, \boldsymbol{\theta}, \boldsymbol{\mu}|\widehat{\mathbf{y}})$ as follows:

$$\begin{aligned}\text{Max } \mathbf{Z}_{\text{DSP}^s} = &\sum_{i\in\mathcal{I}}\sum_{j\in\mathcal{J}}\tau^s_{ij} + \sum_{i\in\mathcal{I}}\sum_{l\in\mathcal{L}}\psi^s_{il} + \sum_{i\in\mathcal{I}}\min\{1, \bar{\phi}_{is}(1+\epsilon_1)\}\kappa^s_i \\ &+ \sum_{i\in\mathcal{I}}\min\{1, (1-\bar{\phi}_{is}(1-\epsilon_1))\bar{\lambda}_{is}(1+\epsilon_2)\eta^s_i + \sum_{j\in\mathcal{J}}Q^{SH}_j\pi^s_j \\ &+ \sum_{k\in\mathcal{K}}\sum_{p\in\mathcal{P}}Q^{DC}_{kp}\theta^s_{kp} + \sum_{r\in\mathcal{R}}\sum_{p\in\mathcal{P}}Q^{CSL}_{rp}\widehat{y}_r\mu^s_{rp} \qquad (3.33)\end{aligned}$$

subject to

$$\tau^s_{ij}+\kappa^s_i-\bar{D}_s(1+\epsilon_3)pop_i\sum_{p\in\mathcal{P}}\omega_p\gamma^s_{jp}+pop_i\pi^s_j \leq pop_i(c_{ij}+VCP_j) \qquad \forall i\in\mathcal{I},\forall j\in\mathcal{J} \qquad (3.34)$$

$$\psi^s_{il}+\eta^s_i-\bar{D}_s(1+\epsilon_3)pop_i\sum_{p\in\mathcal{P}}\omega_p\delta^s_{lp} \leq c_{il}pop_i \qquad \forall i\in\mathcal{I},\forall l\in\mathcal{L} \qquad (3.35)$$

$$\gamma^s_{jp}+\mu^s_{rp} \leq \tilde{c}_{rkjpt'}+VCM_k \qquad \forall r\in\mathcal{R},\forall k\in\mathcal{K},\forall j\in\mathcal{J},\forall p\in\mathcal{P},\forall t'\in\Theta' \qquad (3.36)$$

$$\delta_{lp} + \mu_{rp} \leq \tilde{c}_{rlpt} \qquad \forall r \in \mathcal{R}, \forall l \in \mathcal{L}, \forall p \in \mathcal{P}, \forall t \in \Theta \tag{3.37}$$

$$\kappa_i^s, \eta_i^s, \gamma_{jp}^s, \delta_{lp}^s, \mu_{rp}^s \geq 0 \qquad \forall i \in \mathcal{I}, \forall j \in \mathcal{J}, \forall r \in \mathcal{R}, \forall l \in \mathcal{L}, \forall p \in \mathcal{P} \tag{3.38}$$

$$\tau_{ij}^s, \psi_{il}^s, \pi_j^s, \theta_{kp}^s \leq 0 \qquad \forall i \in \mathcal{I}, \forall j \in \mathcal{J}, \forall k \in \mathcal{K}, \forall l \in \mathcal{L}, \forall p \in \mathcal{P}. \tag{3.39}$$

Let Σ denote the set of all extreme points of DSP^s polyhedron, specified by (3.34)-(3.39). For each extreme point $\sigma \in \Sigma$, we denote the associated decision variables as $\tau_{ij}^{s,\sigma}, \psi_{il}^{s,\sigma}, \kappa_i^{s,\sigma}, \eta_i^{s,\sigma}, \gamma_{jp}^{s,\sigma}, \delta_{lp}^{s,\sigma}, \pi_j^{s,\sigma}, \theta_{kp}^{s,\sigma}, \mu_{rp}^{s,\sigma}$ and the objective function as $D_{s,\sigma}$. If the optimal objective for **DSP**^{s} is D_s^*, then $D_s^* \geq D_{s,\sigma}$, $\forall \sigma \in \Sigma$. Therefore, we restate the **DSP**^{s} as $\min_{D_s \geq 0}\{D_s : D_s \geq D_{s,\sigma}, \forall \sigma \in \Sigma\}$ where

$$\begin{aligned} D_{s,\sigma} = \sum_{i\in\mathcal{I}}\sum_{j\in\mathcal{J}} \tau_{ij}^s + \sum_{i\in\mathcal{I}}\sum_{l\in\mathcal{L}} \psi_{il}^s + \sum_{i\in\mathcal{I}} \min\{1, \bar{\phi}_{is}(1+\epsilon_1)\}\kappa_i^s \\ + \sum_{i\in\mathcal{I}} \min\{1, (1-\bar{\phi}_{is}(1-\epsilon_1))\bar{\lambda}_{is}(1+\epsilon_2)\eta_i^s + \sum_{j\in\mathcal{J}} Q_j^{SH}\pi_j^s \\ + \sum_{k\in\mathcal{K}}\sum_{p\in\mathcal{P}} Q_{kp}^{DC}\theta_{kp}^s + \sum_{r\in\mathcal{R}}\sum_{p\in\mathcal{P}} Q_{rp}^{CSL}\widehat{y}_r\mu_{rp}^s \qquad \forall \sigma \in \Sigma. \end{aligned}$$

3.5.1.2 Benders Master Problem

With the above **DSP** representation, the overall problem can be written as:

$$\text{Min} \qquad Z_{\text{MP}} = \sum_{r\in\mathcal{R}} f_r\, y_r + D \tag{3.40}$$

subject to

$$D \geq D_s \geq \sum_{i\in\mathcal{I}}\sum_{j\in\mathcal{J}} \widehat{\tau}^s_{ij} + \sum_{i\in\mathcal{I}}\sum_{l\in\mathcal{L}} \widehat{\psi}^s_{il} + \sum_{i\in\mathcal{I}} \min\{1, \bar{\phi}_{is}(1+\epsilon_1)\}\widehat{\kappa}^s_i$$
$$+ \sum_{i\in\mathcal{I}} \min\{1, (1-\bar{\phi}_{is}(1-\epsilon_1))\bar{\lambda}_{is}(1+\epsilon_2)\widehat{\eta}^s_i + \sum_{j\in\mathcal{J}} Q^{SH}_j \widehat{\pi}^s_j$$
$$+ \sum_{k\in\mathcal{K}}\sum_{p\in\mathcal{P}} Q^{DC}_{kp}\widehat{\theta}^s_{kp} + \sum_{r\in\mathcal{R}}\sum_{p\in\mathcal{P}} Q^{CSL}_{rp}\widehat{\mu}^s_{rp} y_r \qquad \forall s\in\mathcal{S}, \forall\sigma\in\Sigma \quad (3.41)$$

$$\sum_{r\in\mathcal{R}} Q^{CSL}_{rp} y_r \geq \omega_p \max_{s\in\mathcal{S}}\{\Upsilon_s\} \qquad \forall p\in\mathcal{P} \quad (3.42)$$

$$\sum_{r\in\mathcal{R}}\sum_{t\in\Theta} \tilde{b}_{rlt} y_r \geq 1 \qquad \forall l\in\mathcal{L} \quad (3.43)$$

$$\sum_{r\in\mathcal{R}}\sum_{k\in\mathcal{K}}\sum_{t'\in\Theta'} \tilde{a}_{rkjt'} y_r \geq 1 \qquad \forall j\in\mathcal{J} \quad (3.44)$$

$$D \geq 0, \qquad y_r \in \{0,1\} \qquad \forall r\in\mathcal{R}. \quad (3.45)$$

Due to a huge number of (3.41)-type constraints, this model is difficult to solve, however, not all of those are binding. Therefore, in Benders Decomposition, we start by solving a relaxed **MP** model, where we consider only a subset of (3.41), and obtain a valid lower bound of our overall problem in terms of the **MP**'s optimal solution. At an iteration σ, for each event $s\in\mathcal{S}$, we solve $\mathbf{DSP}^s(\boldsymbol{\lambda}, \boldsymbol{\psi}, \boldsymbol{\alpha}, \boldsymbol{\beta}, \boldsymbol{\gamma}, \boldsymbol{\delta}, \boldsymbol{\pi}, \boldsymbol{\theta}, \boldsymbol{\mu}|\widehat{\mathbf{y}})$, and using the obtained dual solution $(\boldsymbol{\lambda}^{s,\sigma}, \boldsymbol{\psi}^{s,\sigma}, \boldsymbol{\alpha}^{s,\sigma}, \boldsymbol{\beta}^{s,\sigma}, \boldsymbol{\gamma}^{s,\sigma}, \boldsymbol{\delta}^{s,\sigma}, \boldsymbol{\pi}^{s,\sigma}, \boldsymbol{\theta}^{s,\sigma}, \boldsymbol{\mu}^{s,\sigma})$, we generate a cut (3.41) corresponding to the s-th event and σ-th extreme point of the $\mathbf{DSP}^s$ polyhedron. We observe, instead of having one (3.41)-type constraint for each $s\in\mathcal{S}$, the number of cuts to add to **MP** can be reduced by taking the maximum of the RHS over $s\in\mathbf{S}$, thus, only one Benders cut corresponding to the event s with the largest objective value, is added to the **MP** at each BD iteration. We utilize surrogate constraints to ensure that the network provided by the **MP**

solution ($\mathbf{y}$ vector) does not lead to subproblem infeasibility. First, the surrogate constraint (3.42) ensures that aggregate demand of all affected population is met. Next, the surrogate constraint (3.43) ensures that for each UDC $l \in \mathcal{L}$, at least one CSL must open at a location $r \in \mathcal{R}$ that can supply reliefs using any MoT within critical time Γ. Surrogate constraint (3.44) ensures the same for each shelter $j \in \mathcal{J}$. Thus, the $\mathbf{PSP}^s$ are always feasible with respect to any $\mathbf{y}$ vector supplied by **MP** making the corresponding $\mathbf{DSP}^s$ bounded. This way, our $\mathbf{DSP}^s$ solutions always provide Benders optimality cuts rather than the extreme ray based feasibility cuts, hampering BD-convergence rate.

3.5.2 Approaches to Accelerate Benders Decomposition

Since the traditional BD implementations, relying on successive solving of the **MP** and **SP** within an iterative framework, do not perform satisfactorily on large MIP problems, researchers prescribe several algorithmic improvements over time to accelerate BD. Some of these techniques include employing ϵ-optimal approach to obtain first feasible solution of the **MP** instead of solving it to optimality, thereby saving significant solution time (Geoffrion and Graves, 1974). Solving LP relaxation of the **MP** in a number of initial iterations (McDaniel and Devine, 1977), and early-stopping of **MP** in some initial iterations (Üster et al., 2007) have also been suggested. However, the primary drawback of all these approaches is the long time needed to solve the **MP** repeatedly in each iteration. To avoid this repetition and make significant performance improvement, we use CPLEX callback and tune some CPLEX parameters before solving **MP**, inspired by success of our recent work presented in Section 2. The BD acceleration approaches are explained next.

First, we use the CPLEX lazy constraint callback (version 12.4 or later), a control callbacks that allows users to intervene the branch-and-cut tree search process

(Rubin, 2011). Instead of repeatedly solving the **MP** at each iteration as done in traditional BD, we solve it only once. Whenever branch-and-cut finds an incumbent, the callback is invoked to solve all $|\mathbf{S}|$ subproblems ($\mathbf{PSP}^s$) using the incumbent $\mathbf{y}$ vector. A single new cut corresponding to the maximum of the $|\mathbf{S}|$ **PSP** objective values is added to the **MP**. The tree search proceeds till the stopping criteria are met or the optimal solution is obtained. However, note that the callback feature turns off dynamic search and deterministic parallelism of the solver (CPLEX, 2009) that sometime may be disadvantageous.

Second, we examine certain tree search parameter-tuning, since the way to explore the branch-and-cut tree has an expected impact on the strength and timing of the bounds obtained in solving the **MP**. For tree search, we use the conventional search instead of the dynamic one (specified through *MIPSearch*) as the latter is not allowed with callbacks. Specifically, we tune two CPLEX parameters:

1. *MIPEmphasis*: We choose emphasizing optimality over feasibility after some initial trial runs. Though it may take longer than a feasibility-emphasized run, our choice ultimately helps by adding lesser but deeper cuts to **MP**, resulting in faster convergence.
2. *Varsel*: This parameter for variable selection strategy influences which variable is chosen for branching in the search tree, after a node is selected. Based on our trial run experience with default, pseudo, pseudo-reduced, and strong branching alternatives, we use strong branching for our computational study.

3.6 Computational Study

We conduct a series of computational studies to test the performance of our proposed solution methodology. Altering the numbers of disaster events and the nodes in different tiers of our network, we generate 12 classes, each consisting of 10 instances

as shown in Table 3.1. To avoid the tail-off effect, we solve all instances using two early-stopping criteria, whichever is met first: (1) 2% optimality gap between the incumbent and the best lower bound, and (2) time limit of 3600 sec. for C1-C8 and 7200 sec. for C9-C12. Our computational experiments are summarized as follows:

- **Experiment 1:** We solve the instances applying CPLEX branch and cut (B&C) with all its default settings for cut generation, preprocessing and upper bound heuristics.
- **Experiment 2 (BD-I) :** We implement Benders Decomposition (BD)-based solution approach with callback feature of CPLEX (as discussed in §3.5.2).
- **Experiment 3 (BD-II) :** To further improve upon **BD-I** in terms of solution time, we tune several CPLEX parameters (as discussed in §3.5.2) and re-solve the instances.
- **Experiment 4 (B&C with worst BD runtime) :** Here, we demonstrate that the BD-based approaches convincingly outperform B&C. For this, we first record the maximum of **BD-I** and **BD-II**'s solution times for the 10 instances in each class, and then employ B&C by setting that maximum value as the early stopping time.

We implement both B&C and BD using Concert Technology (CPLEX 12.4 with Java API). In BD implementations, we employ CPLEX to solve both the master problem (**MP**) and the dual subproblems (**DSP**^{s}) for each $s \in \mathcal{S}$. We take all runs on desktop computers with Intel Core 2 Duo processor and 8 GB RAM.

3.6.1 Random Test Instance Generation

To conduct our computational study, we generate random test instances in a way that the underlying network structure closely resembles the actual study region along

the Gulf coast of the USA in terms of scale and relative geographical locations of the nodes. We randomly generate several model parameters close to the available real data. We represent the study region by a 500 x 500 rectangle ABCD (see Figure 3.3) with the imaginary coastline along AB.

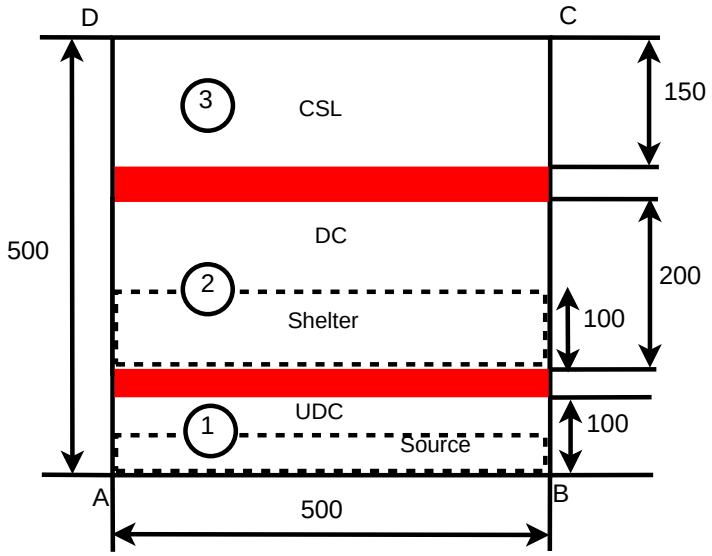

Figure 3.3: Setting for Test Instance Generation

The rectangle is horizontally divided into three zones, from bottom to top, consisting of : (1) evacuation sources and UDCs, (2) available shelter and DC facilities, and (3) potential central storage locations (CSL). To safeguard the shelters and DCs from possible damage by a strong disaster, we keep a 30 unit-wide separation between zones (1) and (2). Similarly, to safeguard the CSLs, we keep a further 20 unit gap between zones (2) and (3). Evacuation sources can be located anywhere within the bottom-most rectangle, but for safety, we consider UDCs located at least 50 units away from AB. The DC nodes can be anywhere in the middle rectangle, but to help

the evacuees reach the shelters quickly, we assume that the shelters are located only at the bottom half of the middle rectangle (2). Now, using uniform distribution, we generate node locations for $\mathcal{I}$, $\mathcal{J}$, $\mathcal{K}$, $\mathcal{L}$, and $\mathcal{R}$ sets within these rectangles, as per the combinations listed in Table 3.1.

Table 3.1: Problem Classes for Computational Study

Class	Source	UDC	Shelter	DC	CSL	Total Nodes	Disaster Event
C1	500	100	50	10	50	700	10
C2	500	100	50	10	50	700	20
C3	500	100	50	10	100	710	10
C4	500	100	50	10	100	710	20
C5	1000	200	100	20	50	1350	10
C6	1000	200	100	20	50	1350	20
C7	1000	200	100	20	100	1370	10
C8	1000	200	100	20	100	1370	20
C9	2000	400	200	40	50	2670	10
C10	2000	400	200	40	50	2670	20
C11	2000	400	200	40	100	2690	10
C12	2000	400	200	40	100	2690	20

We summarize the distributions used to generate the important model parameters in Table 3.2. We use uniform distribution to generate population (pop_i) at the evacuation sources. For shelters, we generate their capacities (Q_j^{SH}) using uniform random distribution in a way that infeasibility issues do not arise due to their capacity constraint violation. We assume that in any single disaster event at most ζ_1=20% of total population living in zone 1 of Figure 3.3, can be affected, whereas about ζ_2= 40% of total number of existing shelters may be turned operative to accommodate the evacuees. Similar approach is taken to generate DC capacities for each relief item (Q_{kp}^{DC}). Here, we assume that stockpiling all supplies for $\Delta = 5$ days is sufficient.

CSL capacity (Q_{rp}^{CSL}) is determined in similar fashion, except for considering ζ_2=10% of the potential CSLs are planned to be opened.

Table 3.2: Distribution of Model Parameters

Parameter	Distribution	Parameter	Distribution
Source:		**UDC:**	
x_i	U [0; 500]	x_l	U [0; 500]
y_i	U [0; 100]	y_l	U [50; 100]
$\bar{\lambda}_i$	U [0.3; 0.6]	**CSL:**	
pop_i	U [300; 3000]	x_r	U [0; 500]
		y_r	U [350; 500]
Shelter:		Q_{rp}^{CSL}	$\frac{\Delta \times \omega_p \times \zeta_1 \sum_{i \in \mathcal{I}} pop_i \times \text{U } [0.8;1.2]}{\zeta_2 \times \lvert\mathcal{R}\rvert}$
x_j	U [0; 500]		where ζ_1=0.2; ζ_2 =0.1
y_j	U [130; 230]	f_r	U[0.9;1.1] $\times \sum_p w_p Q_{rp}^{CSL}$,
VCP_j	U [1; 5]		where $\sum_p w_p = 1, w_p \in [0,1]$
Q_j^{SH}	$\frac{\zeta_1 \times \sum_{i \in \mathcal{I}} pop_i}{\zeta_2 \times \lvert\mathcal{J}\rvert}$ U [0.8; 1.2]	**Event:**	
	where ζ_1=0.2; ζ_2 =0.4	x_s	U [0; 500]
		y_s	U [0; 50]
DC:		C_s	U [1;5]
x_k	U [0; 500]		**Transportation Costs:**
y_k	U [130; 330]	α	U[0.1; 0.2]
VCM_k	U [0.01; 0.10]		$t =$ ST : U [0.005; 0.01]
Q_{kp}^{DC}	$\frac{\Delta \times \omega_p \times \zeta_1 \sum_{i \in \mathcal{I}} pop_i \times \text{U } [0.8;\ 1.2]}{\zeta_2 \times \lvert\mathcal{J}\rvert}$	β_{pt}	t = MT : U [0.0025; 0.005]
	where ζ_1=0.2; ζ_2 =0.4		t = LT : U [0.00125; 0.0025]

As mentioned before, we randomly generate the location and intensity of each disaster event within a 50 unit wide belt along the coastline AB (see Figure 3.3). The intensity of a disaster is expressed by Category (C_s) in a five point Saffir-Simpson scale. Other parameters include unit transportation cost for the evacuees (α), unit distribution cost for each relief item p using different modes of transport t (β_{pt}) such as small trucks (ST), medium size trucks (MT), and large size trucks (LT). For air lifting, we assume \$2 distribution cost per unit-mile. We further consider variable

cost to manage inbound relief items at a DC (VCM_k), and variable cost to serve the evacuees at the shelters (VCP_j). Due to varied storage and handling requirements for different relief supplies, we consider that the fixed opening cost f_r for a CSL at $r \in \mathcal{R}$ is a function of its capacity for p different items. Therefore, we express f_r as the weighted sum of the storage capacities Q_{rp}^{CSL}, for each item p, with weight w_p.

3.6.2 Computational Results

We now discuss our computational experiment results. We solve the **ROCP**(Γ) model by setting the critical time to 24 hours. We first employ CPLEX B&C with its default settings and the fore-mentioned stopping criteria, but do not obtain any acceptable solution in terms of optimality gap. Even in the smallest class C1, many instances fail to obtain a feasible solution within an hour. Instead of attempting B&C on larger classes, we develop the BD implementations. We first employ BD-I using CPLEX with default parameter settings to solve **MP** and **DSP**s. Next, for further performance improvement, we employ BD-II where some CPLEX parameters are tuned to solve **MP**.

The computation results of BD-I and BD-II performances on all 10 instances in C1-C12 classes are summarized in Table 3.4. We also present the outcome of Experiment 4 in the same table. In BD-I and BD-II, for each instance class, we report the average and maximum values of solution times and optimality gaps. Row minimums of the solution times are highlighted in boldfaces. Then, we conduct a performance comparison based on solution time between B&C and either of the BD approaches. We note the maximum of BD-I and BD-II's worst solution times, and set that as the early stopping criterion in B&C to solve the instances of smaller classes C1 - C4. We report the average and maximum optimality gaps for the instances that obtain any feasible solution by this stopping time, and also mention the number

of instances failing to get a feasible solution. For example, in C1 class, three out of 10 instances fail to obtain any feasible solution by 89 sec. The average and maximum optimality gaps of the remaining seven instances are 10.4% and 30.7%, respectively. In C3 and C4, we get no feasible solution (NFS) for any of the 10 instances. We summarize our key observations on the performance comparison of the three approaches as follows:

1. **Solution methodology** is critical to solve large scale realistic problems. BD efficiently decomposes the original large MIP problem into one **master**, and $|\mathcal{S}|$ small **sub-problems** for the separable events. Consequently, the BD implementations solve all 10 instances in C1-C12 classes, while CPLEX B&C fails. Even with the worse of BD-I and BD-II's runtimes as the early stopping time, using B&C, we get no feasible solution for C3 class onwards. In C1 and C2, B&C fails to obtain any feasible solution for three and four out of 10 instances, respectively. For the remaining instances in C1 and C2, B&C finds some feasible solution, but of inferior optimality gap. As B&C cannot obtain any feasible solution for C3 and C4, we do not continue testing on larger instance classes.

2. **CPLEX parameter tuning** as discussed in §3.5.2 to solve the **MP** has a significant effect on solution time (see Figure 3.4). The average runtime for the classes C1-C12 is lower in BD-II than in BD-I, except for C12, where BD-II takes on an average 1.8% more. We observe, the reduction of average solution time is at least 6.4% (in class C3) and at most 24% (in class C10), with an average saving of 18%, indicating that BD-II is the more efficient approach.

3. **The number of events** $|\mathcal{S}|$ influences the solution time of BD. The odd-numbered class instances ($|\mathcal{S}| = 10$) take less time than the instances of even-numbered classes ($|\mathcal{S}| = 20$), which is expected because for the latter, BD solves

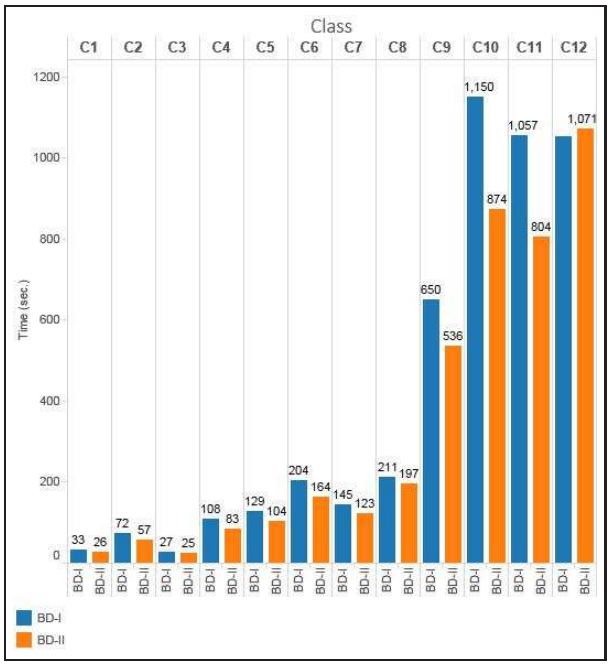

Figure 3.4: Average Runtimes: BD-I, BD-II

twice as many subproblems. The same is observed for maximum runtime.

4. **Network size** also adversely affects the solution time. To isolate the effect of $|\mathcal{S}|$ on runtime as just explained, we consider the odd and even classes separately. We observe an increasing trend in the average solution time (see Figure 3.5) except for a negligible 1 sec decrease in C3 with respect to C1's average runtime.

3.7 Case Study

We apply our robust model ROCP(Γ) on a realistic case for the Gulf coast region with publicly available GIS data. We first present the data sources, followed by our approach to create discrete disaster events, and the experiments conducted to gain managerial insights.

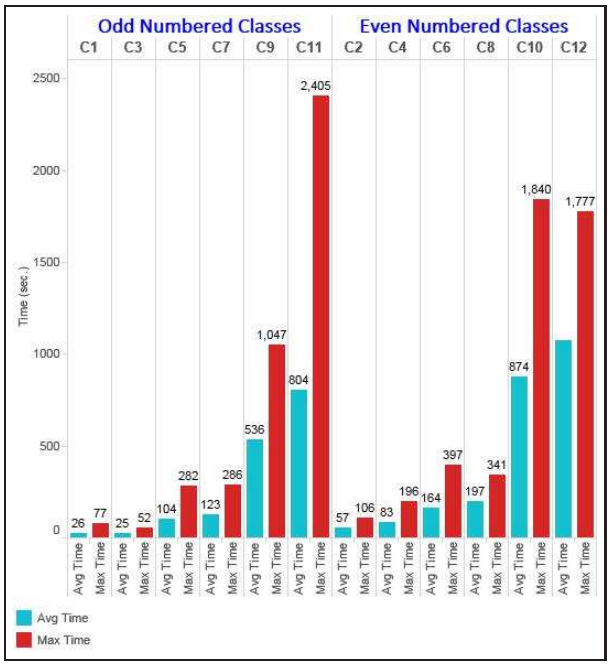

Figure 3.5: Effect of Instance Size on Runtime

3.7.1 Data Collection

We present our study region in Figure 3.6 and summarize in Table 3.3 the information related to each type of node in the underlying network. We partition the study region into three zones: (1) Source and UDC zone, (2) shelter and DC zone, and (3) CSL zone. The approximate widths of the zones 1, 2, and 3 are 150, 200, and 300 miles, respectively. We consider an approximately 150 mile wide belt, running across six states along the Gulf coast as the zone 1. We gather TIGER/Line shapefiles for all five-digit ZIP code tabulation areas (**ZCTA**) belonging to this zone 1 (Source: census.gov), and then, using ArcGIS 10 (ESRI Inc.), determine the centroid locations for 2815 ZCTAs, that represent the source nodes. We obtain population data for these sources from 2010 decennial census (Source: socialexplorer.com). We use the *graduated color scheme* of ArcGIS symbology to represent these ZCTAs by

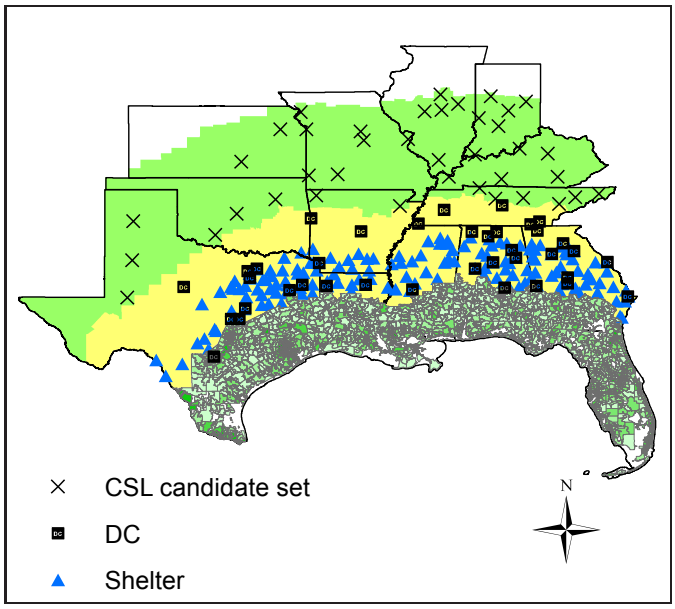

Figure 3.6: Case Study Region

light to dark colors in proportion to their population densities. Next, we collect TIGER/Line shapefiles for the *urban areas* or *urban clusters* (defined in census.gov as *'urban area'*) within our study region to construct the UDC, shelter, DC, and CSL sets. We assume that a large urban area fulfills the infrastructural and space requirements to establish and operate large facilities such as UDCs, shelters, DCs, and CSLs. For UDCs within zone 1, we select all urban clusters that are located, for safety, at least 50 miles from the coastline. Next, for the DC and shelter nodes, we first identify the urban clusters within zone 2. Out of these clusters, as DC nodes, we select the top 38 in terms of available land area. To facilitate the evacuees' quick access to the shelters, we consider the shelter nodes in proximity to the sources.

Table 3.3: Summary of GIS data

Entity	Number of Nodes	Geographic Unit	States
Source	2815	ZIP code	TX,LA,MS,AL,GA,FL
UDC	284	Urban clusters	TX,LA,MS,AL,GA,FL
Shelter	160	Urban clusters	TX,LA,MS,AL,GA, AR, OK
DC	38	Urban clusters	TX,LA,MS,AL,GA, AR, OK
CSL	39	Urban clusters	KS, MI, IL, IN, KY

For this, we identify the urban clusters within 300 miles from the coast and select the top 160, based on available land area as our shelter location set. Similarly, to populate the candidate CSL set, we select land area-wise top 50 urban clusters in the CSL zone 3. After eliminating the clusters that are too close to each other, we finalize 39 candidate CSLs. We determine the centroids of the urban clusters to represent them as UDC, shelter, DC, and CSL nodes, however, we do not assume only one shelter, DC or CSL located at those centroids, rather consider the available aggregated capacities of these facilities. Apart from all node locations and source population, we generate all model parameters using uniform random distribution (see §3.6.1). Storm events are also generated randomly, as explained next.

3.7.2 Disaster Event Creation

In robust optimization, scenario-based uncertainty representation requires much care for scenario planning. The scenarios should capture contrasting but realistic possible outcomes and help to reveal hidden problem characteristics (Kouvelis and Yu, 1997). Keeping this in mind, we use a detailed approach to develop discrete disaster

events for the case study. Based on National Hurricane Center data archive (Source : http://www.nhc.noaa.gov/data/), we first identify all major storms that struck the Gulf coast between 2003 - 2013 and find the approximate latitude/longitude of the storms' intersection point on the coastline. We try to generate the random disaster events located close to these historical storms. Next, we generate random locations along the Gulf coast line using ArcGIS, keeping at least a five mile gap exists between two adjacent storm locations. Out of 67 points obtained this way, we select only those lying within a 20 mile radius of the historic storm's approximated landfall location. We consider these points as the storm events for our case study. Finally, to eliminate several closely located points by clustering them, and to separate the outliers, we apply density-based spatial clustering of applications with noise (DBSCAN) algorithm (Ester et al., 1996) by setting two parameters: (1) minimum two points to define a cluster, and (2) 25 mile cluster radius. In other words, we specify that any two points located within 25 mile radius can be clustered together. Now, within each cluster obtained this way, we replace individual points by their centroids. Following this process, we obtain 18 points that represent independent storm events along the Gulf coast. As we seek a solution that is feasible for the worst case scenario, we consider all 18 events as category five hurricanes. Thus, all the highly populated sources along the Gulf coast are affected by at least one of these 18 category five hurricanes. Although apparently conservative, this assumption balances the fact that we do not consider simultaneous strike of multiple hurricanes, as occasionally happens in reality.

3.7.3 Experiments on the GIS-based System

The source population density presentation by the graduated color scheme in Figure 3.6 reveals a considerable demand variation along the Gulf coast. More specifi-

cally, the ZCTAs close to the large metropolitan areas near the coastline are densely populated, whereas in others, the population is sparse. All our analyses reflect this underlying pattern in population data. Model outcomes are expected to change when applied to a different study region, e.g., east coast of the USA, where population density is more uniform along the Atlantic coastline. Now, we discuss a series of experiments, conducted to illustrate the model's responsiveness to various changes to input data, eliciting different interesting insights.

3.7.3.1 Critical Time vs. System Cost

Critical Time (Γ) plays a vital role in determining the CSL location decisions and overall system cost. In Figure 3.7, we illustrate the effect of changing critical time (Γ) on total cost by solving the ROCP model with different Γ values. Moreover, in Figure 3.8, we list the maps corresponding to significant changes in the solution. With varying Γ, visualization of the solutions in terms of (1) open CSL locations, and (2) CSL $\rightarrow$ {DC, UDC} air transportations, helps to gain interesting insights. In this experiment, to eliminate the effect of varied disaster intensity, we assume that the model is used for worst case decision making when all $|\mathcal{S}|$ events represent category five hurricanes.

Our observations are summarized as follows:

1. Small critical time enforces the use of very expensive air transportation for relief delivery (see Figures 3.8a - 3.8e), thereby, increasing total system cost. As presented in Figure 3.7, for critical time (Γ) up to 18 hours, distribution cost solely dominates other cost components due to the use of air transportation. As Γ increases, the need for air transportation disappears (see Figure 3.8f), reducing the distribution cost to around 15% of the total cost.
2. A trade-off exists between distribution start time and system cost. By starting

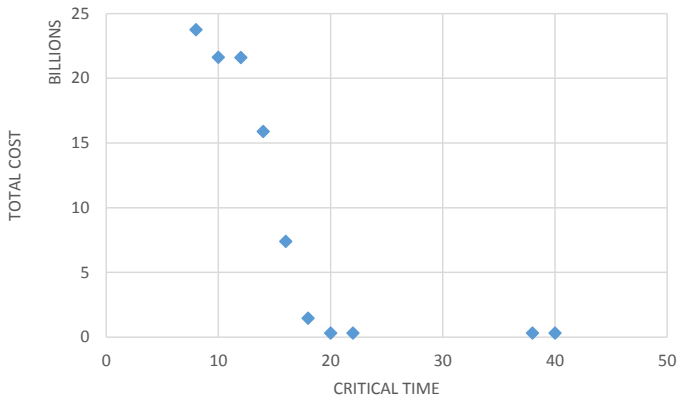

CT (hours)	Total Cost ($)	Distribution Cost %
8	23,755,490,745	98.89
10	21,625,208,806	98.59
12	21,601,187,726	98.70
14	15,894,086,098	98.49
16	7,404,108,406	97.35
18	1,475,005,945	86.69
20	315,022,156	15.76
22-36	314,375,365	15.74
38	314,257,482	15.71
40 onwards	314,111,538	15.67

Figure 3.7: Cost Change with Critical Time

early with large Γ, considerable distribution cost can be saved by completely avoiding air transportation. We note about the possibility of mis-utilization of distribution expense by starting too early, in case the anticipated disaster does not strike at all, however, waiting longer is clearly a more expensive. Based on our problem data setting, by starting the relief dispatch 24 hours before evacuation (i.e., 48 hours before the anticipated storm), the distribution cost counts only 15.74% of the total cost (see Figure 3.7). Even if the disaster does not eventually strike, this distribution cost, as a bad expense, is much less compared to the required expenditure only after a 6 hour delay ($\Gamma = 18$ hours). In our case study problem, 20 hours is as a threshold for Γ, after which, system cost decrease is not that significant.

3. Critical time influences the CSL location decisions. For $\Gamma = 8$ hours, seven CSLs open up at locations that are length-wise well spread-out, but the small Γ forces those to be depth-wise close to the DC/Shelter zone (see Figure 3.8a). As Γ increases, the CSLs gradually spread out depth-wise too, and $\Gamma = 20$ hours onwards, the air transportation reduces to zero.
4. Population density influences the CSL location decisions, by forcing those to open near densely populated regions. With the increase of Γ, when air transportation cost is no longer the single-most dominating factor, the CSLs tend to concentrate more towards the east side of the map, since the coastal population density is significantly higher at the east side than the west.
5. As Γ increases, we observe a gradual decrease in the number of DCs (see Figures 3.8d, 3.8e, 3.8f). For large Γ, distance between the operative DCs and shelters can get longer, still ensuring relief delivery within the critical time along the CSL $\rightarrow$ DC $\rightarrow$ shelter paths. This allows demand consolidation at the operative DCs, reducing their number considerably.

3.7.3.2 Effects of Population Density and Disaster Intensity

In this experiment, we highlight the effects of population density and disaster intensity (in five-point hurricane scale by Simpson and Saffir (1974)) on CSL location decision. To eliminate the effect of large cost incurred by air transportation when critical time is small, we set Γ to 24 hours where no air transportation is required. Also, all the uncertainty measures for evacuee-fraction (ϵ_1), stay-back population fraction going to UDCs (ϵ_2), and disaster duration (ϵ_3) are fixed to 20%. We set up four experiments, considering hurricane intensities at three levels: small (category 1), medium (category 3), and large (category 5). We consider four experiments.

1. We assume that out of 18 random disaster events, ones that are close to low

population density areas, are category 1 hurricanes while the remaining are of category 3.

2. Hurricanes close to low population density areas are of category 5, others are of category 3.
3. Hurricanes close to densely populated areas are of category 1, others are of category 3.
4. Hurricanes close to densely populated areas are of category 5, others are of category 3.

In Figure 3.9 we plot the CSL locations obtained from these four experiments. Moreover, we plot the CSL locations obtained from a separate run, where all 18 events are considered as category 3 (medium) hurricanes. Our key observations are summarized as follows:

1. CSL location decisions are insensitive to disaster intensity at low population density areas. As evident from Figures 3.9a and 3.9b, irrespective of the category (1 or 5) of the hurricane, striking near the less populated sources, exactly same set of CSLs open up. The location decision is more influenced by the induced demand at the densely populated sources, affected by category-3 hurricanes. Therefore, we observe the proximity of the CSL locations obtained from Experiment 1 to those marked by 'X', where all 18 events represent category 3 hurricanes. This outcome is realistic, since the locations of the most populated regions dictate the CSL positions.
2. Since category 1 hurricanes generally do not require mass evacuation, they induce less demand, thereby requiring less number of CSLs to open up. In Figure 3.9c, category 1 hurricanes affect all the densely populated sources and category 3 hurricanes strike fewer, less populated areas. Due to decreased demand with respect to situation in Figure 3.9a, opening only two CSLs prove

sufficient to satisfy the total demand in 3.9c.

3. Effect of disaster intensity is most evident on the densely populated sources. Comparing Figures 3.9c and 3.9d we observe, as hurricane category changes from 1 to 5 in the densely populated areas, in addition to the two CSLs opened in Figure 3.9c, three more are required in 3.9d to satisfy the increased demand for reliefs.

In summary, both population density and disaster intensity have strong influences on CSL location decision. However, instead of treating the factors in isolation, one needs to consider them jointly to better understand their effects.

3.7.3.3 Advantages of RO in Case Study

We conclude this section with a discussion on the advantages of adopting RO to locate CSLs, ensure timely and cost-effective relief distribution to the affected population even in the worst case. Unlike stochastic optimization approach, requiring a difficult-to-estimate probability value for each scenario, RO relieves us from using any probability as we consider minimizing the maximum flow cost over all disaster events. Now, we briefly highlight some approaches that we attempted as alternatives to RO, and explain the outcomes to highlight the benefits of RO in our problem setting.

We assume that only one disaster strikes at a time. If we do not consider the disaster location and intensity uncertainty, we just need to determine the optimal CSL locations that ensure timely distribution in the wake of one particular event while minimizing the overall system cost. However, the location solution for one event becomes suboptimal or even infeasible for another event due to the following reasons. First, the distance between the open CSLs and affected area may be too large to cover within critical time even by air lifting. Second, CSL capacity may

become inadequate if the disaster affects a very large and densely populated area. Third, even with inadequate capacities, if the optimal CSLs for one event supply reliefs to distant sources during another event, the distribution cost may increase significantly.

By considering box uncertainty for the difficult-to-estimate model parameters, we obtain a feasible solution that is protected against fluctuation of those parameters. To observe the effect of not considering such uncertainty, we solve the ROCP model with all ϵ-values set at zero. We consider opening the CSLs only at the locations according to this solution, and solve the associated flow problem. In general, when CSL capacities are adequate, we obtain a feasible flow solution but the flow quantities and assignments alter, increasing the transportation, and thereby the overall system cost.

We note at this point, one may try to prove the advantage of robust optimization by solving the model for each disaster event separately and compare the solutions with the ROCP solution. The solution obtained from the union of $|\mathcal{S}|$ separate location decisions (CSL, DC, shelter, UDC) is definitely worse than the robust solution, but this difference is actually due to centralized and decentralized decision-making, as opposed to robust vs deterministic approaches. We conduct this experiment and as expected, observe that opening CSLs at all of these locations is more than adequate to handle any disaster situation considered in the set $\mathcal{S}$, but the system cost drastically increases.

Based on our observation from the above discussion, we conclude that our RO-based approach provides a cost-effective solution, addressing various sources of uncertainty in an efficient manner.

3.8 Concluding Remarks

In this paper, we introduce a robust emergency relief network design problem. We construct a two-stage model, to determine strategic central supply locations that can send essential relief items to the impacted population in response to any disaster realization from a set of events. In addition to our solution's robustness to disaster location and intensity, we also consider data uncertainties due to human behavior during emergency, causing deviation from the nominal model parameters. Two such sources of data uncertainties, namely, the fraction of total population actually evacuating a source and the fraction from the balance stay-back population going to UDCs, are considered in our model. Moreover, we consider uncertainty due to inaccurate estimation of disaster duration that affects true demand value for the relief items. By considering different modes of transport with varied unit costs to distribute reliefs, we explain the trade-off between the critical time to start sending reliefs from CSLs and the overall system cost. We observe, by employing the state of the art branch-and-cut algorithm, we cannot solve realistically large problem instances. By exploiting the model structure, we apply Benders Decomposition (BD) to split the model into master problem (**MP**) and subproblem (**SP**), the latter further splits into separable LPs for each event. By adding appropriate surrogate constraints to **MP**, we ensure subproblem feasibility, thereby avoid adding feasibility cuts that hamper BD's convergence rate. We use CPLEX lazy constraint callback to solve the **MP** to avoid its repeated solving at each BD iteration as happens in traditional BD implementation. For further performance improvement, we solve the **MP** by tuning certain CPLEX parameters based on our trial experiments. We conduct a detailed computational study with these two BD implementations and observe significant solution time improvement by CPLEX parameter tuning. We apply the

robust model to solve a realistic, GIS-data based problem with the entire Gulf coast as the study region. Following a systematic approach, we create a set of disaster events that cover all major densely populated habitats along the Gulf coast, thereby ensuring the solution's robustness to the worst case scenario. We observe the effects of critical time, disaster intensity, and population density on the solution in terms of CSL location decision and the system cost. We explain the advantages of using robust optimization based approach based on the insights gained.

We conclude by indicating the future research directions. One may introduce economies of scale in the modes of transport by considering LTL/FTL. We may consider dispatching reliefs from CSLs by grouping certain items, that have specialized handling requirements, together. From data uncertainty perspective, one can add scenarios of partial road network damage to varied extent. In this paper, we focus on determining the high level allocation decisions for people and relief flows, therefore, do not consider making detailed routing decisions. However, if we add road damage scenarios, instead of using node-pair Euclidean distances, we should use underlying real road network, determine the shortest path distance between node-pairs in different scenarios.

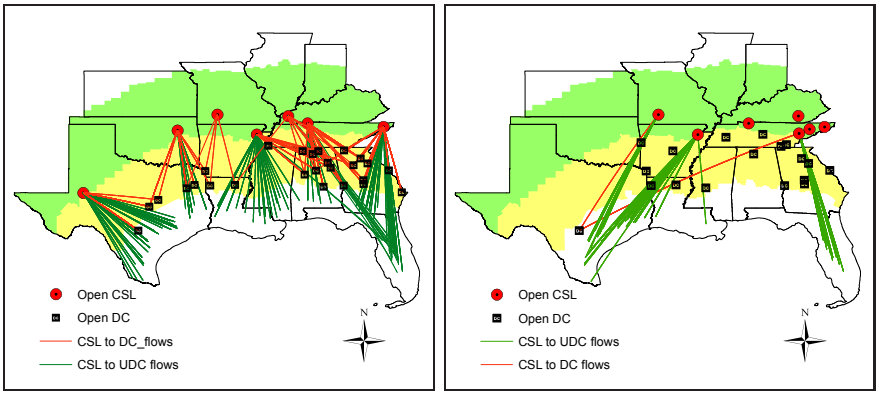

(a) Critical Time $\Gamma = 8$ hours (b) Critical Time $\Gamma = 12$ hours

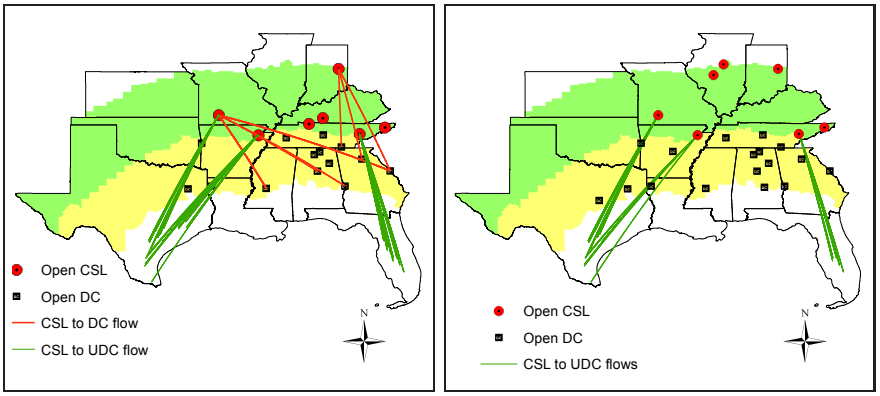

(c) Critical Time $\Gamma = 14$ hours (d) Critical Time $\Gamma = 16$ hours

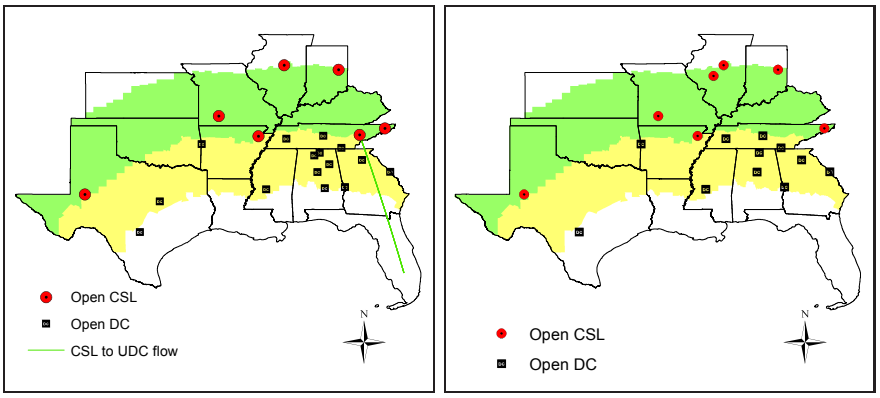

(e) Critical Time $\Gamma = 18$ hours (f) Critical Time $\Gamma = 20$ hours

Figure 3.8: CSL Location and Flow by **Air transportation** Changing With Critical Time Γ

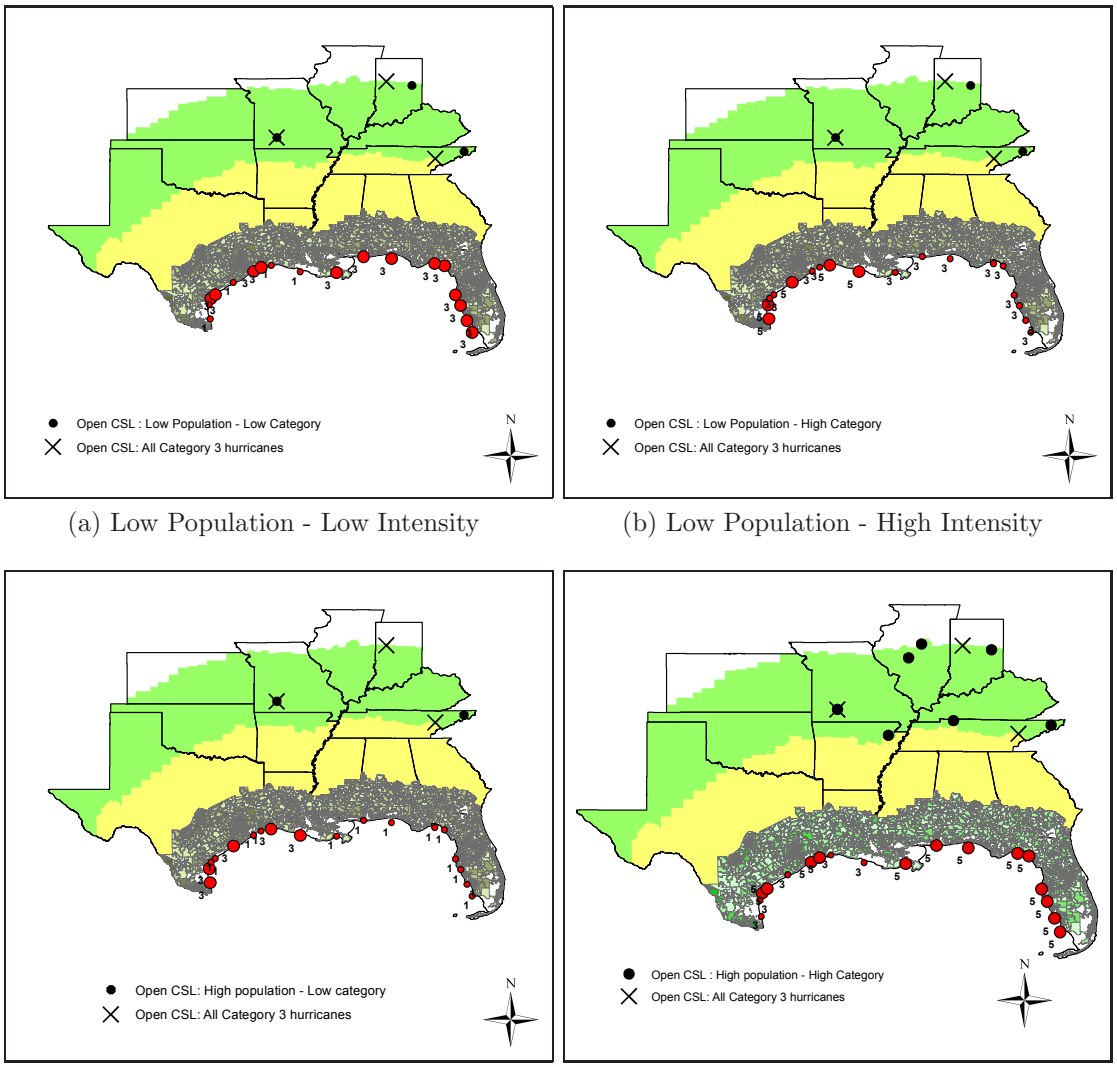

(a) Low Population - Low Intensity

(b) Low Population - High Intensity

(c) High Population - Low Intensity

(d) High Population - High Intensity

Figure 3.9: Joint Effects of Population Density and Disaster Intensity on CSL Location

Table 3.4: Computational Results

	BD-I				BD-II				B&C			
	Runtime (sec.)		Gap %		Runtime (sec.)		Gap %		Time Limit	Gap%		No feasible
Class	Avg	Max	Avg	Max	Avg	Max	Avg	Max	(sec.)	Avg	Max	solution
C1	33	89	1.8	2.0	**26**	**77**	1.8	2.0	89	10.4	30.7	3
C2	72	177	1.6	2.0	**57**	**106**	1.6	2.0	177	14.3	25.1	4
C3	27	52	1.5	2.0	**25**	**52**	1.7	2.0	52	NFS	NFS	10
C4	108	227	1.7	2.0	**83**	**196**	1.7	2.0	227	NFS	NFS	10
C5	129	333	1.6	2.0	**104**	**282**	1.6	2.0	–	–	–	–
C6	204	545	1.7	2.0	**164**	**397**	1.7	2.0	–	–	–	–
C7	145	326	1.6	2.0	**123**	**286**	1.6	2.0	–	–	–	–
C8	211	**322**	1.6	2.0	**197**	341	1.6	2.0	–	–	–	–
C9	650	1948	1.4	2.0	**536**	**1047**	1.5	2.0	–	–	–	–
C10	1150	2217	1.7	2.0	**874**	**1840**	1.8	2.0	–	–	–	–
C11	1057	3200	1.7	2.0	**804**	**2405**	1.6	2.0	–	–	–	–
C12	**1051**	1994	1.5	2.0	1071	**1777**	1.5	2.0	–	–	–	–

4. COMBINING WORST CASE AND AVERAGE CASE CONSIDERATIONS IN AN INTEGRATED EMERGENCY RESPONSE NETWORK DESIGN PROBLEM

4.1 Introduction and Motivation

Every year natural disasters strike at different parts of the world, causing staggering loss of lives, properties, and damage of infrastructure. Over the past decade, mankind have experienced several mega-disasters such as the Indian Ocean tsunami (2004), the hurricanes Katrina (2005), Rita (2005), Ike (2008), Irene (2011), Sandy (2012), the earthquakes in China (2008), Haiti (2010), and Japan (2011). In recent past, initiatives are taken by operations research community to address different aspects of the overly complex issues related to emergency logistics in order to reduce the sufferings of the human society. Past experiences of disasters taught the emergency managers the importance of effective pre-disaster preparedness that is critical for the success of post-disaster response. Therefore, several studies focus on the disaster preparedness phase to identify the strategic locations to pre-position essential relief supplies to ensure fast distribution of those to the affected population in the wake of a disaster. Researchers propose several pre-positioning models for the two- or three-tier systems, consisting of demand points, intermediate facilities in case of three-tiered system, and the supply points, to find the optimal locations and capacities of the facilities in one of these tiers, along with determining the supply to demand point assignments.

There is another line of research focusing on the operational aspect in the post-disaster setting, primarily in the context of vehicle routing or location-routing problems under several disaster-related constraints such as road or infrastructure damage,

limited vehicle availability, short response time. Although literatures exist focusing on both pre- and post-disaster problems, a strategic level integration of these two is necessary under single framework for decision making with a holistic view of the entire system. Our research is to bridge this gap by integrating the supply and demand sides, observing that the intermediate tier of shelters acts as the interface between the two sides of the network.

Acknowledging that cost minimization is not always a suitable objective in humanitarian logistics problem context, researchers use various objective measures such as maximizing coverage (Jia et al., 2007; Balçik and Beamon, 2008), minimizing casualties (Salmeron and Apte, 2010), minimizing response time (Duran et al., 2011). However, in reality, although in post-disaster situation funds are not scarce due to generous global aids, in pre-disaster situation, infrastructure building as a preparedness step, may not have sufficient fund availability. Therefore, we consider the importance of system cost minimization, as found in literature (Horner and Downs, 2010; Rawls and Turnquist, 2011, 2012; Li et al., 2011; Doyen et al., 2012).

We consider a three-tier emergency response network, consisting of evacuation sources (demand points), shelters, and DCs (supply points). We introduce uncertainty in the location and intensity of a storm in terms of varied disaster scenarios, causing the induced demand fluctuation at sources. In this work, we attempt to combine the approaches in stochastic and robust optimization literature to address scenario-based uncertainties by considering a new objective measure. For a strategic level integration of the supply and demand sides, we consider a multi-objective problem with objectives: (1) fast evacuation, and (2) cost minimization due to evacuee- and relief-flows. For objective (1), we consider minimizing *critical distance*, the maximum travel distance for an evacuee to reach a shelter. For objective (2), we consider minimizing the fixed cost to open DCs and shelters to satisfy the demand induced

by any of the disaster scenarios, along with a weighted sum of two more flow-related cost components. First, minimizing the maximum flow cost (robust optimization approach), and second, minimizing the average flow cost (stochastic optimization approach), both, over all scenarios. Combining them together helps in the situation when the worst case scenario is significantly different from the most other scenarios. In such case, if we consider minimizing only the average flow cost, the worst case scenario flow cost can be exorbitant. On the other hand, minimizing only the worst case cost produces a conservative solution, building redundancy in the system. However, considering the weighted sum of these two cost components together in the objective function, we achieve a balance. Thus, we offer a flexible decision making tool to explore the trade-offs between the worst case and average system cost minimization, and to observe their implications on solution.

From the methodological perspective, we develop a Benders decomposition (BD) based solution approach that is essential to solve large scale realistic problem because the state-of-the-art solver is inadequate for large networks with many scenarios. We develop three BD models to apply in different situations based on the decision maker's emphasis on cost minimization at the worst, average, or in-between situations. Exploiting the model structure, we decompose the overall problem and further separate the subproblem into smaller LPs, that enables us to solve large instances where an off-the-shelf solver fails. We employ various acceleration approaches and present their outcomes by conducting a detailed computational study on a realistic network. Finally, we apply the model to GIS-based case study with scenario-based demand uncertainty representation on coastal Texas region. We discuss the effects of varying (1) critical distance, (2) relative weights on the worst case and average cost terms in the objective function and illustrate the interactions between these factors.

The remainder of this section is organized as follows. As the current problem is

built upon the works presented in Sections 2 and 3, with the similar general problem setting, we refer our readers to §2.2 and §3.2 for discussion on the related literature. We explain the problem setting in §4.2, followed by introduction to the notation and model formulation in §4.3. In §4.4, a general solution approach is discussed for the multi-objective model, followed by the Benders Decomposition (BD) framework with its necessary modifications to apply to different problem classes. Several possible performance enhancements are considered to solve large scale problems efficiently. In §4.5, a GIS data based case study is conducted, with computational experiments on a realistic network, and the analytical results are presented. The computational results and comparisons of the solution methodologies are reported in §4.5.3. Finally, we summarize our conclusions in §4.6.

4.2 Problem Setting

We consider a three-tier system consisting of evacuation source, shelter and DC (see Figure 4.1) similar to the system described in Section 2. However, we simplify the problem setting by considering only single capacity level at the shelters, thus replacing the staircase structure by a single value for the fixed cost of opening a shelter. Moreover, instead of considering multiple relief items having different unit transportation costs and different consumption levels, we consider aggregation of these items in the form of survival kits, containing several relief items at pre-determined quantities. We now consider per head demand of these kits instead of accounting for each relief item separately. We now describe the three tiers of our system. Sources represent the habitats near the coastline, most vulnerable to hurricane-type disaster. On receiving evacuation order from the authorities, a certain fraction of the population from each likely to be impacted source take refuge in the shelters, operative at a safe distance from the coastline. Large distribution centers (DC), geographically

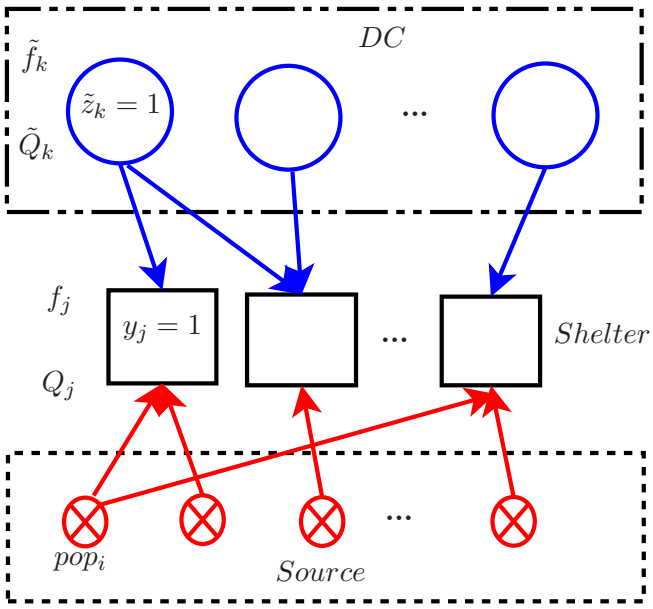

Figure 4.1: Problem Setting

located farther away from the coastal area, stockpile essential relief items and supply to the assigned shelters as need arises in the wake of a disaster. Thus, the shelters, staying at the middle tier, receiving both the relief- and evacuee-flows, connects the supply and demand sides. We justify our consideration of DC and shelter as separate entities in Section 2. We present a detailed discussion on considering centralized storage location for a different problem setting in §3.3.3, which is applicable to DC as well in our current setting. In brief, DCs, with adequate space, specialized storage and handling equipment, help in inventory aggregation. A dedicated DC provides operational advantage by facilitating bulk transportation. On the other hand, the shelters, operating as makeshift arrangements at public buildings, can accommodate evacuees during emergency, but are barely equipped for bulk logistical operation. As the DCs and sources are located at the opposite sides of the shelters, the evacuee- and relief-flows are less likely to intervene each other, thus, reducing the delay in distribution from DC to shelter.

4.2.1 Uncertainty Representation

Unlike the deterministic problem in Section 2, in this work, we include a set of randomly generated disaster scenarios. We consider uncertainties in disaster location and intensity that affect the overall demand in the system. The number of evacuees leaving a source depends on whether the source is facing a mild tropical storm or a high category hurricane. Also, as a hurricane's strength gradually decreases as it moves inland, the location of a source node with respect to the coastline strongly influences the evacuee-volume. We generate a set of random storm scenarios. Each element of this set is a demand vector representing the nominal number of evacuees leaving each source under that scenario. For each scenario and each source, we further estimate an evacuation fraction, based on the source location relative to the coast and the disaster intensity (see detailed description in §4.5.2). Multiplying the nominal demand with this evacuation fraction, we obtain estimated demand at each source. We do not further model the uncertainty caused by human behavior when some evacuees do not adhere to the suggested evacuation plan by not going to their assigned shelters. Our focus in this study is to understand the effect of minimizing the worst case and average flow costs together, according to their relative importances, along with reducing fixed cost of infrastructure building. We consider only the uncertainty in source demand data, but note that other sources of uncertainties may also be included in the model as the respective scenario-indexed vectors.

4.2.2 Problem Characteristics and Assumptions

Our goal is to design a relief network that reduces (1) evacuation time and (2) logistics cost. To ensure fast evacuation (objective (1)), as in section 2, we minimize the maximum source to shelter travel distance of the evacuees (critical distance). For objective (2), we consider total system cost reduction in two stages. The first

stage involves fixed costs due to pre-disaster opening of DC and shelter facilities. The second stage includes weighted sum of two cost components: (a) worst case evacuee- and relief-flow costs, and (b) average flow cost, over all scenarios. A small value of the critical distance (CD) ensures fast evacuation and reduces the evacuees' transportation cost. However, it increases the DC to shelter relief distribution cost, thus escalating the overall system cost. In this work, as opposed to total flow cost minimization, we consider the minimization of the weighted sum of maximum and average flow costs over all scenarios. Therefore, a non-trivial interaction is expected between the CD and the weighted logistics cost based objective. To understand the effects of CD, relative weights assigned to the worst case and average case transportation cost components, we construct a two-stage optimization model to design a strategic network. Before presenting our model, we first highlight the important **design characteristics and assumptions**.

1. Disaster scenarios are discrete and independent. We assume that any two scenarios do not occur simultaneously. Each scenario is equally likely, with the sum of their probabilities of occurrence being equal to one.

2. Considering the demand uncertainty as discussed in §4.2.1, we estimate the number of evacuees representing demand at that source. After this estimation, our model ensures total coverage of this estimated population, unlike several studies that allow resource shortage and with the help of penalty cost, try to minimize its adverse effect on the system.

3. The system is multi-sourcing. Evacuees from one source can go to multiple shelters, and a shelter can receive evacuee-inflow from multiple sources. The same is true for the supply side, between DC and shelter.

4. We consider limited capacities for the DC and shelters. The fixed costs of opening these facilities are proportional to their capacities.

5. We use different unit costs for evacuee and relief transportation, the latter being significantly lesser considering the bulk transportation of the relief items. We assume that the evacuees mainly use their personal transports.

6. Instead of considering the total system cost minimization objective as used in any optimization problem in a regular business environment, we introduce a variation in the objective function to measure the goodness of the solution. We combine the robust and stochastic optimization concepts in the form of a weighted sum of the worst case and the average case transportation costs over all disaster scenarios as a part of our objective. Now, in addition to minimizing the fixed costs of opening DCs and shelters (first stage), based on the decision-maker's emphasis on minimizing the worst or average transportation cost or a balance between them (second stage), our model prescribes a strategic solution.

For an integrated relief network with these assumptions and design characteristics, we determine (1) optimal locations to open the shelters and DCs, (2) source-to-shelter and DC-to-shelter assignments and corresponding flows, and (3) the critical travel distance for an evacuee to reach a shelter, so as to minimize: (a) maximum travel distance for evacuees, (b) weighted sum of the worst case and average case transportation costs due to evacuee- and relief- flows.

We next present our integrated multi-objective model.

4.3 Model Formulation

We first introduce the following notation.

Sets and Indices

$\mathcal{I}$	Set of sources of evacuation, $i \in \mathcal{I}$
$\mathcal{J}$	Set of existing shelter locations, $j \in \mathcal{J}$
$\mathcal{K}$	Set of existing DC locations, $k \in \mathcal{K}$
$\mathcal{S}$	Set of disaster events, $s \in \mathcal{S}$

Model Parameters

pop_i	Total population at source $i \in \mathcal{I}$
pop_{is}	Evacuating population from source $i \in \mathcal{I}$ during scenario $s \in \mathcal{S}$
Q_j^{SH}	Shelter capacity at location $j \in \mathcal{J}$ (persons)
$\tilde{Q}_k^{DC}$	DC capacity at $k \in \mathcal{K}$ for storing relief (units)
f_j	Fixed cost for opening a shelter at location $j \in \mathcal{J}$
$\tilde{f}_k$	Fixed cost for opening a DC at location $k \in \mathcal{K}$
d_{ij}	Distance from a node $i \in \mathcal{I} \cup \mathcal{K}$ to node $j \in \mathcal{J}$
α	Unit transportation cost for an evacuee (\$/person-mile)
c_{ij}	$:= \alpha\ d_{ij}$, Transportation cost to move a person from i to j
β	Unit transportation cost for relief (\$/unit-mile)
$\tilde{c}_{kj}$	$:= \beta\ d_{kj}$, unit cost to send relief from node $k \in \mathcal{K}$ to node $j \in \mathcal{J}$
CD	Critical Distance
ϕ	Per head demand for relief item (units/person)
p_s	Probability of occurrence of scenario $s \in \mathcal{S}$
ω_1	Weight of maximum flow cost over all scenarios $s \in \mathcal{S}$
ω_2	Weight of expected flow cost over all scenarios $s \in \mathcal{S}$

Decision Variables

x_{ij}^s	Number of people from source $i \in \mathcal{I}$ going to shelter $j \in \mathcal{J}$ during $s \in \mathcal{S}$
$\tilde{x}_{kj}^s$	Units of relief shipped from DC $k \in \mathcal{K}$ to shelter $j \in \mathcal{J}$ during $s \in \mathcal{S}$

y_j 1, if shelter opens at $j \in \mathcal{J}, 0$ otherwise

$\tilde{z}_k$ 1, if DC opens at $k \in \mathcal{K}, 0$ otherwise

u_{ij} 1, if origin $i \in \mathcal{I}$ is assigned to shelter $j \in \mathcal{J}, 0$ otherwise.

We present the problem P as follows:

$$\text{Min} \qquad Z_1 = \{\max_{i\in\mathcal{I}, j\in\mathcal{J}} u_{ij} d_{ij}\} \tag{4.1}$$

$$\begin{aligned}\text{Min} \qquad Z_2 = \sum_{k\in\mathcal{K}} \tilde{f}_k \tilde{z}_k + \sum_{j\in\mathcal{J}} f_j y_j + \omega_1 \max_{s\in\mathcal{S}}\{\sum_{i\in\mathcal{I}}\sum_{j\in\mathcal{J}} c_{ij} x_{ij}^s + \sum_{k\in\mathcal{K}}\sum_{j\in\mathcal{J}} \tilde{c}_{kj}\tilde{x}_{kj}^s\} \\ + \omega_2 \sum_{s\in\mathcal{S}} p_s\{\sum_{i\in\mathcal{I}}\sum_{j\in\mathcal{J}} c_{ij} x_{ij}^s + \sum_{k\in\mathcal{K}}\sum_{j\in\mathcal{J}} \tilde{c}_{kj}\tilde{x}_{kj}^s\}\end{aligned} \tag{4.2}$$

subject to

$$\sum_{j\in\mathcal{J}} x_{ij}^s \geq pop_{is} \qquad \forall i \in \mathcal{I},\, \forall s \in \mathcal{S} \tag{4.3}$$

$$\sum_{i\in\mathcal{I}} x_{ij}^s \leq Q_j^{SH} y_j \qquad \forall j \in \mathcal{J},\, \forall s \in \mathcal{S} \tag{4.4}$$

$$\sum_{k\in\mathcal{K}} \tilde{x}_{kj}^s \geq \phi \sum_{i\in\mathcal{I}} x_{ij}^s \qquad \forall j \in \mathcal{J},\, \forall s \in \mathcal{S} \tag{4.5}$$

$$\sum_{j\in\mathcal{J}} \tilde{x}_{kj}^s \leq \tilde{Q}_k^{DC} \tilde{z}_k \qquad \forall k \in \mathcal{K},\, \forall s \in \mathcal{S} \tag{4.6}$$

$$x_{ij}^s \leq M\, u_{ij}, \;\; u_{ij} \leq y_j \qquad \forall i \in \mathcal{I},\, \forall j \in \mathcal{J},\, \forall s \in \mathcal{S} \tag{4.7}$$

$$x_{ij}^s, \tilde{x}_{kj}^s \geq 0 \qquad \forall i \in \mathcal{I}, \forall j \in \mathcal{J}, \forall k \in \mathcal{K}, \forall s \in \mathcal{S} \tag{4.8}$$

$$u_{ij}, y_j, \tilde{z}_k \in \{0, 1\} \qquad \forall i \in \mathcal{I}, \forall j \in \mathcal{J}, \forall k \in \mathcal{K}. \tag{4.9}$$

We now describe the multi-objective model P. The objective (4.1) minimizes the maximum distance between any origin and shelter. The objective (4.2) minimizes

the weighted sum of two cost components along with the fixed costs of infrastructure building. The first two terms of (4.2) represent the fixed costs of opening the DCs and shelters respectively. The third term represents the maximum cost for evacuee and relief transportation over all $|\mathcal{S}|$ scenarios with an associated cost ω_1. The fourth term in the objective (4.2) represents the average of the transportation costs for all $|\mathcal{S}|$ scenarios, with ω_2 as the associated weight factors. Thus, we want to obtain a solution that not only minimizes the first stage cost for infrastructure building but also reduces the transportation cost in the worst case and average case, according to their relative emphasis expressed by the decision-maker while specifying (ω_1, ω_2). Among the constraints, (4.3) ensures that under each scenario $s \in \mathcal{S}$, for every source node $i \in \mathcal{I}$, the estimated number of evacuees pop_{is} are accommodated by the open shelters. The shelter capacity constraint (4.4) ensures that for any scenario $s \in \mathcal{S}$, total evacuee inflow from all the affected sources into a shelter $j \in \mathcal{J}$ must not exceed its capacity. Observe, if $y_j = 0$, i.e., a shelter is closed, its available capacity becomes zero, as expressed by the right hand side of (4.4). Constraint (4.5) ensures demand fulfillment at a shelter $j \in \mathcal{J}$. Total supply from all open DCs to the shelter j must be adequate to satisfy the accommodated evacuees' need for the relief items. Constraint (4.6) is the DC capacity constraint. It ensures that the total outbound relief from a DC $k \in \mathcal{K}$ must not exceed its capacity. Similar to (4.4), if a DC location is not open, $\tilde{z}_k$ becomes zero, eliminating its available capacity, therefore, no relief flow occurs from that DC. Constraints (4.7) ensure that shelters and origin-to-shelter links are created properly based on flow. In the first part of (4.7), M stands for a very large value (big-M), to ensure appropriate upper bound of x_{ij}^s variables, based on the u_{ij} values. Finally, constraints (4.8) and (4.9) state the variable range requirements.

4.4 Solution Approach

We first observe that the model (4.1) - (4.9) can be converted from multi-objective to single objective using the similar approach discussed in §2.4. For this, first, by introducing a non-negative continuous auxiliary variable CD for the critical distance, we simplify the minimax-type objective (4.1) to minimization-type (4.10) as follows:

$$\begin{array}{ll} \text{Min} & CD \\ \text{Min} & Z_2 \end{array} \tag{4.10}$$

subject to

$$u_{ij} d_{ij} \leq CD \qquad \forall i \in \mathcal{I}, \forall j \in \mathcal{J} \tag{4.11}$$

$$CD \geq 0 \tag{4.12}$$

(4.3) to (4.9).

Since at optimality, CD, the maximum source to shelter distance obtains a value equal to one of the (i, j) links, we pre-process to populate a sorted distance list $\mathcal{D} := \{d_{ij} | i \in \mathcal{I}, j \in \mathcal{J}\}$. From the practical application perspective, we do not even need to consider all possible d_{ij} values if one list entry differs negligibly from its adjacent entry. Therefore, we populate $\mathcal{D}$ with an increasing series of integers, with meaningful difference between the list elements. Now, for each chosen $\widehat{CD} \in \mathcal{D}$, we can solve the model P with only objective (4.2) subject to constraints (4.3) - (4.9). However, to avoid any source-to-shelter assignment with $d_{ij} > \widehat{CD}$, we construct a binary accessibility matrix $[a_{ij}]$:

$$a_{ij} = \begin{cases} 1, & \text{if } d_{ij} \leq \widehat{CD} \qquad \forall i \in \mathcal{I},\ j \in \mathcal{J} \\ 0, & \text{otherwise,} \end{cases} \tag{4.13}$$

and, with big-M, we redefine the unit transportation cost of the evacuees m_{ij} as:

$$m_{ij} := \alpha \times d_{ij} + M\,(1 - a_{ij}) \qquad \forall i \in \mathcal{I}, \forall j \in \mathcal{J}. \tag{4.14}$$

Thus, for a given $\widehat{CD}$, we solve the following single objective model P($\widehat{CD}$):

$$\text{P }(\widehat{CD})\ \text{Min } Z_2 = \sum_{k\in\mathcal{K}} \tilde{f}_k \tilde{z}_k + \sum_{j\in\mathcal{J}} f_j y_j + \omega_1 \max_{s\in\mathcal{S}}\{\sum_{i\in\mathcal{I}}\sum_{j\in\mathcal{J}} m_{ij} x^s_{ij} + \sum_{k\in\mathcal{K}}\sum_{j\in\mathcal{J}} \tilde{c}_{kj}\tilde{x}^s_{kj}\}$$
$$+ \omega_2 \sum_{s\in\mathcal{S}} p_s\{\sum_{i\in\mathcal{I}}\sum_{j\in\mathcal{J}} m_{ij} x^s_{ij} + \sum_{k\in\mathcal{K}}\sum_{j\in\mathcal{J}} \tilde{c}_{kj}\tilde{x}^s_{kj}\} \tag{4.15}$$

$$\text{subject to} \qquad (4.3) \text{ to } (4.6), \quad \text{and} \quad (4.8) \text{ to } (4.9).$$

After obtaining a single-objective model, we simplify the min-max part of the Objective (4.15) by introducing a non-negative, continuous, auxiliary variable Ψ to get the following form:

$$\text{P }(\widehat{CD})\ \text{Min } Z_2 = \sum_{k\in\mathcal{K}} \tilde{f}_k \tilde{z}_k + \sum_{j\in\mathcal{J}} f_j y_j$$
$$+ \omega_1 \Psi + \omega_2 \sum_{s\in\mathcal{S}} p_s\{\sum_{i\in\mathcal{I}}\sum_{j\in\mathcal{J}} m_{ij} x^s_{ij} + \sum_{k\in\mathcal{K}}\sum_{j\in\mathcal{J}} \tilde{c}_{kj}\tilde{x}^s_{kj}\} \tag{4.16}$$

subject to

$$\sum_{i\in\mathcal{I}}\sum_{j\in\mathcal{J}} m_{ij} x^s_{ij} + \sum_{k\in\mathcal{K}}\sum_{j\in\mathcal{J}} \tilde{c}_{kj}\tilde{x}^s_{kj} \le \Psi \qquad \forall s \in \mathcal{S} \tag{4.17}$$

$$\Psi \ge 0 \tag{4.18}$$

(4.3) to (4.6), and (4.8) to (4.9).

Next, discuss how Benders Decomposition (BD) is applicable to the above model.

4.4.1 Benders Decomposition Framework

We observe that in the MIP problem P($\widehat{CD}$), if y_j and $\tilde{z}_k$ values are known, then the remaining problem becomes a LP with only continuous variables x_{ij}^s and $\tilde{x}_{kj}^s$. Therefore, to solve large scale instances of P($\widehat{CD}$), Benders Decomposition(BD) can be effective. In BD, the overall model is decomposed into a master problem (**MP**) and a subproblem (**SP**). In an iterative framework, by transferring one-another's solution, the overall problem's solution gradually converges towards optimality. The MP mainly contains the integer variables and one continuous variable that connects the **MP** with **SP**. However, in our problem P($\widehat{CD}$), even when the binary vectors $\mathbf{y}, \mathbf{z}$ are fixed, the LP subproblem is not easy to solve. When the relative weights (ω_1, ω_2) are fractional, both the worst case and average transportation cost minimization terms stay together in the objective , and hinder the possibility of separating the **SP** into $|\mathbf{S}|$ independent small LPs and solve efficiently. Therefore, as $|\mathbf{S}|$ increases, the traditional BD framework becomes ineffective, as we have to solve increasingly large **SP**, with minimax type term present in the objective. However, when only one of these weighted terms corresponding to either worst case or average transportation cost is present (either $\omega_1 = 0$, or $\omega_2 = 0$), the **SP** becomes separable. With this observation, we devise different variations of BD implementations to solve the P($\widehat{CD}$) problem efficiently for different weight combinations (ω_1, ω_2). In particular, we develop three distinct BD versions as follows:

- BD-I : When $\omega_1 = 0, \omega_2 = 1$, i.e., minimizing average flow cost over all scenarios, along with fixed costs.
- BD-II : When $\omega_1 = 1, \omega_2 = 0$, i.e., minimizing the maximum flow cost over all scenarios, along with fixed costs.

- BD-III : When $(\omega_1, \omega_2) \in (0, 1)$, i.e., minimizing weighted sum of average and worst case flow costs over all scenarios, along with fixed costs.

We discuss these three implementations next.

4.4.1.1 BD-I : (ω_1 = 0, ω_2 = 1)

With $\omega_1 = 0$, $\omega_2 = 1$, we obtain the following problem P($\widehat{CD}|\omega_1 = 0, \omega_2 = 1$):

$$\text{P } (\widehat{CD}|(0,1)) \text{ Min Z} = \sum_{k\in\mathcal{K}} \tilde{f}_k \tilde{z}_k + \sum_{j\in\mathcal{J}} f_j y_j + \sum_{s\in\mathcal{S}} p_s \{ \sum_{i\in\mathcal{I}} \sum_{j\in\mathcal{J}} m_{ij} x^s_{ij} + \sum_{k\in\mathcal{K}} \sum_{j\in\mathcal{J}} \tilde{c}_{kj} \tilde{x}^s_{kj} \} \tag{4.19}$$

subject to

$$\sum_{i\in\mathcal{I}} \sum_{j\in\mathcal{J}} m_{ij} x^s_{ij} + \sum_{k\in\mathcal{K}} \sum_{j\in\mathcal{J}} \tilde{c}_{kj} \tilde{x}^s_{kj} \leq \Psi \qquad \forall s \in \mathcal{S} \tag{4.20}$$

$$\Psi \geq 0$$

(4.3) to (4.6), and (4.8) to (4.9).

This is a two-stage model to minimize the cost of opening the DCs and shelters at the first stage, and average flow cost over all scenarios in the second stage. Observe, absence of the variable Ψ from the objective function makes the constraint (4.20) redundant. In this setting, considering the binary vectors $(\mathbf{y}, \mathbf{z})$ as fixed, we can easily employ BD to decompose the overall problem P($\widehat{CD}|(0,1)$) into one **MP** and $|\mathcal{S}|$ separable smaller subproblems. Eliminating constraint (4.20), for each $s \in \mathcal{S}$, we obtain the primal subproblem $\mathbf{PSP}^s(\mathbf{x}, \tilde{\mathbf{x}}|\widehat{\mathbf{y}}, \widehat{\mathbf{z}})$ as follows.

$$\text{Min } Z_{PSP^s} = p_s \{ \sum_{i\in\mathcal{I}} \sum_{j\in\mathcal{J}} m_{ij} x^s_{ij} + \sum_{k\in\mathcal{K}} \sum_{j\in\mathcal{J}} \tilde{c}_{kj} \tilde{x}^s_{kj} \} \tag{4.21}$$

subject to

$$\sum_{j\in\mathcal{J}} x_{ij}^s \geq pop_{is} \qquad \forall i \in \mathcal{I} \tag{4.22}$$

$$\sum_{i\in\mathcal{I}} x_{ij}^s \leq Q_j^{SH}\widehat{y}_j \qquad \forall j \in \mathcal{J} \tag{4.23}$$

$$\sum_{k\in\mathcal{K}} \tilde{x}_{kj}^s \geq \phi \sum_{i\in\mathcal{I}} x_{ij}^s \qquad \forall j \in \mathcal{J} \tag{4.24}$$

$$\sum_{j\in\mathcal{J}} \tilde{x}_{kj}^s \leq \tilde{Q}_k^{DC}\widehat{\tilde{z}}_k \qquad \forall k \in \mathcal{K} \tag{4.25}$$

$$x_{ij}^s, \tilde{x}_{kj}^s \geq 0 \qquad \forall i \in \mathcal{I}, \forall j \in \mathcal{J}, \forall k \in \mathcal{K}. \tag{4.26}$$

For each $s \in \mathcal{S}$, defining dual variables $\alpha_{is}, \beta_{js}, \gamma_{js}, \mu_{ks}$ corresponding to constraints (4.22) - (4.25), the Dual Subproblem $\mathbf{DSP}^s(\boldsymbol{\alpha}, \boldsymbol{\beta}, \boldsymbol{\gamma}, \boldsymbol{\mu}|\widehat{\mathbf{y}}, \widehat{\mathbf{z}})$ is as follows:

$$\text{Maximize } Z_{DSP^s} = \sum_{i\in\mathcal{I}} pop_{is}\alpha_{is} - \sum_{j\in\mathcal{J}} Q_j^{SH}\widehat{y}_j\beta_{js} - \sum_{k\in\mathcal{K}} \tilde{Q}_k^{DC}\widehat{\tilde{z}}_k\mu_{ks} \tag{4.27}$$

subject to

$$\alpha_{is} - \beta_{js} - \phi\gamma_{js} \leq p_s m_{ij} \qquad \forall i \in \mathcal{I}, \forall j \in \mathcal{J} \tag{4.28}$$

$$\gamma_{js} - \mu_{ks} \leq p_s \tilde{c}_{kj} \qquad \forall k \in \mathcal{K}, \forall j \in \mathcal{J} \tag{4.29}$$

$$\alpha_{is}, \beta_{js}, \gamma_{js}, \mu_{ks} \geq 0 \qquad \forall i \in \mathcal{I}, \forall j \in \mathcal{J}, \forall k \in \mathcal{K}. \tag{4.30}$$

Let Θ denote the set of all extreme points of the $\mathbf{DSP}^s$ polyhedron specified by (4.28) - (4.30). For each extreme point $\theta \in \Theta$, we denote the associated variables $\alpha_{is}^\theta, \beta_{js}^\theta, \gamma_{js}^\theta, \mu_{ks}^\theta$ and the objective function D_s^θ. If the optimal objective value is D_s^*, then $D_s^* \geq D_s^\theta, \forall\theta \in \Theta$. We can restate $\mathbf{DSP}^s$ as $\min_{D_s\geq 0}\{D_s : D_s \geq D_s^\theta, \forall\theta \in \Theta\}$

where

$$D_s^\theta = \sum_{i\in\mathcal{I}} pop_{is}\alpha_{is}^\theta - \sum_{j\in\mathcal{J}} Q_j^{SH}\widehat{y}_j\beta_{js}^\theta - \sum_{k\in\mathcal{K}} \tilde{Q}_k^{DC}\widehat{\tilde{z}}_k\mu_{ks}^\theta.$$

With the above representation of $\mathbf{DSP}^s$ by using the extreme points of its polyhedron, we reformulate the overall problem as:

$$\text{Min } Z_{MP} = \sum_{k\in\mathcal{K}} \tilde{f}_k\tilde{z}_k + \sum_{j\in\mathcal{J}} f_j y_j + \sum_s D_s \tag{4.31}$$

subject to

$$\sum_{k\in\mathcal{K}} \tilde{Q}_k^{DC}\tilde{z}_k \geq \phi \max_{s\in\mathcal{S}}\{\sum_{i\in\mathcal{I}} pop_{is}\} \tag{4.32}$$

$$\sum_{j\in\mathcal{J}} Q_j^{SH} y_j \geq \max_{s\in\mathcal{S}}\{\sum_{i\in\mathcal{I}} pop_{is}\} \tag{4.33}$$

$$D_s \geq \sum_{i\in\mathcal{I}} pop_{is}\widehat{\alpha}_{is}^\theta - \sum_{j\in\mathcal{J}} Q_j^{SH}\widehat{\beta}_{js}^\theta y_j - \sum_{k\in\mathcal{K}} \tilde{Q}_k^{DC}\widehat{\mu}_{ks}^\theta\tilde{z}_k \qquad \forall\theta\in\Theta, \forall s\in\mathcal{S} \tag{4.34}$$

$$D_s \geq 0, \qquad y_j, \tilde{z}_k \in \{0,1\} \qquad \forall s\in\mathcal{S}, \forall k\in\mathcal{K}, \forall j\in\mathcal{J}. \tag{4.35}$$

This model is difficult to solve due to a huge number of type (4.34) constraints, however, not all of those are binding. Therefore, in Benders Decomposition, we start by solving the master problem (**MP**) by considering only a subset of (4.34). As **MP** is a relaxation of the original model since it does not contain all (4.34) type constraints in the overall problems reformulation, its optimal solution provides a valid lower bound of our overall problem. At an iteration θ, we solve the $|\mathcal{S}|$ independent $\mathbf{DSP}^s(\boldsymbol{\alpha}, \boldsymbol{\beta}, \boldsymbol{\gamma}, \boldsymbol{\mu}|\widehat{\mathbf{y}}, \widehat{\mathbf{z}})$ problems, and using the obtained dual solutions we generate $|\mathcal{S}|$ (4.34) cuts corresponding to the θ-th extreme point of the DSP^s polyhedron, and add it to the **MP**. We emphasize at this point, there is no need to aggregate

$|\mathcal{S}|$ individual BD cuts to make a single cut before adding to **MP**. In fact, such aggregation generally weakens the cut and negatively affects the convergence rate. Moreover, for BD-I problem setting, it is enough to add only the optimality cuts, based on extreme points of DSP polyhedron, because even if the distance d_{ij} between an evacuation source i and a shelter j is larger than given $\widehat{CD}$, we assume link (i, j) as connected, however, usage of such link incurs a huge penalty cost. Therefore, the **PSP**^{s} is always feasible with respect to any $(\widehat{\mathbf{y}}, \widehat{\mathbf{z}})$ pair, hence, the corresponding **DSP**^{s} is always bounded. Therefore, we only need to add Benders optimality cuts rather than feasibility cuts, based on the extreme rays of the **DSP**^{s}, that may hamper BD convergence. To this end, we also utilize surrogate constraints to ensure that the network provided by the **MP** solution, based on the values of $(\mathbf{y}, \tilde{\mathbf{z}})$, does not lead to subproblem infeasibility. Specifically, constraint (4.32) ensures aggregate demand satisfaction for the relief items by the open DCs for any scenario $s \in \mathcal{S}$, and constraint (4.33) ensures all evacuees' accommodation by opening enough shelters, again, for any scenario $s \in \mathcal{S}$.

4.4.1.2 BD-II : ($\omega_1 = 1$, $\omega_2 = 0$)

With $\omega_1 = 1$, $\omega_2 = 0$, we obtain the following problem P($\widehat{CD}|\omega_1 = 1, \omega_2 = 0$):

$$\text{P } (\widehat{CD}|(1,0)) \text{ Min Z} = \sum_{k \in \mathcal{K}} \tilde{f}_k \tilde{z}_k + \sum_{j \in \mathcal{J}} f_j y_j + \Psi \tag{4.36}$$

subject to

$$\sum_{i\in\mathcal{I}}\sum_{j\in\mathcal{J}} m_{ij}x^s_{ij} + \sum_{k\in\mathcal{K}}\sum_{j\in\mathcal{J}} \tilde{c}_{kj}\tilde{x}^s_{kj} \leq \Psi \qquad \forall s \in \mathcal{S}$$

$$\Psi \geq 0$$

(4.3) to (4.6), and (4.8) to (4.9).

Here we have the model P $(\widehat{CD}|(1,0))$ to minimize the fixed costs of opening the DCs and shelters, and the maximum flow cost over all scenarios. In this setting, if the binary vectors $(\mathbf{y}, \mathbf{z})$ are fixed, the remaining LP problem essentially converts to solving $|\mathcal{S}|$ separable, independent subproblems and selecting the PSP^s with maximum objective value. Therefore, we can easily employ BD to decompose the overall problem P$(\widehat{CD}|(0,1))$ into one **MP** and $|\mathcal{S}|$ separable smaller subproblems as before. The **PSP**$^s(\mathbf{x}, \tilde{\mathbf{x}}|\widehat{\mathbf{y}}, \widehat{\mathbf{z}})$ is as follows.

$$\text{Min } Z_{PSP^s} = \sum_{i\in\mathcal{I}}\sum_{j\in\mathcal{J}} m_{ij}x^s_{ij} + \sum_{k\in\mathcal{K}}\sum_{j\in\mathcal{J}} \tilde{c}_{kj}\tilde{x}^s_{kj} \tag{4.37}$$

$$\text{subject to} \qquad (4.22) - (4.26).$$

Similar to BD-I, we construct the Dual Subproblem **DSP**$^s(\boldsymbol{\alpha}, \boldsymbol{\beta}, \boldsymbol{\gamma}, \boldsymbol{\mu}|\widehat{\mathbf{y}}, \widehat{\mathbf{z}})$ for each $s \in \mathcal{S}$, by defining dual variables $\alpha_{is}, \beta_{js}, \gamma_{js}, \mu_{ks}$ corresponding to constraints (4.22) - (4.25):

$$\text{Maximize } Z_{DSP^s} = \sum_{i\in\mathcal{I}} pop_{is}\alpha_{is} - \sum_{j\in\mathcal{J}} Q^{SH}_j \widehat{y}_j \beta_{js} - \sum_{k\in\mathcal{K}} \tilde{Q}^{DC}_k \widehat{\tilde{z}}_k \mu_{ks} \tag{4.38}$$

subject to

$$\alpha_{is} - \beta_{js} - \phi\gamma_{js} \leq m_{ij} \qquad \forall i \in \mathcal{I}, \forall j \in \mathcal{J} \tag{4.39}$$

$$\gamma_{js} - \mu_{ks} \leq \tilde{c}_{kj} \qquad \forall k \in \mathcal{K}, \forall j \in \mathcal{J} \tag{4.40}$$

$$\alpha_{is}, \beta_{js}, \gamma_{js}, \mu_{ks} \geq 0 \qquad \forall i \in \mathcal{I}, \forall j \in \mathcal{J}, \forall k \in \mathcal{K}. \tag{4.41}$$

Following the same discussion in §4.4.1.1, we solve $|\mathcal{S}|$ separate $\mathbf{DSP}^s$ problems, and corresponding to each extreme point θ of the $\mathbf{DSP}^s$ polyhedron, construct a BD optimality cut to add to the **MP**. However, we observe, instead of adding all $|\mathcal{S}|$ BD cuts at each iteration θ, it is sufficient to add only one, corresponding to scenario index $s \in \mathcal{S}$ with the maximum $\mathbf{DSP}^s$ objective value in that iteration. Next, we present the **MP** in BD-II setting.

$$\text{Min } Z_{MP} = \sum_{k \in \mathcal{K}} \tilde{f}_k \tilde{z}_k + \sum_{j \in \mathcal{J}} f_j y_j + D \tag{4.42}$$

subject to $\quad (4.32) - (4.33)$

$$D \geq \max_{s \in \mathcal{S}} \{ \sum_{i \in \mathcal{I}} pop_{is} \widehat{\alpha}^{\theta}_{is} - \sum_{j \in \mathcal{J}} Q^{SH}_j \widehat{\beta}^{\theta}_{js} y_j - \sum_{k \in \mathcal{K}} \tilde{Q}^{DC}_k \widehat{\mu}^{\theta}_{ks} \tilde{z}_k \} \qquad \forall \theta \in \Theta \tag{4.43}$$

$$D \geq 0 \tag{4.44}$$

$$y_j, \tilde{z}_k \in \{0, 1\} \qquad \forall k \in \mathcal{K}, \forall j \in \mathcal{J}. \tag{4.45}$$

4.4.1.3 BD-III : ($\omega_1, \omega_2 \in (0, 1)$)

When both the weights (ω_1, ω_2) take fractional values, we lose the advantage of separating the problem as discussed in §4.4.1.1 and §4.4.1.2. In order to be able to obtain separable subproblems in Benders decomposition setting, we introduce in the

original model auxiliary variables $\psi_s \geq 0$ for each scenario $s \in \mathcal{S}$.

$$\text{P } (\widehat{CD}|(\omega_1,\omega_2)) \text{ Min Z} = \sum_{k\in\mathcal{K}} \tilde{f}_k \tilde{z}_k + \sum_{j\in\mathcal{J}} f_j y_j + \omega_1 \Psi + \omega_2 \sum_{s\in\mathcal{S}} p_s \{\sum_{i\in\mathcal{I}}\sum_{j\in\mathcal{J}} m_{ij} x_{ij}^s + \sum_{k\in\mathcal{K}}\sum_{j\in\mathcal{J}} \tilde{c}_{kj}\tilde{x}_{kj}^s\} \quad (4.46)$$

subject to

$$\sum_{i\in\mathcal{I}}\sum_{j\in\mathcal{J}} m_{ij} x_{ij}^s + \sum_{k\in\mathcal{K}}\sum_{j\in\mathcal{J}} \tilde{c}_{kj}\tilde{x}_{kj}^s \leq \psi_s \qquad \forall s \in \mathcal{S} \quad (4.47)$$

$$\psi_s \leq \Psi, \qquad \forall s \in \mathcal{S} \quad (4.48)$$

$$\Psi, \psi_s \geq 0$$

(4.3) to (4.6), and (4.8) to (4.9).

We consider a decomposition different from the previous two cases. We keep the decision vectors $\mathbf{y}, \tilde{\mathbf{z}}$ and $\boldsymbol{\psi}$ in the **MP** and $\mathbf{x}, \tilde{\mathbf{x}}$ in the **SP**. For a solution $(\mathbf{y}, \tilde{\mathbf{z}}, \boldsymbol{\psi})$ supplied by the **MP**, the primal subproblem now becomes separable into $|\mathcal{S}|$ smaller LPs, called $\mathbf{PSP}^s(\mathbf{x}, \tilde{\mathbf{x}}|\widehat{\mathbf{y}}, \widehat{\tilde{\mathbf{z}}}, \widehat{\boldsymbol{\psi}})$ as follows:

$$\text{Min } Z_{PSP^s} = \omega_2 p_s \{\sum_{i\in\mathcal{I}}\sum_{j\in\mathcal{J}} m_{ij} x_{ij}^s + \sum_{k\in\mathcal{K}}\sum_{j\in\mathcal{J}} \tilde{c}_{kj}\tilde{x}_{kj}^s\} \quad (4.49)$$

subject to

$$\sum_{i\in\mathcal{I}}\sum_{j\in\mathcal{J}} m_{ij} x_{ij}^s + \sum_{k\in\mathcal{K}}\sum_{j\in\mathcal{J}} \tilde{c}_{kj}\tilde{x}_{kj}^s \leq \widehat{\psi}_s \quad (4.50)$$

$(4.22) - (4.26)$.

Next, for each $s \in \mathcal{S}$, defining dual variables $\pi_s, \alpha_{is}, \beta_{js}, \gamma_{js}, \mu_{ks}$ corresponding to constraints (4.50), (4.22) - (4.25), the Dual Problem $\mathbf{DSP}^s(\boldsymbol{\alpha}, \boldsymbol{\beta}, \boldsymbol{\gamma}, \boldsymbol{\mu} | \widehat{\mathbf{y}}, \widehat{\mathbf{z}}, \widehat{\boldsymbol{\psi}})$ is as follows:

$$\text{Maximize } Z_{DSP^s} = \sum_{i \in \mathcal{I}} pop_{is} \alpha_{is} - \sum_{j \in \mathcal{J}} Q_j^{SH} \widehat{y}_j \beta_{js} - \sum_{k \in \mathcal{K}} \tilde{Q}_k^{DC} \widehat{\tilde{z}}_k \mu_{ks} - \widehat{\psi_s} \pi_s \tag{4.51}$$

subject to

$$-m_{ij}\pi_s + \alpha_{is} - \beta_{js} - \phi\gamma_{js} \leq \omega_2 p_s m_{ij} \qquad \forall i \in \mathcal{I}, \forall j \in \mathcal{J} \tag{4.52}$$

$$-\tilde{c}_{kj}\pi_s + \gamma_{js} - \mu_{ks} \leq \omega_2 p_s \tilde{c}_{kj} \qquad \forall k \in \mathcal{K}, \forall j \in \mathcal{J} \tag{4.53}$$

$$\pi_s, \alpha_{is}, \beta_{js}, \gamma_{js}, \mu_{ks} \geq 0 \qquad \forall i \in \mathcal{I}, \forall j \in \mathcal{J}, \forall k \in \mathcal{K}. \tag{4.54}$$

Based on the **MP** solution vector $(\mathbf{y}, \tilde{\mathbf{z}}_\mathbf{k}, \boldsymbol{\psi_s})$, if **PSP** is feasible, solving each $\mathbf{DSP}^s$, we obtain an optimality cut for the θ-th extreme point of DSP^s polyhedron as follows:

$$D_s \geq \sum_{i \in \mathcal{I}} pop_{is} \widehat{\alpha}_{is}^{\theta} - \sum_{j \in \mathcal{J}} Q_j^{SH} \widehat{\beta}_{js}^{\theta} y_j - \sum_{k \in \mathcal{K}} \tilde{Q}_k^{DC} \widehat{\mu}_{ks}^{\theta} \tilde{z}_k - \widehat{\pi}_s^{\theta} \psi_s, \qquad \forall \theta \in \Theta. \tag{4.55}$$

On the other hand, at the θ-th iteration, we add the following feasibility cut using an extreme ray of the dual subproblem when $\mathbf{PSP}^s$ is infeasible:

$$0 \geq \sum_{i \in \mathcal{I}} pop_{is} \widehat{\alpha}_{is}^{\theta} - \sum_{j \in \mathcal{J}} Q_j^{SH} \widehat{\beta}_{js}^{\theta} y_j - \sum_{k \in \mathcal{K}} Q_k^{DC} \widehat{\mu}_{ks}^{\theta} \tilde{z}_k - \widehat{\pi}_s^{\theta} \psi_s, \qquad \forall \theta \in \Theta. \tag{4.56}$$

Now, we present the **MP** for BD-III setting as follows:

$$\text{Min } Z_{MP} = \sum_{k \in \mathcal{K}} \tilde{f}_k \tilde{z}_k + \sum_{j \in \mathcal{J}} f_j y_j + \omega_1 \Psi + \sum_s D_s \tag{4.57}$$

subject to $(4.32) - (4.33), (4.55) - (4.56)$

$$\psi_s \leq \Psi \qquad \forall s \in \mathcal{S} \quad (4.58)$$

$$D_s \geq 0, y_j, \tilde{z}_k \in \{0,1\} \qquad \forall s \in \mathcal{S}, \forall k \in \mathcal{K}, \forall j \in \mathcal{J}. \quad (4.59)$$

As discussed in §4.4.1.2, again, at each BD iteration, we do not need to aggregate the $|\mathcal{S}|$ number of cuts before adding to **MP**. In fact, keeping the optimality cuts (4.55) and feasibility cuts (4.56) disaggregated, helps faster BD-convergence.

4.4.2 Approaches to Accelerate Benders Decomposition

We present various BD acceleration methods suggested by researchers over time in §2.4.1 and §3.5.1. Based on the success in our works presented in Sections 2 and 3, we employ those acceleration techniques, and attempt two new, model-specific techniques. In this section, we briefly explain all the techniques used in this study.

4.4.2.1 Lazy Constraint Callback

We utilize lazy constraint callback of CPLEX (version 12.4 or later) (Rubin, 2011) in our three current BD implementations described in §4.4.1.1 - §4.4.1.3. Lazy constraint callback is one type of control callbacks that CPLEX offers its users to intervene the branch-and-cut tree search process. Unlike the traditional BD implementation, where the **MP** is solved repeatedly in each iteration with single or multiple new cut addition, this callback implementation solves the **MP** only once. During the branch-and-cut execution, whenever the solver finds an incumbent, a new cut is constructed, added to the **MP** and the tree search proceeds till the stopping criteria are met or the optimal solution is obtained. This avoidance of repeated solving of the **MP** saves a significant computation time. However, it is important to note that the use of callback turns off dynamic search and deterministic parallelism

of the solver (CPLEX, 2009), forcing CPLEX to use single thread, therefore, callback is not always guaranteed to perform better.

4.4.2.2 Tuning CPLEX Parameters

In BD framework, how the branch-and-cut tree is explored has an expected impact on the strength and the timing of the bounds obtained in solving the **MP**. Thus, we examine tuning of certain tree search parameters to increase the efficiency of our implementation. We specify the tree search method to use during solving a problem through the CPLEX parameter *MIPSearch*. However, we note, if callback is used, CPLEX can no longer use dynamic search and only its conventional search method needs to be utilized. We tune the parameter *MIPEmphasis*, that specifies our emphasis on optimality or feasibility while CPLEX conducts the tree search. We try with its two settings : (a) balancing between optimality and feasibility, and (b) emphasizing optimality over feasibility. We choose the setting (b) after some initial trials, because for our problem it is important to add good quality cuts at the early stage of BD execution. Lastly, although in our previous two studies, we tune the variable selection strategy for branching at an incumbent node by specifying the parameter *Varsel* value to favor strong branching, for this study, our trial runs suggest negative impact on performance while tuning this parameter. Therefore, we leave this parameter to its default value.

4.4.2.3 Cut Strengthening

We conduct cut strengthening to further improve BD performance. For a details discussion on cut strengthening, its possible advantages, and the definition of *strongness* of a cut, we direct the reader to §2.4.2.2. The main idea behind this exercise is to explore the possibility of obtaining a stronger cut from several existing alternate optimal solutions of DSP. We now explain a problem-specific, two-phased

cut strengthening scheme. We observe, in the DSP objective function, the dual variables associated with $\widehat{y}_j$ and $\widehat{\tilde{z}}_k$ parameters do not have any impact on the optimum objective value if the corresponding $\widehat{y}_j$ and $\widehat{\tilde{z}}_k$ are zeros. Those dual variables can be modified without impacting the objective, provided that the feasibility is maintained by satisfying all **DSP** constraints (Üster and Agrahari, 2011). Although the **DSP** constraints slightly differ in BD-I, BD-II, and BD-III, our cut strengthening approach is similar in all these different implementations. Therefore, we explain the two-phased process for **DSP** of BD-III (see (4.51) - (4.54)), having the most general form among these three, as follows:

Phase 1. Instead of solving the **DSP**, we solve a *reduced* version of it where we consider only the β_{js} and μ_{ks} variables corresponding to non-zero $\widehat{y}_j$ and $\widehat{\tilde{z}}_k$ values obtained from **MP**. We consider all other dual variables for all their indices. The reduced **DSP** for each scenario $s \in \mathcal{S}$ is given as follows:

$$\text{Maximize } Z_{DSP^s} = \sum_{i \in \mathcal{I}} pop_{is}\alpha_{is} - \sum_{j \in \mathcal{J}_\mathcal{O}} Q_j^{SH}\widehat{y}_j\beta_{js} - \sum_{k \in \mathcal{K}_\mathcal{O}} \tilde{Q}_k^{DC}\widehat{\tilde{z}}_k\mu_{ks} - \widehat{\psi_s}\pi_s \quad (4.60)$$

subject to

$$-m_{ij}\pi_s + \alpha_{is} - \beta_{js} - \phi\gamma_{js} \leq \omega_2 p_s m_{ij} \qquad \forall i \in \mathcal{I}, \forall j \in \mathcal{J}_\mathcal{O} \qquad (4.61)$$

$$-\tilde{c}_{kj}\pi_s + \gamma_{js} - \mu_{ks} \leq \omega_2 p_s \tilde{c}_{kj} \qquad \forall k \in \mathcal{K}_\mathcal{O}, \forall j \in \mathcal{J}_\mathcal{O} \qquad (4.62)$$

$$\pi_s, \alpha_{is}, \beta_{js}, \gamma_{js}, \mu_{ks} \geq 0 \qquad \forall i \in \mathcal{I}, \forall j \in \mathcal{J}_\mathcal{O}, \forall k \in \mathcal{K}_\mathcal{O}, \qquad (4.63)$$

where $\mathcal{J}_\mathcal{O} := \{j \in \mathcal{J} | \widehat{y}_j = 1\}$ and $\mathcal{K}_\mathcal{O} := \{k \in \mathcal{K} | \widehat{\tilde{z}}_k = 1\}$.

Phase 2. For second phase, we fix all the dual variable values obtained in first phase and only solve for the remaining variables. The second phase **DSP** model is

as follows:

$$\text{Maximize } Z_{DSP^s} = -\sum_{j\in\mathcal{J}_\mathcal{C}} Q_j^{SH}\widehat{y}_j\beta_{js} - \sum_{k\in\mathcal{K}_\mathcal{C}} \tilde{Q}_k^{DC}\widehat{\tilde{z}}_k\mu_{ks} \tag{4.64}$$

subject to

$$-m_{ij}\widehat{\pi}_s + \widehat{\alpha}_{is} - \beta_{js} - \phi\widehat{\gamma}_{js} \leq \omega_2 p_s m_{ij} \qquad \forall i \in \mathcal{I}, \forall j \in \mathcal{J}_\mathcal{C} \tag{4.65}$$

$$-\tilde{c}_{kj}\widehat{\pi}_s + \widehat{\gamma}_{js} - \mu_{ks} \leq \omega_2 p_s \tilde{c}_{kj} \qquad \forall k \in \mathcal{K}_\mathcal{C}, \forall j \in \mathcal{J}_\mathcal{C} \tag{4.66}$$

$$\beta_{js}, \gamma_{js}, \mu_{ks} \geq 0 \qquad \forall i \in \mathcal{I}, \forall j \in \mathcal{J}_\mathcal{C}, \forall k \in \mathcal{K}_\mathcal{C}, \tag{4.67}$$

where $\mathcal{J}_\mathcal{C} := \{j \in \mathcal{J} | \widehat{y}_j = 0\}$ and $\mathcal{K}_\mathcal{C} := \{k \in \mathcal{K} | \widehat{\tilde{z}}_k = 0\}$. After solving these two phases, we construct the Benders optimality or feasibility cuts as described by (4.55) and (4.56), respectively, with the help of the final dual variable values and add to the **MP** in each iteration. For the second phase, instead of employing CPLEX to solve the LP (4.64) - (4.67), we use an efficient solution approach. We can rewrite the constraint (4.65) and (4.66) as follows:

$$\beta_{js} \geq -m_{ij}\widehat{\pi}_s - \omega_2 p_s m_{ij} + \widehat{\alpha}_{is} - \phi\widehat{\gamma}_{js} \qquad \forall i \in \mathcal{I}, \forall j \in \mathcal{J}_\mathcal{C} \tag{4.68}$$

$$\mu_{ks} \geq -\tilde{c}_{kj}\widehat{\pi}_s + \widehat{\gamma}_{js} - \omega_2 p_s \tilde{c}_{kj} \qquad \forall k \in \mathcal{K}_\mathcal{C}, \forall j \in \mathcal{J}_\mathcal{C}. \tag{4.69}$$

In the optimal solution of the second phase problem, β_{js} obtains the following value:

$$\beta_{js} = \begin{cases} \max_{i\in\mathcal{I}}\{-m_{ij}\widehat{\pi}_s - \omega_2 p_s m_{ij} + \widehat{\alpha}_{is} - \phi\widehat{\gamma}_{js}\} = \Upsilon_j, \forall j \in \mathcal{J}_\mathcal{C}, & \text{when } \Upsilon_j > 0 \\ 0, & \text{otherwise,} \end{cases}$$

and μ_{ks} obtains the following:

$$\mu_{ks} = \begin{cases} \max_{j \in \mathcal{J}_\mathcal{C}} \{-\tilde{c}_{kj}\widehat{\pi}_s + \widehat{\gamma}_{js} - \omega_2 p_s \tilde{c}_{kj}\} = \Gamma_j, \forall k \in \mathcal{K}_\mathcal{C} & \text{when } \Gamma_j > 0 \\ 0, & \text{otherwise.} \end{cases}$$

Solving the second phase LP in this manner reduces significant computational overhead.

4.4.2.4 Adding Initial Cut to MP

In the traditional BD framework, the **MP** is solved for the first time without any Benders cut. After solving the subproblem, based on the first **MP** solution, we generate an optimality or feasibility cut, depending on whether the primal subproblem gets a feasible solution, and second BD iteration onwards we continue adding cuts. However, solving the first BD iteration with no cut may cause delay in convergence. Therefore, we attempt to enhance BD performance by providing the with **MP** additional information about the overall problem from the very beginning, in the form of an initial cut. To obtain this cut, we first solve LP relaxation of the overall problem, where we remove the integrality requirement of the $\mathbf{y}$ and $\tilde{\mathbf{z}}$ variables. After solving the LP-relaxed problem, we retain the ψ_s values unchanged, but fix the binary variables *conservatively*, i.e., if any y_j or $\tilde{z}_k$ obtains positive value in the LP-relaxed solution, we round it up to one. We do this in order to avoid any infeasibility in the original problem due to opening of inadequate shelter or DC. Next, using this $(\mathbf{y}, \mathbf{z}, \boldsymbol{\psi})$ solution vector, we solve the $|\mathcal{S}|$ separate subproblems and depending on feasibility of each subproblem $s \in \mathcal{S}$, an optimality or feasibility cut is generated as discussed before and added to the **MP**. Thus, instead of solving the **MP** for the first time without any cut, we provide significant amount of additional information in the form of $|\mathcal{S}|$ initial cuts, expecting faster convergence.

4.5 Case Study

We apply our proposed model on a realistic problem instance in coastal Texas region. The study region is same as the one described in §2.6, with identical settings for the evacuation, shelter, and DC zones, respectively (see Figure 2.6). The evacuation zone consists of the most disaster-prone areas in the five coastal Texas counties: Brazoria, Chambers, Galveston, Harris, and Matagorda. Each source node represents a block group (census 2010). However, unlike considering the four settings (see Table 2.6 and Figure 2.6.1) used in section 2, namely: *coast*, *(coast + A)*, *(coast + A + B)*, and *(coast + A + B + C)*, respectively, depicting the gradual expansion of the evacuation source zone with the disaster intensity increase, in this study, we generate a large number of scenarios by randomly selecting a subset of the evacuation source nodes. The scheme of scenario generation will be explained shortly in §4.5.2. The shelter zone consists of nine shelter hubs identified in "State Evacuation and Sheltering Plan"(Texas, 2006) and 47 additional neighboring counties considered by us. These counties are spatially spread out, enveloping the entire evacuation zone. These 56 candidate shelter nodes do not necessarily indicate the precise locations to establish the physical shelters with certain accommodation capacities, but represent the available aggregated capacities in those 56 counties. Next, 48 counties, located farther away from the coast, enveloping the entire shelter zone, constructs our DC zone. The names of the counties and the geographic units used to construct these three zones are summarized in Table 2.5. We use the TIGER/Line shapefiles for census 2010 (source: census.gov) for visual representation of these three zones (see Figure 2.6).

4.5.1 Data Collection and Random Parameter Generation

We summarize the data sources for different model parameters in Table 4.1. Some of the parameters are collected from the GIS databases, while the remaining ones are randomly generated using uniform distribution with realistic intervals.

Table 4.1: Distribution of Model Parameters

Parameter	**Distribution**
Source, shelter, DC node locations	TIGER/Line shapefiles (census.gov)
pop_i, pop_j	Census 2010 population data (socialexplorer.com)
Q_j^{SH}	$pop_j \times U[0.4; 0.6]$
f_j	$Q_j^{SH} \times U[50; 100]$
ϕ	U [3; 6]
$\tilde{Q}_k^{DC}$	$\phi \frac{\sum_{i \in \mathcal{I}} pop_i \times \text{U}[0.9;\ 1.1]}{\zeta \times \lvert\mathcal{K}\rvert}$, where $\zeta = 0.1$
$\tilde{f}_k$	$\tilde{Q}_k^{DC} \times U[10; 20]$
α	U[0.1;0.2]
β	U[0.01;0.05]
$(\omega_1, \omega_2) \in [0, 1]$	$\omega_1 + \omega_2$=1

For the population at each evacuation source, we use the block group population data from census 2010. In practice, instead of constructing dedicated shelters, existing infrastructure such as public building, school.church, stadium, and auditorium are converted to makeshift shelters. Therefore, we assume that capacity of a shelter location (one per county) is proportional to the county's population. Specifically, we consider a candidate shelter capacity as 40%-60% of that county's population (census 2010). Moreover, we assume that a shelter's capacity is linearly related to its associated fixed opening cost, incurred for converting the pre-existing facilities

to shelters that can accommodate the inbound evacuees. Consequently, in this cost structure, if a densely populated county is considered as a candidate shelter, both its capacity and fixed cost will be high. We generate remaining model parameters such as unit transportation cost for evacuee and relief flows, per head demand for relief items using uniform distribution as shown in Table 4.1. As explained before, the relative weights (ω_1, ω_2) for the worst case and average case transportation cost terms in the objective function are supplied by the decision maker. Both are fractions between 0 and 1, summing up to 1.

4.5.2 Scenario Generation

We define a disaster scenario by its intensity and impact area. In our study region, there are total 1085 source nodes, but an extreme scenario where all or most of these nodes will be affected by a high-intensity storm is very unlikely. Therefore, we consider a subset of these source nodes as the *affected* sources to construct each scenario. To enforce enough variability among the scenarios, we consider dividing $|\mathcal{S}|$ into n equal number of groups. In each group, we randomly select a predetermined number of source nodes out of 1085, as the *affected* sources in that scenario. Next, based on the location of the affected sources relative to the coastline, we estimate a distance factor (DF_{is}). For this, we use the four settings described in Table 2.6. Based on whether a source node is within coast, A, B, or C (see Figure 2.6.1), we set the DF_{is} value as follows:

$$DF_{is} = \begin{cases} 1.0, & i \in Coast \\ 0.9, & i \in A \\ 0.8, & i \in B \\ 0.7, & i \in C. \end{cases}$$

However, the volume of the evacuating population largely depends on disaster intensity. A category five disaster can reach deeper inland, causing significant damage compared to a low intensity tropical storm. Therefore, we estimate the evacuation fraction (ν_{is}) as a weighted sum of the distance and intensity factor:

$$\nu_{is} = W_1 \ DF_{is} + W_2 \frac{Catg_s}{5} \qquad \forall i \in \mathcal{I}, \forall s \in \mathcal{S}. \tag{4.70}$$

We set $W_1 = 0.4$ and $W_2 = 0.6$ in our study. Now, evacuating population from a source i in scenario s is calculated as $pop_{is} = \nu_{is} pop_i$.

4.5.3 Computational Experiments

We solve our problem instance, created by using both the GIS-based and randomly generated parameters (see §4.5.1), for an increasing sequence of critical distance (CD) values such as {180,190,200,...,260} and for changing relative weights (ω_1, ω_2), specifically, (0.0,1.0),(0.2,0.8),(0.4,0.6),(0.6,0.4),(0.8,0.2), and (1.0,0.0). We first attempt to solve the instance for all CD and weight combinations by CPLEX B&C with two early stopping criteria: 3600 sec. runtime or 2% optimality gap, whichever is encountered first. However, B&C performs poorly for the weight combination (1.0,0.0), where we minimize the fixed cost and the worst case transportation cost. For the other weight combinations, as the number of scenarios increases, B&C takes longer to solve, and 150 scenario onwards, B&C stops finding any feasible solution by 3600 secs.

To demonstrate the efficiency of our proposed Benders Decomposition based solution approaches, we conduct a detailed computational study. We solve the special cases at two extreme weight vectors (0.0,1.0) and (1.0,0.0) by the BD-based approaches described in §4.4.1.1 and §4.4.1.2. For the remaining weight vectors in-between, we employ several BD-enhancements as explained in §4.4.1.3. We im-

plement both B&C and BD-based approaches using Concert Technology (CPLEX 12.4 with Java API). In BD implementations, we employ CPLEX to solve the master and the $|\mathcal{S}|$ subproblems. We take all runs on desktop computers with Intel Core 2 Duo processor and 8 GB RAM. In Tables 4.2 and 4.3, we report the solution times by employing our different approaches for all the combinations of CD values and weight vectors that we consider. Before presenting the computational results, we first explain these experiments, based on CPLEX B&C and several BD-enhancement attempts. We conduct all experiments with same two early stopping criteria: 3600 sec. or 2% optimality gap, whichever is met first.

- **CPLEX B&C :** We solve the test instance by CPLEX B&C keeping all the default settings of the solver for cut generation, preprocessing, and upper bound heuristics. We use this B&C solution time to benchmark the performance of other approaches.

- **Experiment 1 :** We employ our Benders Decomposition implementation with lazy constraint callback. We use CPLEX with its default settings to solve the **MP** and all $|\mathcal{S}|$ subproblems, that are LPs.

- **Experiment 2 :** To improve the BD performance upon Experiment 1, we include a two-phased cut strengthening scheme (see §4.4.2.3). We apply CPLEX to solve the **MP** and the first phase of **DSP**, but avoid using the solver in the second phase of **DSP** and apply an efficient alternative method.

- **Experiment 3 :** In the BD framework of Experiment 2, we include CPLEX parameter tuning (see §4.4.2.2) while solving **MP**. Specifically, we set the *MIPEmphasis* parameter to optimality instead of keeping the default setting to balance optimality and feasibility.

- **Experiment 4 :** In the callback-based BD framework (Experiment 1), we combine the two-phased cut strengthening scheme (Experiment 2) and CPLEX parameter tuning (Experiment 3) together.

- **Experiment 5 :** Instead of solving the first **MP** conventionally, i.e., without any additional information about the overall problem, we provide an initial cut to **MP** at the very first BD iteration. The details of constructing this cut is explained in §4.4.2.4.

- **Experiment 6 :** Here, in addition to inclusion of an initial cut to the first **MP**, we conduct CPLEX parameter tuning (as in Experiment 3) to solve **MP**.

4.5.4 Computational Results

We solve the test instance with different values of CD and different weight vectors (ω_1, ω_2). First, for the two special cases: $(\omega_1 = 0, \omega_2 = 1)$ and $(\omega_1 = 1, \omega_2 = 0)$, we attempt to solve the instance for different CDs by CPLEX B&C and callback based BD implementations. As shown in Table 4.2 with best runtimes highlighted in boldfaces, for the $(\omega_1 = 0, \omega_2 = 1)$ case, BD with Experiment 1 setting, i.e., with no enhancement, outperforms B&C except for CD values 190 and 200. However, CPLEX parameter tuning (Experiment 3 setting) boosts the BD performance, reflected by the faster solution time under the column BD (tuned) of Table 4.2. In the other special case $(\omega_1 = 1, \omega_2 = 0)$, where we minimize the first stage fixed cost and the worst case flow cost over all scenarios in a robust optimization setting, we observe that B&C cannot find any feasible solution within 3600 sec. However, due to the advantage of decomposition and further having subproblem separability, BD (tuned) efficiently solves the test instance for all CD values.

In Table 4.3, we present the solution times for B&C and all other experiment settings described in §4.5.3 to solve the instance with non-zero weight vector (ω_1, ω_2),

Table 4.2: Runtime (sec.) Comparison Between B&C and BD for Special Cases ($|\mathcal{S}|$ = 100)

	$(\omega_1 = 0, \omega_2 = 1)$			$(\omega_1 = 0, \omega_2 = 1)$
CD	B&C	BD	BD (tuned)	BD (tuned)
180	1243	918	**520**	971
190	1060	1162	**768**	931
200	1195	1586	**1102**	588
210	1315	934	**781**	665
220	1348	1053	**796**	967
230	1332	**835**	918	1057
240	1326	827	**803**	726
250	1340	925	**711**	692
260	1380	949	**707**	650

i.e., when both ω_1 and ω_2 are fractions, summing up to one. Here, the number of scenarios $|\mathcal{S}| = 100$. Row minimums, the best runtimes out of all experiments, are highlighted in boldfaces. We observe, B&C can solve the instance by 3600 sec for all CD values and weight combinations we consider, and the same is true for EXPT 1 to EXPT 6. Therefore, we skip reporting the closing optimality gap in Table 4.3, since all values are below 2% gap, one of our early stopping conditions. We now discuss our main observations from this computational study.

- Changing CD or the weight vector (ω_1, ω_2) values do not significantly affect B&C runtime in our problem. For all considered combination of these parameters, B&C solution times are in same order of magnitude. However, for BD implementations EXPT 1 - EXPT 4, the solution time noticeably decreases as we increase CD, particularly for CD = 220 onwards.

- For each CD and weight vector combination, represented by a row in Table 4.3,

at least one of the BD implementations outperform B&C. The most successful attempt is the EXPT 3: CPLEX parameter tuning within BD framework.

- In this problem, inclusion of cut strengthening does not help (EXPT 2), except for a few cases. The two phase method, in isolation, indeed causes computational overhead, increasing the solution time.

- In EXPT 5 and EXPT 6, the attempt to add initial cut to the first **MP** leads to a very poor performance, although the solution time is less than 3600 sec., our specified early stopping time. We observe, the time to solve the LP relaxation (LP-R) of the overall problem is considerably high, leading to an increase of the total solution time. Although the time consumed by the BD module, after solving the LP-R, construction and insertion of the initial cut, this approach is not recommended, since other approaches clearly perform better. We further observe the benefit of tuning by comparing the EXPT 5 and EXPT 6 solution times, the latter being less in general, where we tune certain CPLEX parameter as mentioned before.

- Out of all six experiments involving some BD enhancement, EXPT 3 performs best, followed by EXPT 4. This indicates that tuning of the right CPLEX parameter, on top of the basic callback-based BD implementation, is most suited for our problem. Cut strengthening is partially helpful, as we observe some best runtime entries under EXPT 4 (highlighted in bold). For those cases, tuning proves beneficial by making up for the overhead of cut strengthening process, and decreases the overall solution time.

Thus far, we establish that for the problem instance with $|\mathcal{S}| = 100$, BD outperforms B&C for any of the weights (ω_1, ω_2) that we consider. Next, we take some trial

runs to identify the threshold problem size that the B&C can no longer solve, but BD can still solve in reasonable time with acceptable solution quality. We observe, for instance with scenarios $|\mathcal{S}| = 150$, B&C cannot find a feasible solution within 3600 sec. for any CD and weight combination. However, callback based BD (Experiment 1 setting) solves them all, except for one case when CD = 200, weight vector is ($\omega_1 = 0.8, \omega_2 = 0.2$). With further enhancement by CPLEX parameter tuning (Experiment 3 setting), that case also resolves and several other solution times also improve. We present the solution times and the closing optimality gaps in Table 4.4.

4.5.5 Analysis

In Figures 4.2 and 4.3 (combined), we illustrate the change in the strategic location decision for the DCs and shelters, while two parameters: critical distance (CD) and relative weight vector (ω_1, ω_2) are altered. We show the opened DC and shelter locations in our study region map, for the CD values of 180, 220, and 260 miles. For ω_1, the relative weight on worst case transportation cost, we consider the values: 0, 0.2, 0.8, and 1. The ω_2 value changes respectively, keeping their sum equal to one. In Figures 4.2 and 4.3, row-wise we present the maps for a fixed ω_1, for the three CD values that we mention above. Therefore, we explore the effects of changing CD by row-wise comparison of three maps, and the effects of changing ω_1 by comparing them column-wise. We now discuss our important observations.

For small CD values, the shelters open up close to the evacuation zone. As CD increases, the shelters get spread out, and some get closer to the DC zone, facilitating supply side transportation cost reduction. This pattern is observed across each row of these two figures. DC locations also alter, but not as noticeably as the shelters.

In this problem parameter setting, we assume that the accommodation capacity as well as the fixed cost of opening a shelter are proportional to the population of

the underlying county. The population density of the candidate shelter county is shown in the maps using "graduated color scheme" of ArcGIS (ESRI Inc.), where thicker color indicates high density. For this reason, in all 15 maps of the Figures 4.2 and 4.3, we find that some shelters open up at distant locations from the evacuation zone, always avoiding the candidates in thicker colored. Similarly, we observe that some open DCs, located at the southwest side of each map are far from the open shelters. such location decisions are due to the significantly higher opening costs for the DC candidates located closer to the shelter zone.

The effect of changing the relative weights (ω_1, ω_2) on shelter location can be explained by column-wise comparing the four maps in Figures 4.2 and 4.3 (combined). For the fractional weights, i.e., where ω_1 and ω_2 are both non-zeros, we observe a gradual shift of the shelters towards the evacuation zone. DC locations alter accordingly, to reduce the supply side transportation cost component. This phenomenon becomes more prominent by comparing the first row of Figure 4.2 and the last row of Figure 4.3. When $\omega_1 = 1$, i.e., the focus is on minimizing the maximum transportation cost, the shelters are very close to the evacuation zone (see Figures 4.3d, 4.3e,4.3f). On the other hand, $\omega_2 = 1$, we observe (see Figures 4.2a, 4.2b, 4.2c) that the shelters are more fanned out, while being constrained by the respective CD values. This pattern is explained by the increasing importance placed on minimizing the worst case scenario transportation cost. Out of a large number of scenarios, a few cause this worst case to materialize. If the source nodes, affected by this worst case disaster situation, are geographically concentrated at a small region, then, as ω_1 increases, the shelters open up close to that region to reduce the evacuees' transportation cost. DC locations, also by adjusting accordingly, try to reduce the relief transportation cost. However, if we focus on minimizing the average transportation cost over all scenarios, the shelters need not be located close to the evacuation zone.

Those can open up in the middle, between the DC and evacuation zones, and balance the transportation costs at the supply and demand sides, respectively.

Therefore, we observe that the change of CD and relative importance given to the average and worst case cost minimization, can alter the location decision. Comparison of the obtained solutions in Figures 4.2 and 4.3 reveals that the combination of lower CD and higher ω_1 is the most restrictive setting, reflected by the highest objective function value in our problem. On the other hand, larger CD and lower ω_1 value combination produces the least restrictive solution, with the smallest objective function value.

4.6 Conclusion

In this research, we introduce a new model to combine the aspects of robust and stochastic optimization in the presence of data uncertainty. The demand uncertainty is presented by a set of disaster scenarios, each having equal probability of occurrence. We consider a strategic, multi-objective three-tier network design problem, focusing on fast evacuation and flow cost minimization. The second objective is expressed as the weighted sum of the worst case and expected costs over all scenarios. By altering the relative weights, the decision-maker can change his emphasis on worst case or expected system cost minimization. We demonstrate the conversion of the multi-objective model to single-objective. But the presence of min-max type term (worst case flow cost) in the second objective makes the problem hard. Large scale problems of this nature, particularly, with a huge number of scenarios, are very difficult to solve. Therefore, we devise a Benders Decomposition based solution approach to solve the large instances efficiently. The strength of BD lies in the ability to split the overall model into a master problem and completely separable, independent flow problems for each scenario. We present variations of BD, appropriate for

different relative weight combinations. We conduct a detailed computational study with various BD-acceleration schemes, and finally apply it to a GIS-based case study on coastal Texas region. We observe the effects of changing (1) critical distance, and (2) relative weights on worst or average case cost minimization terms, and gain interesting insights. We conclude by indicating future research directions. In this work, we consider only scenario-based demand uncertainty. An extension of this work can include other types of uncertainties such as infrastructure unavailability due to damage of road network, shelter or DC facilities. We consider the critical distance of evacuees as a proxy of fast evacuation in this study, however, traffic congestion is a real issue during mass evacuation. Inclusion of the evacuation side operational decisions in a more comprehensive model can be considered for future work.

Table 4.3: Comparison of B&C and BD Runtimes (sec.) with Fractional Weights (ω_1, ω_2) $(|\mathcal{S}| = 100)$

CD	ω_1	ω_2	B&C	EXPT 1	EXPT 2	EXPT 3	EXPT 4	EXPT 5	EXPT 6
180	0.2	0.8	1,318	**1,084**	1,098	1,173	1,193	1,223	1,095
180	0.4	0.6	1,978	2,007	2,112	1,309	1,616	**1,147**	1,157
180	0.6	0.4	1,216	1,947	1,987	**1,048**	1,050	2,291	1,634
180	0.8	0.2	1,199	1,884	1,953	**677**	679	1,495	1,657
190	0.2	0.8	1,851	625	613	**512**	515	886	934
190	0.4	0.6	2,078	2,384	2,517	1,969	1,932	2,378	1,495
190	0.6	0.4	1,310	2,456	3,039	**1,040**	1,705	2,728	1,397
190	0.8	0.2	1,193	1,432	1,416	992	**957**	2,191	1,537
200	0.2	0.8	1,629	993	1,022	952	994	1,046	**841**
200	0.4	0.6	1,612	1,603	3,062	1,414	**1,098**	2,304	1,918
200	0.6	0.4	1,856	1,946	1,880	**750**	762	1,977	1,085
200	0.8	0.2	1,311	2,399	2,859	1,301	1,437	1,675	**1,226**
210	0.2	0.8	2,292	779	794	690	**668**	3,139	1,936
210	0.4	0.6	1,771	1,689	1,616	644	**596**	2,549	1,252
210	0.6	0.4	1,542	845	1,018	**596**	667	2,943	1,120
210	0.8	0.2	1,517	1,269	1,138	878	**819**	2,586	1,922
220	0.2	0.8	1,805	162	163	**162**	164	2,441	1,099
220	0.4	0.6	1,771	434	436	**196**	198	2,319	1,867
220	0.6	0.4	1,524	1,679	1,645	**573**	577	2,709	2,075
220	0.8	0.2	1,564	1,411	1,395	**478**	483	2,250	1,686
230	0.2	0.8	2,307	124	125	**122**	122	4,123	1,922
230	0.4	0.6	1,764	174	174	**152**	152	3,209	1,418
230	0.6	0.4	1,967	229	230	**179**	204	2,532	1,938
230	0.8	0.2	1,536	606	611	**201**	202	3,516	1,366
240	0.2	0.8	2,402	167	168	**162**	163	2,930	2,067
240	0.4	0.6	2,238	**152**	153	153	154	2,896	2,174
240	0.6	0.4	1,501	**185**	187	194	195	2,863	2,171
240	0.8	0.2	1,668	601	664	**277**	278	1,496	1,389
250	0.2	0.8	2,311	150	151	**150**	151	3,188	2,313
250	0.4	0.6	1,720	143	144	**133**	134	3,754	2,252
250	0.6	0.4	2,462	402	436	**271**	273	2,728	1,727
250	0.8	0.2	1,619	661	725	**269**	270	3,221	1,606
260	0.2	0.8	1,835	915	895	**471**	473	2,458	2,218
260	0.4	0.6	1,839	1,237	1,331	**760**	770	2,556	1,657
260	0.6	0.4	2,741	522	526	**425**	429	1,606	2,067
260	0.8	0.2	1,549	1,150	1,126	587	**573**	2,783	1,552

Table 4.4: BD Runtimes (sec.) and Optimality Gaps (%) ($|\mathcal{S}| = 150$)

	weights		BD (EXPT 1)		BD (EXPT 2)	
CD	ω_1	ω_2	Runtime (sec.)	Gap%	Runtime (sec.)	Gap%
180	0.2	0.8	3,041	2.00	**1,512**	1.10
180	0.4	0.6	**757**	1.53	1,557	1.96
180	0.6	0.4	2,334	2.00	**1,655**	1.47
180	0.8	0.2	1,908	1.97	**1,302**	1.18
190	0.2	0.8	**2,681**	2.00	3,265	2.00
190	0.4	0.6	1,697	2.00	**1,526**	2.00
190	0.6	0.4	**1,467**	1.97	1,510	1.99
190	0.8	0.2	1,157	1.97	**1,150**	2.00
200	0.2	0.8	2,011	1.99	**735**	1.99
200	0.4	0.6	3,052	2.00	**1,985**	2.00
200	0.6	0.4	2,673	2.00	**2,209**	1.93
200	0.8	0.2	3,611	2.31	**1,640**	1.59
210	0.2	0.8	1,699	1.99	**1,608**	1.99
210	0.4	0.6	2,219	2.00	**1,072**	2.00
210	0.6	0.4	2,037	1.99	**1,019**	2.00
210	0.8	0.2	1,371	1.99	**861**	1.88
220	0.2	0.8	2,193	1.99	**1,279**	2.00
220	0.4	0.6	**1,237**	1.98	1,252	1.15
220	0.6	0.4	1,291	1.98	**816**	1.97
220	0.8	0.2	1,654	1.99	**874**	1.90
230	0.2	0.8	**181**	1.48	197	1.98
230	0.4	0.6	**185**	0.00	233	0.16
230	0.6	0.4	**363**	1.65	476	1.85
230	0.8	0.2	1,174	1.99	**469**	1.98
240	0.2	0.8	**217**	1.76	246	1.97
240	0.4	0.6	**191**	0.00	231	0.99
240	0.6	0.4	**239**	0.56	300	1.76
240	0.8	0.2	717	2.00	**413**	1.89
250	0.2	0.8	**218**	0.00	246	1.70
250	0.4	0.6	**193**	0.00	229	0.00
250	0.6	0.4	401	1.71	**380**	1.90
250	0.8	0.2	680	1.96	**453**	1.98
260	0.2	0.8	**216**	0.00	221	0.00
260	0.4	0.6	**195**	0.00	254	1.17
260	0.6	0.4	**340**	1.39	435	1.72
260	0.8	0.2	757	1.98	**410**	1.99

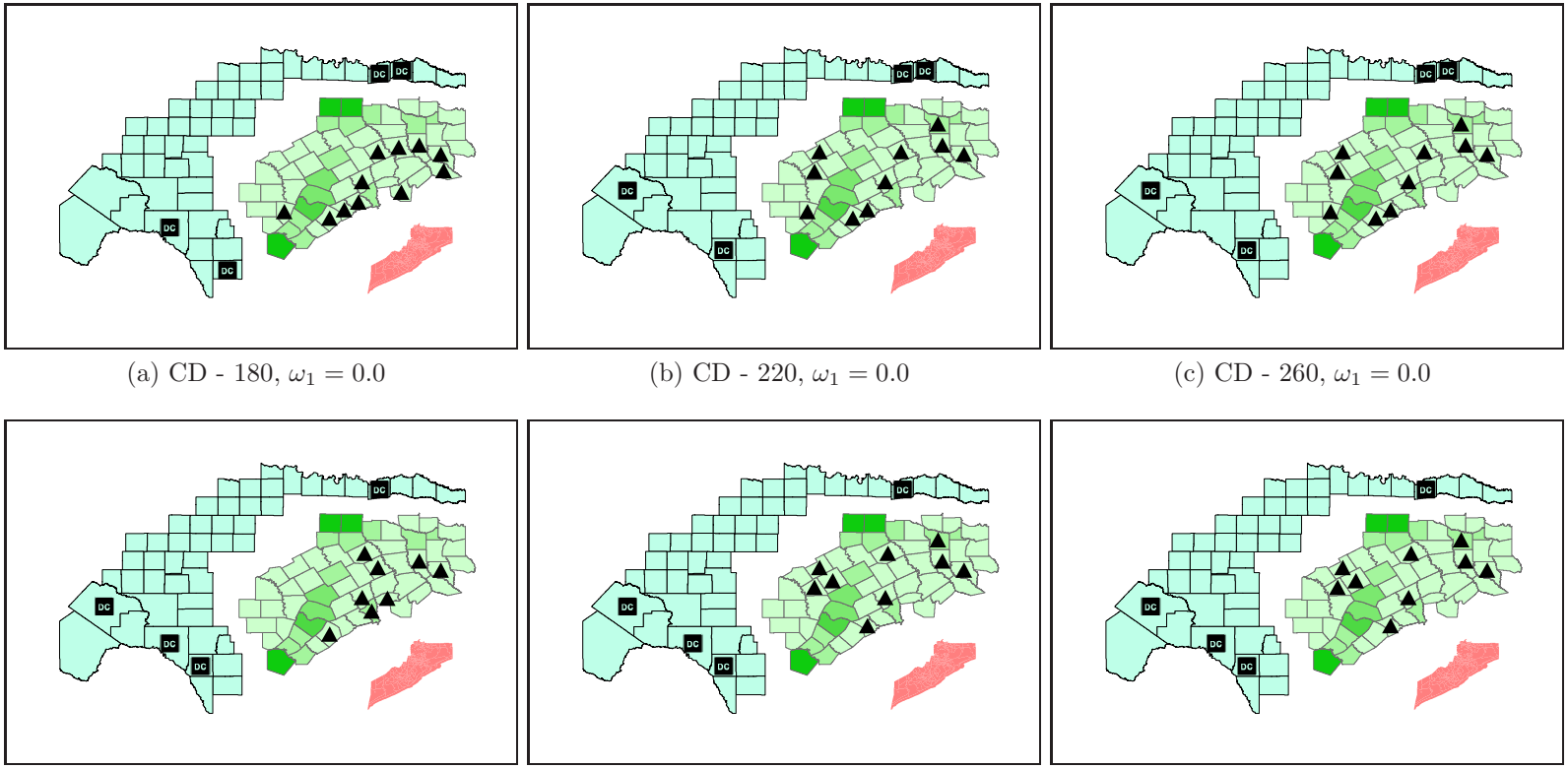

(a) CD - 180, $\omega_1 = 0.0$ (b) CD - 220, $\omega_1 = 0.0$ (c) CD - 260, $\omega_1 = 0.0$

(d) CD - 180, $\omega_1 = 0.2$ (e) CD - 220, $\omega_1 = 0.2$ (f) CD - 260, $\omega_1 = 0.2$

Figure 4.2: Effects of Changing CD and Relative Weights on Location Decision - Part A

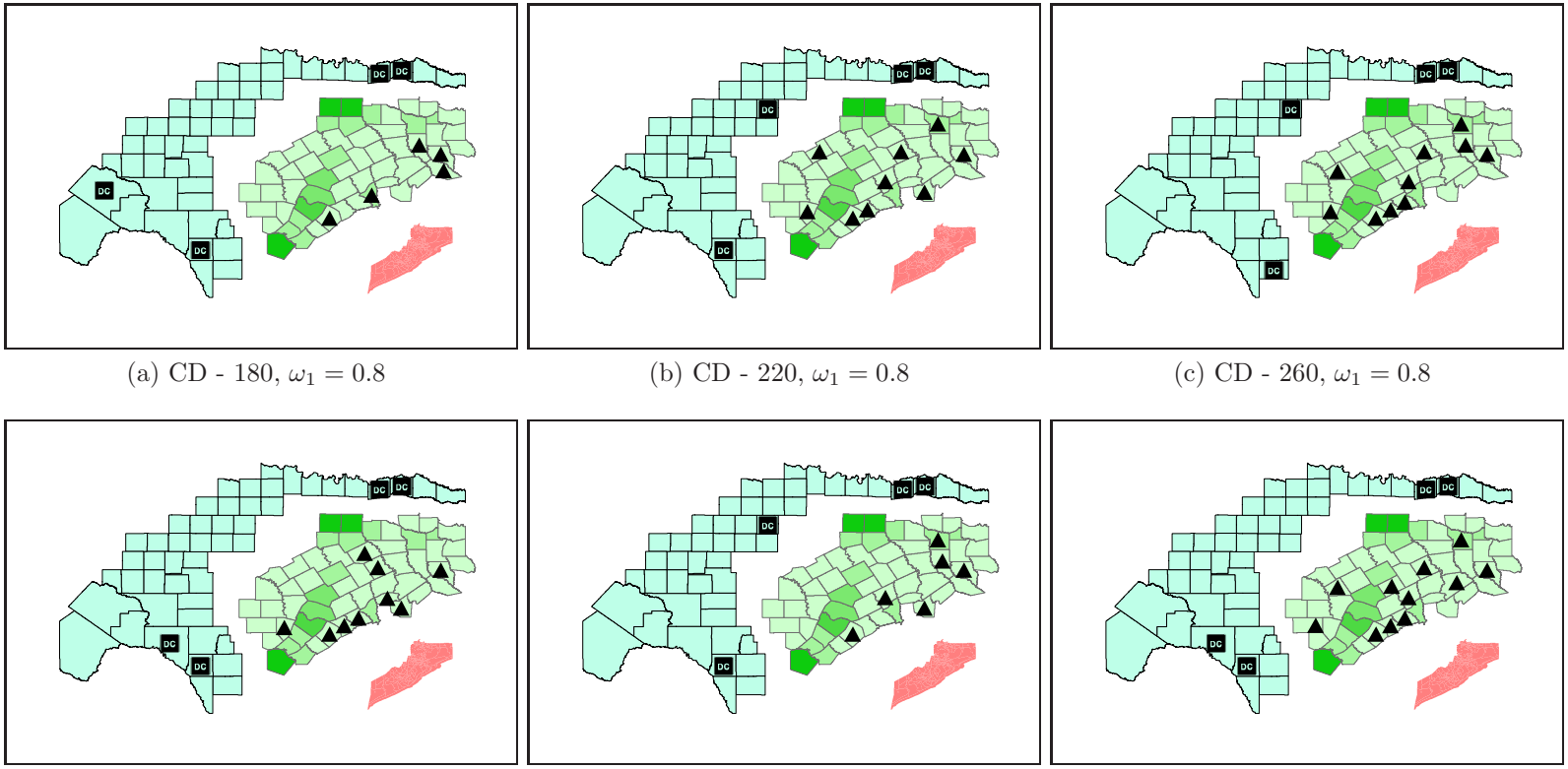

(a) CD - 180, $\omega_1 = 0.8$ (b) CD - 220, $\omega_1 = 0.8$ (c) CD - 260, $\omega_1 = 0.8$

(d) CD - 180, $\omega_1 = 1.0$ (e) CD - 220, $\omega_1 = 1.0$ (f) CD - 260, $\omega_1 = 1.0$

Figure 4.3: Effects of Changing CD and Relative Weights on Location Decision - Part B

5. CONCLUSIONS AND FUTURE DIRECTIONS

5.1 Conclusions

In this dissertation, we present three closely related works on strategic response network design. In our first work, we introduce a deterministic multi-objective emergency relief network design problem, integrating the evacuation and distribution decision in a mixed integer linear model. We devise a Benders Decomposition (BD)-based solution approach, relying on lazy constraint callback function of CPLEX to solve large problem instances. We apply the integrated Network for Emergency Evacuation and Distribution of Supplies (NEEDS) model to solve a realistic problem with available GIS-based data. Our model can be used as a decision-making tool to explore the trade-offs between cost and critical distance.

In our next work, we introduce data uncertainties due to disaster location, intensity, and duration, non-compliance of instruction during emergency, all contributing to demand uncertainty. We present a robust emergency relief network design problem, where in a two-stage model, we determine the strategic central supply locations that can send relief items to the impacted population in response to any realization of disaster from a set of events. By considering different modes of transport with varied unit transportation costs, we explore the trade-off between the *critical time* to start sending reliefs from CSLs and the overall system cost. We develop a decomposition-based solution methodology, as the state of the art branch-and-cut algorithm fails to solve realistically large problem instances. By exploiting the model structure, we apply Benders Decomposition (BD) that successfully splits the model, first, into master problem (**MP**) and subproblem (**SP**), and then, separates the **SP** into smaller LPs for each event. We apply the robust model to solve a GIS-data based case with the

entire Gulf coast as the study region. We observe how the change of critical time, disaster intensity, and population density affects the solution.

In our third work, we again consider data uncertainty, presented by a set of equally likely disaster scenarios. We revisit the problem setting of the first work with some simplifications, but present a new problem with an objective function that considers minimization of the worst case as well as the average cost over all disaster scenarios in a weighted sum fashion. As with the NEEDS model, here also we consider two objectives: first, minimization of maximum travel distance for all evacuees, and second, the cost based objective as mentioned above. We develop an efficient solution approach and apply it to a large scale GIS-based case study on coastal Texas. We study the effects of changing the critical distance, and relative weights on worst or average case cost minimization terms.

5.2 Future Directions

The models and solution methods developed in this dissertation can be extended in the future in the various directions. Our first model has already been extended in the second and third works, therefore, we only discuss the future work directions for our second and third works.

1. **Other robustness criteria:** In our second work, instead of using absolute robustness, other robustness criteria such as relative robustness or robust deviation can be applied to observe any change in the solution value or runtime performance.

2. **Economies of Scale:** In addition to different modes of transport, we may introduce economies of scale by considering LTL/FTL.

3. **Consolidation:** We may consider dispatching reliefs from CSLs by grouping

certain items together.

4. **Uncertainty in infrastructure:** We can add road network unavailability, partial or full post-disaster damage of the different network entities.

5. **Low-level decisions:** As we focus on determining the high level allocation decisions for people and relief flows, we do not consider making detailed routing decisions. However, road network damage and traffic congestion are some important issues during mass evacuation. Inclusion of such decisions by forming a more comprehensive model can be considered as future work.

6. **Algorithmic improvement:** While considering any of the above extensions, the problem is likely to become more complex. Some new algorithmic approach may be developed to solve those problems with added difficulty. Various heuristic approaches may be useful for that purpose.

REFERENCES

Alem, D. J., R. Morabito. 2012. Production planning in furniture settings via robust optimization. *Computers & Operations Research* **39**(2) 139–150.

Altay, N., W. G. Green III. 2006. OR/ MS research in disaster operations management. *European Journal of Operational Research* **175** 475–493.

Apte, A. 2009. Humanitarian Logisitics: A New Field of Research and Action, Foundations and Trends® in Technology. *Information and Operations Management* **3**(1) 1–100.

Atamtürk, A., M. Zhang. 2007. Two-stage robust network flow and design under demand uncertainty. *Operations Research* **55**(4) 662–673.

Azad, N., G. K. D. Saharidis, H. Davoudpour, H. Malekly, S. A. Yektamaram. 2013. Strategies for protecting supply chain networks against facility and transportation disruptions: an improved Benders decomposition approach. *Annals of Operations Research* **210**(1) 125–163.

Balçik, B., B. M. Beamon. 2008. Facility location in humanitarian relief. *International Journal of Logistics: Research and Applications* **11**(2) 101–121.

Baron, O., J. Milner, H. Naseraldin. 2011. Facility location: A robust optimization approach. *Production and Operations Management* **20**(5) 772–785.

Ben-Tal, A., L. El Ghaoui, A. Nemirovski. 2009. *Robust Optimization*. Princeton University Press, Princeton.

Ben-Tal, A., A. Nemirovski. 2008. Selected topics in robust convex optimization. *Mathematical Programming* **112**(1) 125–158.

Benders, J. F. 1962. Partitioning procedures for solving mixed variables programming problems. *Numerische Mathematik* **4**(1) 238–252.

Bertsimas, D., D.B. Brown, C. Caramanis. 2011. Theory and applications of robust optimization. *SIAM Review* **53**(3) 464–501.

Bertsimas, D., M. Sim. 2003. Robust discrete optimization and network flows. *Mathematical Programming* **98**(1-3) 49–71.

Bertsimas, D., M. Sim. 2004. The price of robustness. *Operations Research* **52**(1) 35–53.

Bozorgi-Amiri, A., M.S. Jabalameli, S.M.J. Mirzapour Al-e Hashem. 2013. A multi-objective robust stochastic programming model for disaster relief logistics under uncertainty. *OR Spectrum* **35**(4) 905–933.

Brachman, M. L., R. L. Church. 2009. Planning for a Disaster: A Review of the Literature with a Focus on Transportation Related Issues. Tech. Rep. Report No. 1, Geotrans Laboratory, UCSB, Santa Barbara, CA. `http://geog.ucsb.edu/geotrans/publications/FiRSTreport_final.pdf`, Online; Accessed 24-March-2014.

Cacchiani, V., A. Caprara, L. Galli, L. Kroon, G. Maróti, P. Toth. 2012. Railway rolling stock planning: Robustness against large disruptions. *Transportation Science* **46**(2) 217–232.

Caunhye, A. M., X. Nie, S. Pokharel. 2012. Optimization models in emergency logistics: A literature review. *Socio-Economic Planning Sciences* **46**(1) 4–13.

Çelik, M., Ö. Ergun, B. Johnson, P. Keskinocak, Á. Lorca, P. Pekgün, J. Swann. 2012. Humanitarian Logistics. *INFORMS TutORials in Operations Research* **9** 18–49.

CPLEX. 2009. IBM ILOG CPLEX V12.1 User's Manual for CPLEX.

Croxton, K. L., B. Gendron, T. L. Magnanti. 2003. A comparison of mixed-integer programming models for nonconvex piecewise linear cost minimization problems. *Management Science* **49**(9) 1268–1273.

Daskin, M. S. 1995. *Network and Discrete Location: Models, Aplications and Algorithms*. John Wiley and Sons, Inc., New York, NY.

Deb, K. 2001. *Multi-objective Optimization using Evolutionary Algorithms*. Wiley, UK.

Doyen, A., N. Aras, G. Barbarosoğlu. 2012. A two-echelon stochastic facility location model for humanitarian relief logistics. *Optimization Letters* **6**(6) 1123–1145.

Duran, S., M. A. Gutierrez, P. Keskinocak. 2011. Improving Pre-positioning of emergency items for CARE International. *Interfaces* **41**(3) 223–237.

Ester, M., H. P. Kriegel, J. Sander, X. Xu. 1996. A density-based algorithm for discovering clusters in large spatial databases with noise. AAAI Press, 226–231.

Fort Bend County Office of Emergency Management. 2012. Hurricanes. `http://www.fbcoem.org/go/doc/1528/258151/`, Online; Accessed 24-March-2014.

Gabrel, V., C. Murat, A. Thiele. 2014. Recent advances in robust optimization: An overview. *European Journal of Operational Research* **235**(3) 471–483.

Geoffrion, A. M., G. W. Graves. 1974. Multicommodity distribution system design by Benders decomposition. *Management Science* **20**(5) 822–844.

Gutiérrez, G. J., P. Kouvelis, A.A. Kurawarwala. 1996. A robustness approach to uncapacitated network design problems. *European Journal of Operational Research* **94**(2) 362–376.

Horner, M. W., J. A. Downs. 2010. Optimizing hurricane disaster relief goods distribution: model development and application with respect to planning strategies. *Disasters* **3** 821–844.

Huang, S., M. Lindell, C. Prater, H. Wu, L. Siebeneck. 2012. Household Evacuation Decision Making in Response to Hurricane Ike. *Natural Hazards Review* **13**(4) 283–296.

Jia, H., F. Ordonez, M. M. Dessouky. 2007. Solution approaches for facility location of

medical supplies for large-scale emergencies. *Computers and Industrial Engineering* **52** 257–276.

Koster, A. M., M. Kutschka, C. Raack. 2013. Robust network design: Formulations, valid inequalities, and computations. *Networks* **61**(2) 128–149.

Kouvelis, P., G. Yu. 1997. *Robust discrete optimization and its applications*, vol. 14. Springer.

Li, L., M. Jin, L. Zhang. 2011. Sheltering network planning and management with a case in the Gulf Coast region. *Int. J. Production Economics* **131** 431–440.

Lu, Q., S. George, B.and Shekhar. 2005. Capacity constrained routing algorithms for evacuation planning: A summary of results. *Lecture Notes in Computer Science* **3633** 291–307.

Magnanti, T. L., R. T. Wong. 1981. Accelerating Benders Decomposition: Algorithmic Enhancement and Model Selection Criteria. *Operations Research* **29**(3) 464–484.

McDaniel, D., M. Devine. 1977. A Modified Benders' Partitioning Algorithm for Mixed Integer Programming. *Management Science* **24**(3) 312–319.

Mulvey, J. M., R. J. Vanderbei, S. A. Zenios. 1995. Robust optimization of large-scale systems. *Operations Research* **43**(2) 264–281.

Noh, H., Y. C. Chiu, H. Zheng, M. Hickman, P. Mirchandani. 2009. Approach to modeling demand and supply for a short-notice evacuation. *Transportation Research Record* **2091** 91–99.

Polonis, T., C. Phinney, M. Penney, K. Dhanji, C. Moore. 2013. Hurricane Planning. `https://www.preparingtexas.org/Resources/documents/2013%20Conference%20Presentations/Hurricane%20Planning.pdf`, Online; Accessed 24-March-2014.

Rawls, C.G., M. A. Turnquist. 2010. Pre-positioning of emergency supplies for dis-

aster response. *Transportation Research Part B* **44** 521–534.

Rawls, C.G., M. A. Turnquist. 2011. Pre-positioning planning for emergency response with service quality constraints. *OR Spectrum* **33** 481–498.

Rawls, C.G., M. A. Turnquist. 2012. Pre-positioning and dynamic delivery planning for short-term response following a natural disaster. *Socio-Economic Planning Sciences* **46** 46–54.

Rezaei-Malek, M., R. Tavakkoli-Moghaddam. 2014. Robust humanitarian relief logistics network planning. *Uncertain Supply Chain Management* **2**(2) 73–96.

Rubin, P. 2011. Benders decomposition then and now. `http://orinanobworld.blogspot.com/2011/10/benders-decomposition-then-and-now.html`, Online; Accessed 24-March-2014.

Saharidis, G. K. D., M. Minoux, M. G. Ierapetritou. 2010. Accelerating Benders method using covering cut bundle generation. *International Transactions in Operational Research* **17**(2) 221–237.

Salmeron, J., A. Apte. 2010. Stochastic optimization for natural disaster asset prepositioning. *Production and Operations Management* **19**(5) 561–574.

Sherali, H. D., T. B. Carter, A. G. Hobeika. 1991. A location-allocation model and algorithm for evacuation planning under hurricane/flood conditions. *Transportation Research Part B:Methodological* **25**(6) 439 – 452.

Simpson, Robert H, H Saffir. 1974. The hurricane disaster potential scale. *Weatherwise* **27**(8) 169.

Soyster, A. L. 1973. Technical note - convex programming with set-inclusive constraints and applications to inexact linear programming. *Operations Research* **21**(5) 1154–1157.

Üster, H., H. Agrahari. 2011. A Benders Decomposition Approach for a Distribution Network Design Problem with Consolidation and Capacity Considerations.

Operations Research Letters **39**(2) 138–143.

Üster, H., G. Easwaran, E. Akçalı, S. Çetinkaya. 2007. Benders decomposition with alternative multiple cuts for a multi-product closed-loop supply chain network design model. *Naval Research Logistics* **54**(8) 890–907.

Üster, H., P. Kewcharoenwong. 2011. Strategic Design and Analysis of a Relay Network in Truckload Transportation. *Transportation Science* **45**(4) 505–523.

Van Roy, T. J. 1986. A cross decomposition algorithm for capacitated facility location. *Operations Research* **34**(1) 145–163.

Wu, H., M. K. Lindell, C. S. Prater. 2012. Logistics of hurricane evacuation in Hurricanes Katrina and Rita . *Transportation Research Part F: Traffic Psychology and Behaviour* **15**(4) 445 – 461.